THE UNIVERSITY OF MANITOBA

STRUCTURAL ANALYSIS OF ARCHED-FOLDED PLATES OF REVOLUTION

by

Roland Chee-Pang Hui

A THESIS

SUBMITTED TO THE FACULTY OF GRADUATE STUDIES

IN PARTIAL FULFILMENT OF THE REQUIREMENTS FOR THE DEGREE

OF MASTER OF SCIENCE

DEPARTMENT OF CIVIL ENGINEERING

WINNIPEG, MANITOBA

October, 1974

STRUCTURAL ANALYSIS OF ARCHED-FOLDED PLATES OF REVOLUTION

by

ROLAND HUI

A dissertation submitted to the Faculty of Graduate Studies of the University of Manitoba in partial fulfillment of the requirements of the degree of

MASTER OF SCIENCE

ACKNOWLEDGMENTS

The writer gratefully acknowledges the cordial assistance and guidance given to him by Dr. A. H. Shah in the preparation of this thesis. His superior knowledge on the subject is sincerely appreciated.

The writer also wishes to thank Professor J. I. Glanville for his many constructive comments and enthusiasm on the subject. His valuable contributions are gratefully recognized.

SUMMARY

An arched-folded plate of revolution, formed by rotating a folded cross-section about a fixed line, is investigated under the action of uniformly distributed surface loads.

An attempt to analyze the above structure by ordinary one dimensional structural theories, namely, arch and curved-beam theories for the longitudinal action and moment distribution for transverse action while ensuring compatibility between two folds, is the main objective of this thesis.

The comparisons of numerical results for a two-folds roof system obtained by the structural and finite element analyses, are also included.

TABLE OF CONTENTS

CHAPTER I

INTRODUCTION

1.1 Object of Study

A prismatic folded-plate structure, formed by a system of thin plates spanning longitudinally and monolithically connected to each other along longitudinal joints has obtained increasing popularity in past decades. It is now well known that folded plate construction utilizes the strength characteristic of shell structures, such that its inherent stiffness allows for a longer span. Yet, contrasted with curved shell, the folded plate offers the advantage of simpler and less expensive formwork. Although mainly used for roof system, the folded plate has been adapted to bins, bridges, floors and even foundations, resulting in an economic, rational and pleasing design.

The analysis of folded plate structures has received considerable attention since the first publication in 1930. G. Ehlers[1] of Germany was one of the first to propose a folded-plate theory based on a linear variation of longitudinal stress in each plate but neglected the effect of the relative displacement of the joints. Further development of the theory in the 1930's was made by H. Craemer[2] and E. Gruber[3]. They took into account the transverse moments at the joints arising from continuity of construction. This method was introduced to

North America in 1947 in a paper by G. Winter and M. Pei[4]. They described the folded plate theory neglecting relative joint displacements and developed a convenient iteration procedure for the determination of the longitudinal stress pattern after the moment distribution procedure. The more rigorous theory which takes into account the effect of relative joint displacements was first proposed by Gruber and Gruening[5] in 1932. The theory was simplified by W. Z. Vlassow[6] in 1936 with an approach that used linear algebraic equations for calculation of the longitudinal stresses and ridge moments instead of solving fourth order simultaneous differential equations. The theory involving relative joints displacements was also developed by I. Gaafar[7] and D. Yitzhaki[8] who introduced different procedures which reduced the number of equations required for solution to approximately one half that of Vlassow's method. In addition, an iteration method was developed to account for relative joint displacement. Further theoretical developments reconsidered the use of simple beam theory in each plate and the use of one-way slab in the transverse direction was introduced by H. Simpson[18]. Utilization of the two-dimensional theory of elasticity for determination of membrane stresses and two-way slab theory for determination of bending and twisting of the slab was introduced by Goldberg and Leve[9]. The ASCE Task Committee on Folded Plate Construction summarized the literature on analysis of folded plates structures into the following four basic categories:

(a) beam method,

(b) folded plate theory neglecting relative joint displacement,

(c) folded plate theory considering relative joint displacement, and

(d) elasticity method.

A full bibliography on folded plates has been presented in the report by this committee in 1963[10].

The behaviour of prismatic folded plate structures is now well understood. Figure 1.1 shows some typical folded plate structures together with almost unlimited range of possible cross-section arrangements. The structures carry the superimposed loads to the end diaphragms or gable frames through considerable bending action in the longitudinal direction. The tensile longitudinal stresses require a large amount of reinforcement and thus limit the longitudinal clear span of a reinforced concrete folded plate. There are two ways to overcome such difficulty. One method is to apply prestressing forces to folded plate structures[11] where possibility of cracking, tensile stresses and deflections can be significantly reduced. Another method is to utilize the fact that an arched construction can resist loads more effectively than a straight one. Therefore, an arched folded plate will be able to resist loads more effectively than a conventional straight folded plate. An attempt, using structural theories, to analyze such structure under the action

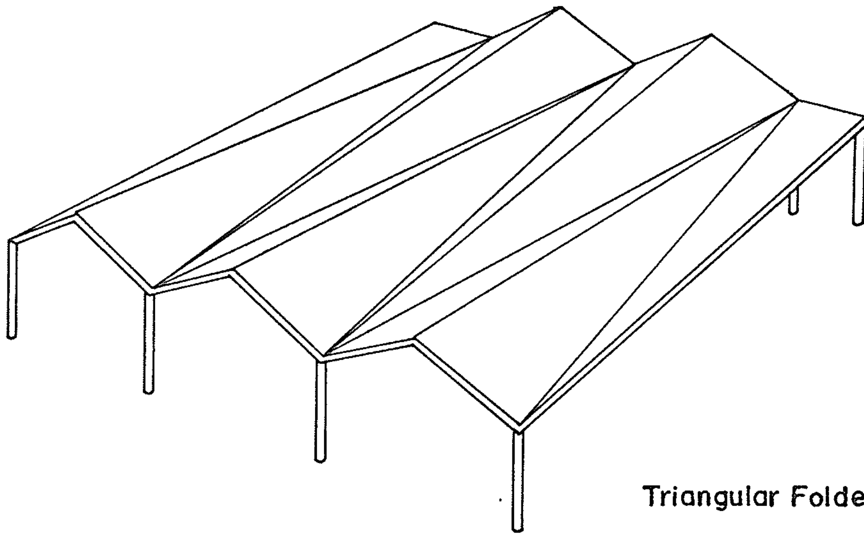

Triangular Folded Plate Structure

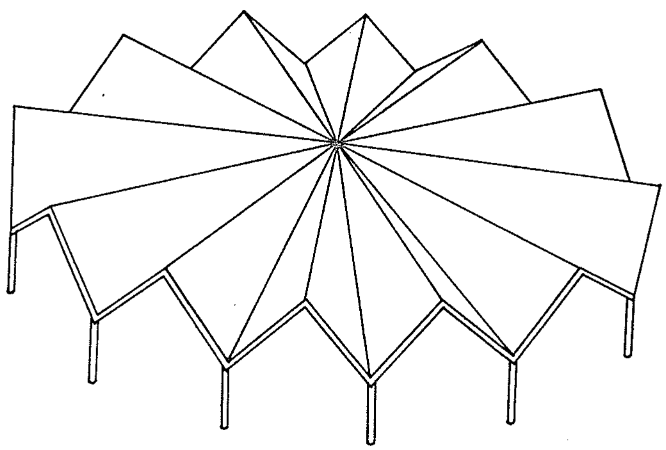

Umbrella Folded Plate Structure

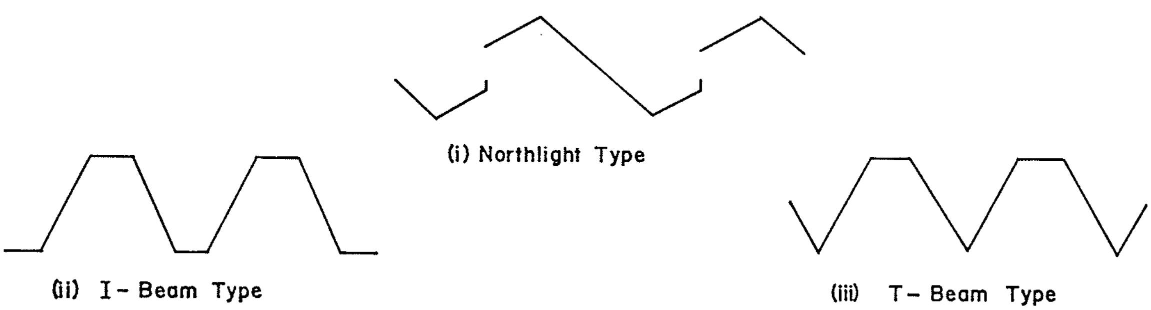

Typical Cross-Sections

Fig. 1.1 Typical Folded Plate Structures

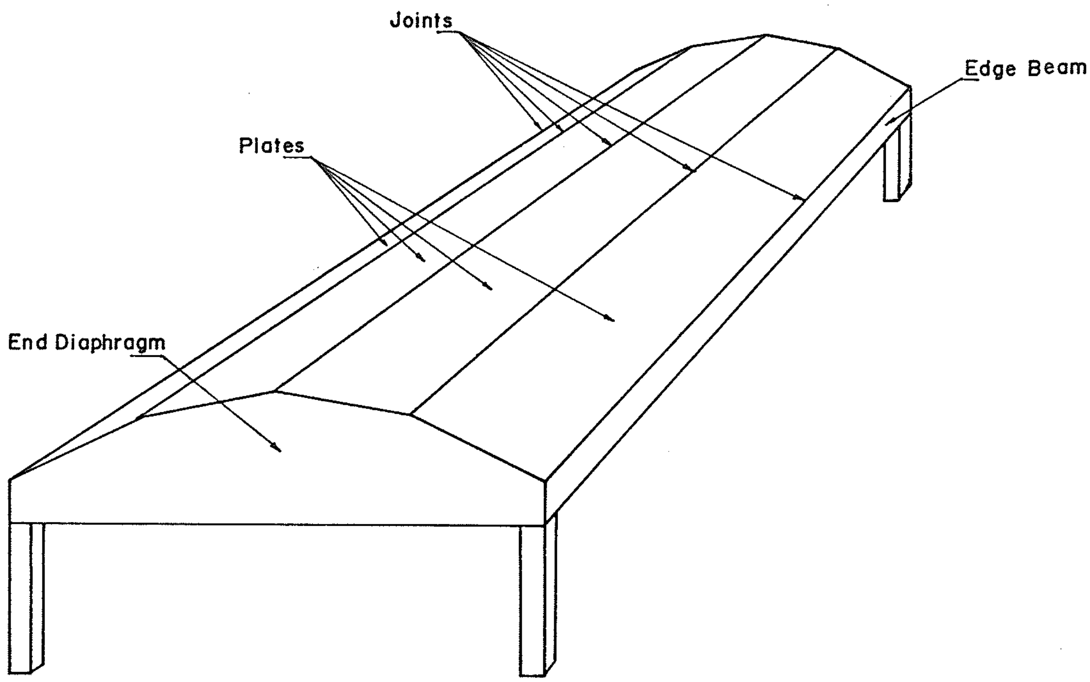

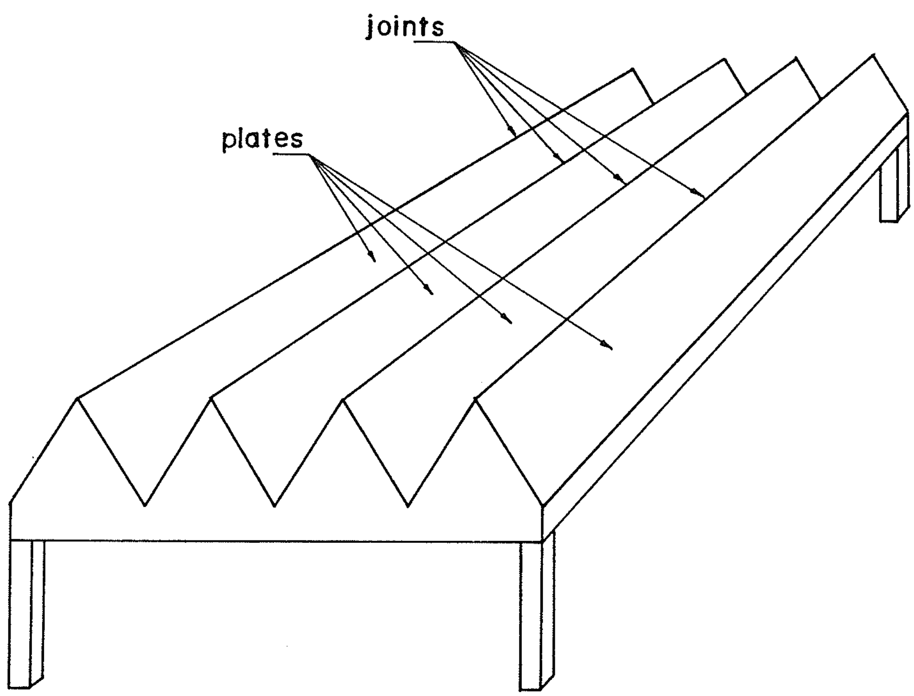

Fig. 1.1 Continued

of loads, becomes the main objective of this thesis.

1.2 Geometry and Previous Study

There are two distinct different types of arched folded plate structures. By translating a folded cross-section along a given curve, an arched folded plate of translation is formed (Figure 1.2a). However, by rotating a folded cross-section about a fixed line, an arched folded plate of revolution is formed (Figure 1.2b). Both structures have the strength characteristic of a double curvature shell and yet it is simple in forming due to the straight edges in one direction.

Since each unit of the arched folded plate of translation is an inclined straight line translating along a shallow curve, each unit can be analyzed as a translational shallow shell in the longitudinal direction. Using the governing equations of a general shallow shell given by K. Marguerre[12] and the Levy-type solution given by K. Apeland and E. Popov[13], the problem of an arched folded plate of translation, simply supported along the two transverse edges, has been solved by Shah and Lansdown[14].

Each unit of the arched folded plate of revolution is formed by rotating an inclined straight line about an axis. It can also be considered as a section from a circular cone shown in Figure 1.3a. The plan view of two inclined lines of rotation, which form such unit, is shown in Figure 1.3b. Since each unit of the arched folded plate of revolution is actually part of a circular cone, it can be analyzed by Shell theory. The solution is quite complex, and currently being examined. Only simply supported boundary condition along the two

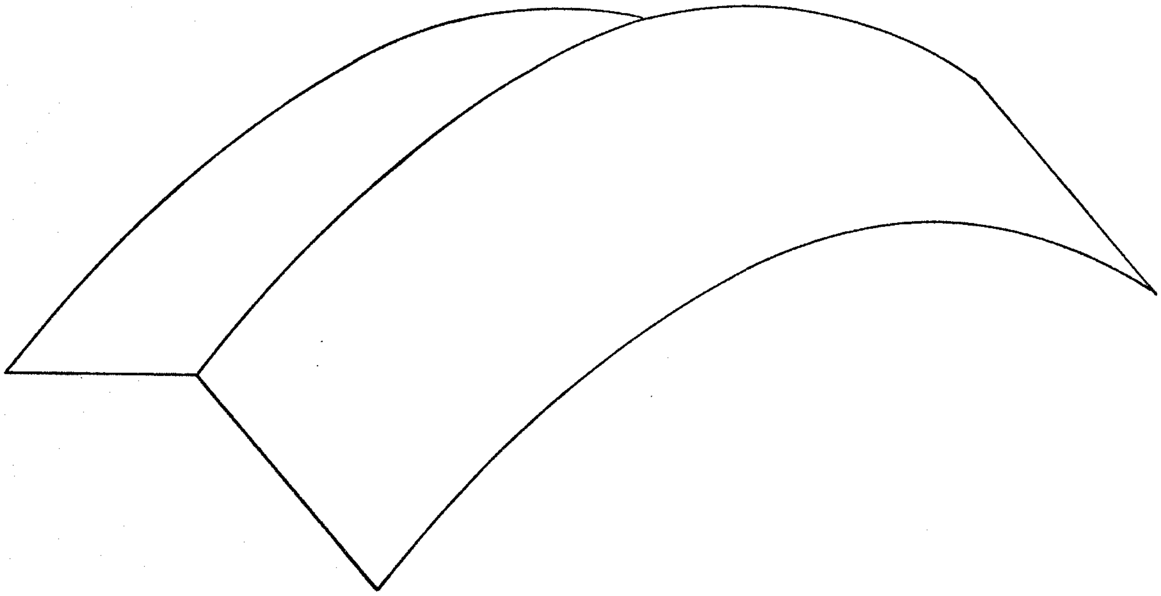

(a) Translational Type

(b) Rotational Type

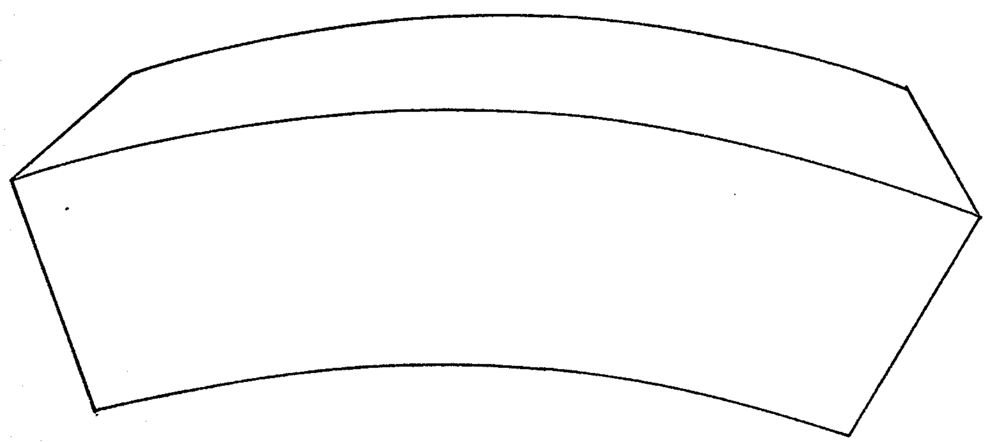

Fig. 1.2 Arched Folded Plate

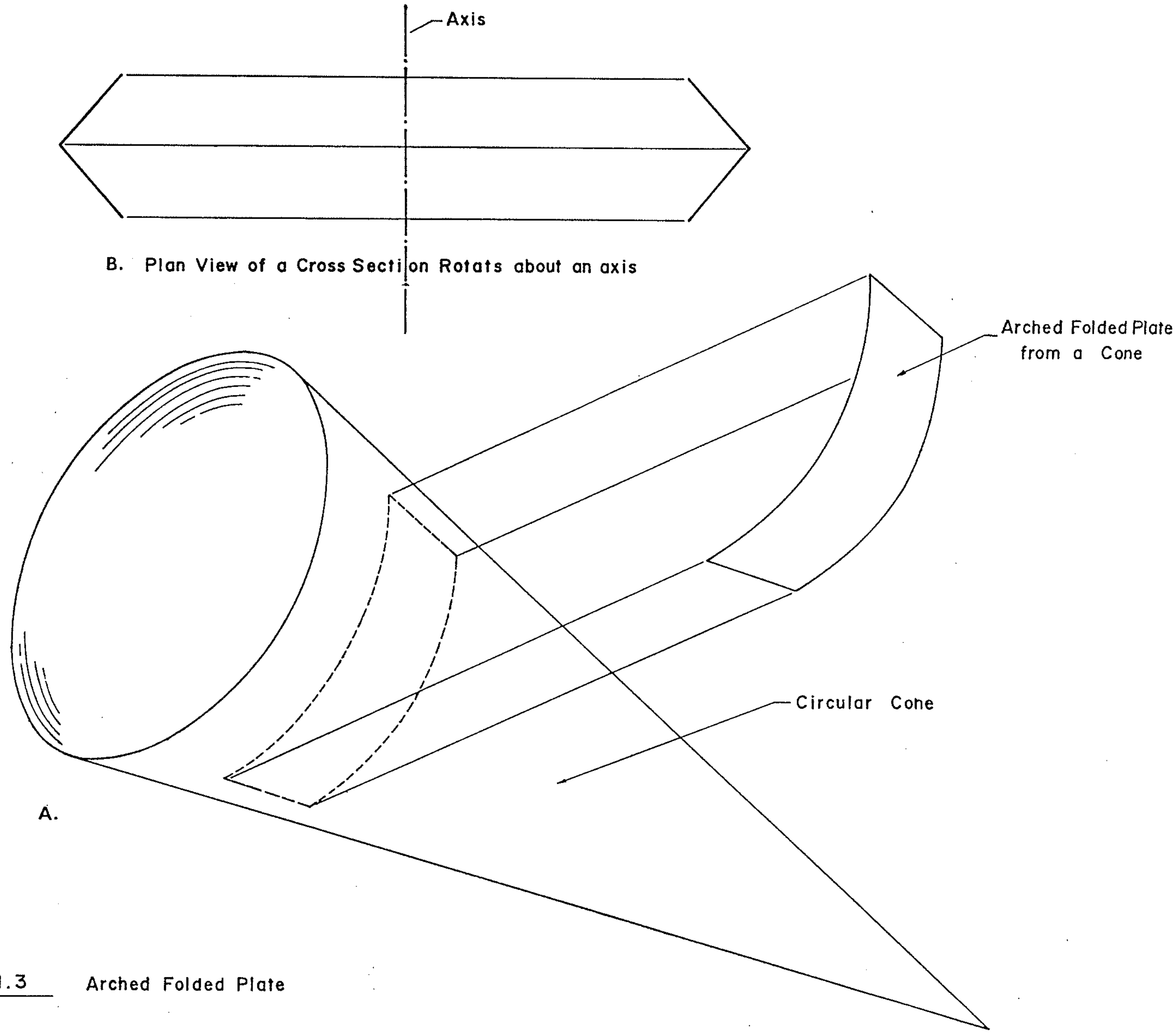

Fig. 1.3 Arched Folded Plate

transverse edges can be solved by any shell theory. This thesis, however, combines ordinary one dimensional structural theories for longitudinal action and moment distribution for transverse action, while ensuring compatibility between two folds, and can solve any boundary conditions along the transverse edges.

1.3 Assumptions and Limitations

In order to apply one-dimensional structural theories to arched folded plate structures (Figure 1.4), certain assumptions must be made. Limitations are thereby introduced in the applicability of the theory. Some basic assumptions similar to those in the conventional folded plate theory are:

(1) The material is elastic, isotropic, and homogeneous.

(2) The principle of superposition holds.

(3) The plates carry loads transversely only by bending normal to their planes (i.e. transverse continuous one-way slab action).

(4) The plates carry loads longitudinally by bending and axial force within their planes (i.e. longitudinal arch-curved beam action).

(5) The variation of longitudinal stress across the entire cross-section of each unit is planar. It varies linearly across the width and over the depth.

(6) Displacements due to axial forces, bending moments are considered.

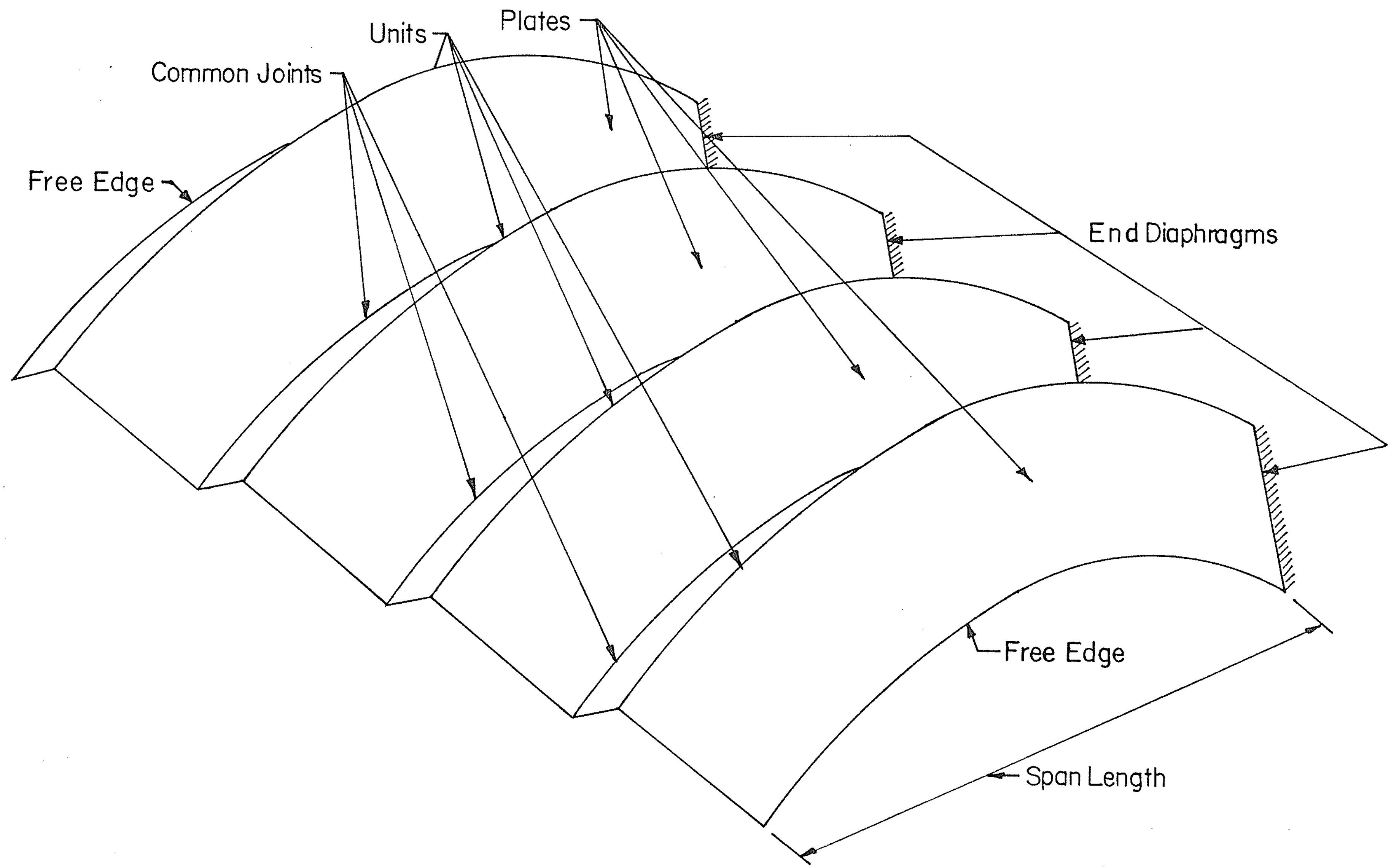

Figure 1.4 Arched Folded Plates Structure

(7) The longitudinal distribution of all loads on all units must be symmetrical.

(8) The cross-section of each unit is constant throughout its span length (i.e. prismatic arched folded plates).

Additional assumptions are:

(9) The arched folded plate is symmetrical in the longitudinal direction.

(10) The end supporting members along the two transverse edges must provide built-in boundary conditions.

(11) The open cross-section of each unit may have shapes other than the basic $\wedge$ shape.The ratio of the largest sectional dimension to the radius of curvature must be in the order of 1/10 or less. The ratio of span-width should be more than 5.

(12) Each unit can be subjected to inplane and out of plane loadings which can be forces or moments. Loadings within and normal to structure's plane of curvature are termed inplane and out of plane loads respectively.

(13) Individual unit possess torsional resistance. Torsional stresses due to twisting moments are ignored. Rotational deflections of the cross-section due to twisting are considered.

(14) Shear stresses in each cross-section have negligible effect on the deflection of the cross-section.

(15) The actual deflections are small compared to the overall configuration of the structure.

(16) The two outer longitudinal edges of the structure are assumed to be free of supports. It can be supported by edge beams which are considered as simple supports, but not without modification of the theory.

The limitations which the preceding assumptions impose are generally those associated with arch/curved beam theory and one-way slab action. Certain restrictions on the configuration of the structure are also introduced. It is noted that the theory herein is considered to be applicable to reinforced concrete (a nonhomogeneous material) and to structures composed of properly jointed prefabricated sections (initially discontinuous) for which, effectively, a homogeneous continuous structure results from the design. A further limitation, such as maintaining an angle between adjoining plates of not less than 15° and not more than 165° has been recommended by R. B. Moorman[15] in order to avoid violating the assumption of superposition.

1.4 Outline of the Method of Analysis

The theory of arched folded plates of revolution presented here considers the longitudinal action of each unit to be governed by arch and curved-beam theories, and the transverse action to be that of a continuous one-way slab. The procedure of analysis employed here is similar to those developed by D. Yitzhaki[16] in the conventional folded plate theory and subsequently adopted by D. Billington[17] in his book. This analysis is divided into the following three parts.

(1) Elementary Analysis (first presented in North America by M. Pei[4]) consisting of three separate analyses.

(a) Transverse Slab Analysis:

All surface loads are considered to be carried transversely to the joints by the plates acting as continuous one-way slabs. The interior joints are assumed unyielding along their entire span length. Moment-distribution can be used here to give transverse moments at the joints and the resulting reactions can be used in joint loads with the same longitudinal distribution as the loads. No longitudinal stresses are developed at this stage.

(b) Longitudinal Arch/Curved Beam Analysis:

The reactions from (a) are applied as loads which will be transmitted longitudinally to the end supporting diaphragms by each unit acting as an arch and as a curved beam. These vertical joint reactions must first be transferred to the shear center of every unit. Longitudinal hinges are then introduced along the joints to eliminate transverse moments. In addition, each unit is allowed to behave individually under load. The analysis is now separated into the following two steps.

(i) Circular Arch Analysis, in which the inplane loads are accounted for.

(ii) Curved Beam Analysis, in which the out of plane loads are taken care of.

Longitudinal stresses in each unit are developed from (i) and (ii). These stresses are initially determined on the assumption that each unit carries its loads and behaves independently of every other unit. Free-edge stresses in two separate units at a common joint are usually different. Cross-section deflections in each unit, computed on the same basis as longitudinal stresses, will also show that relative displacements exists between successive joints. The incompatibility cannot be allowed in the overall structure, and corrections must then be applied.

(2) Correction Analysis

The relative joint displacements in (b) violate the basic assumption of unyielding supports in (a). Self-equalized forces are applied at each common joint in order to correct such discrepancies. However, this will further introduce unequal longitudinal edge stresses. Equalized edge stresses can be obtained by the application of self-equalized shear correction forces, however this will destroy the displacement compatibility established previously.

An overall compatibility at every common joint can be established by using iteration technique. In this study, simultaneous equations are set up in such a way that the conditions of displacement and stress compatibility at each common joint are simultaneously satisfied.

(3) Superposition

The results of the elementary analysis (a) are combined with those of the correction analysis to give final forces, moments, stresses and displacements.

CHAPTER II

BENDING OF A CURVED BEAM

2.1 Introduction

Beams with curved axes under loads normal to the plane of their curvatures are classified as curved beams. The problem of bending of curved beams has been intensively investigated. Many well-known elasticians including Barré de Saint-Venant[19], H. Marcus[20] and A. J. S. Pippard[21] have made valuable contributions.

In this chapter a beam with circular axis is examined. The Saint-Venant's equations which relate displacements to forces are derived. By considering the equilibrium conditions of the beam, equilibrium equations are obtained. The expressions for forces, moments and displacements are presented for a variety of loadings.

2.2 Saint-Venant's Equations and Equations of Equilibrium[25]

Consider the cantilever curved beam having the constant cross-sectional properties shown in Figure 2.1. The beam has a local cartesian coordinates system xyz with the origin O at the centroid of the cross-section of the beam. The shear center S is assumed to coincide with the centroid. The x and y axes are in the directions of the principal axes of inertia of the cross-section, while the z-axis coincides with the tangent to the elastic line at O. The xz-plane also coincides with the plane of initial curvature of the beam. The positive directions of x, y, and z are defined as shown. The arc s is defined as the arc length of the center line measured from the fixed end. Other variables, which appear in Figure 2.1, are defined as follows:

M_x = bending moment acting on the cross-section at 0 about x-axis,

M_z = twisting moment at 0 about z-axis,

N_y = shear force in y direction,

v = centroid displacement in the direction of y-axis,

β = angle of twist of the cross-section about z-axis, counterclockwise rotation being positive,

ϕ = angle of twist per unit length at the same cross-section,

EI_{xx} = flexural rigidity,

K = torsional rigidity,

R = initial radius of curvature of the center line,

R_1 = radius of curvature of the deformed center line at 0 in the yz principal plane.

Furthermore, it is assumed that the effect of cross-sectional warping is negligible. The original plane section after twist is assumed to remain plane, such that the torsional rigidity could be calculated simply as the product of the torsional constant J and the shear modulus G_c of the material. Based on the above definitions and assumptions, the following equations can be derived,

$$\left.\begin{aligned} \frac{EI_{xx}}{R_1} &= M_x \\ K\phi &= M_z \end{aligned}\right\} \tag{2.1}$$

where, $K = G_c J$.

The radius of curvature R_1 and the twist ϕ must be expressed as functions of displacement v and the angle β. Small deflection theory implies that v and β will be small quantities. The final values of R_1 and ϕ are obtained by superimposing the separate effects produced on the beam by the linear displacement v and the angular displacement β.

If an element ds of a curved bar (Figure 2.2a) is subjected to a small displacement dv in the y-direction at a cross-section 0_1, the element will rotate with respect to the axis CO through an angle dv/ds. Due to this displacement, the axis CO_1 will displace into the new CO_2 axis. The angle 0_1CO_2 is equal to dv/R. The twist per unit length ϕ will be

$$(\phi)_1 = \frac{dv}{R} \times \frac{1}{ds} = \frac{dv}{Rds} \tag{2.2}$$

In addition, a displacement dv will also produce a new curvature $\frac{1}{R_1}$ of the center line of the beam in the yz plane, which will be given by

$$\left(\frac{1}{R_1}\right)_1 = - \frac{d^2v}{ds^2} \tag{2.3}$$

The same element is now subjected to a small angular displacement β (Figure 2.2b). The corresponding curvature will be given by

$$\left(\frac{1}{R_1}\right)_2 = \frac{\sin\beta}{R} \doteq \frac{\beta}{R} \tag{2.4}$$

The twist per unit length ϕ, produced by the angular displacement $d\beta$ will be

$$(\phi)_2 = \frac{d\beta}{ds} \tag{2.5}$$

Equation (2.4) is obtained by the following manipulations in Figure 2.3,

$$OO_1 = d, \quad CO = R, \quad d = R - R\cos\theta$$

$$v = d\sin\beta = (R - R\cos\theta)\sin\beta = R\sin\beta - R\cos\theta\sin\beta$$

$$\frac{dv}{d\theta} = R\sin\theta\sin\beta, \quad \frac{d^2v}{d\theta^2} = R\cos\theta\sin\beta$$

where, $ds = Rd\theta$.

Therefore, curvature $= \dfrac{d^2v}{ds^2} = \left.\dfrac{d^2v}{R^2d\theta^2}\right|_{d\theta \to 0}$

$$= \left.\frac{R\cos\theta\sin\beta}{R^2}\right|_{d\theta \to 0}$$

$$= \frac{\sin\beta}{R}$$

The summation of equations (2.2) and (2.5), equations (2.3) and (2.4) gives the following equations,

$$\left.\begin{aligned} \frac{1}{R_1} &= \frac{\beta}{R} - \frac{d^2v}{ds^2} \\ \phi &= \frac{d\beta}{ds} + \frac{dv}{Rds} \end{aligned}\right\} \tag{2.6}$$

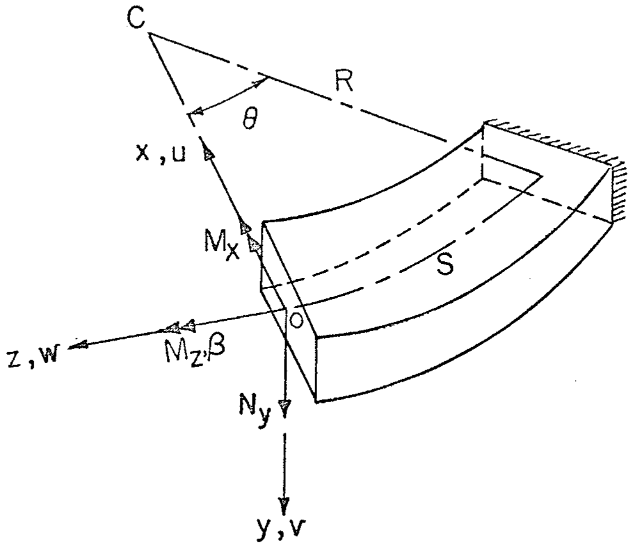

Figure 2.1 Internal Forces and Moments of a Curved Beam

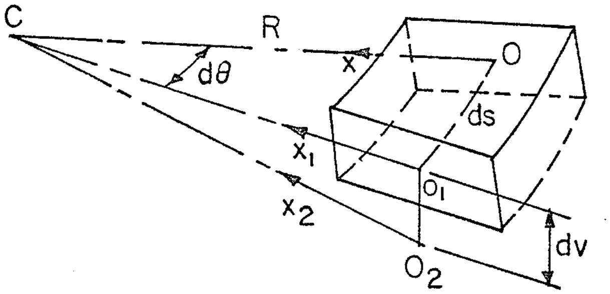

Figure 2.2 (a) Curved Beam Element subjected to dv

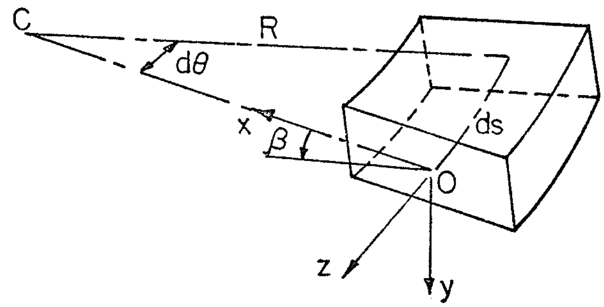

(b) Element subjected to β

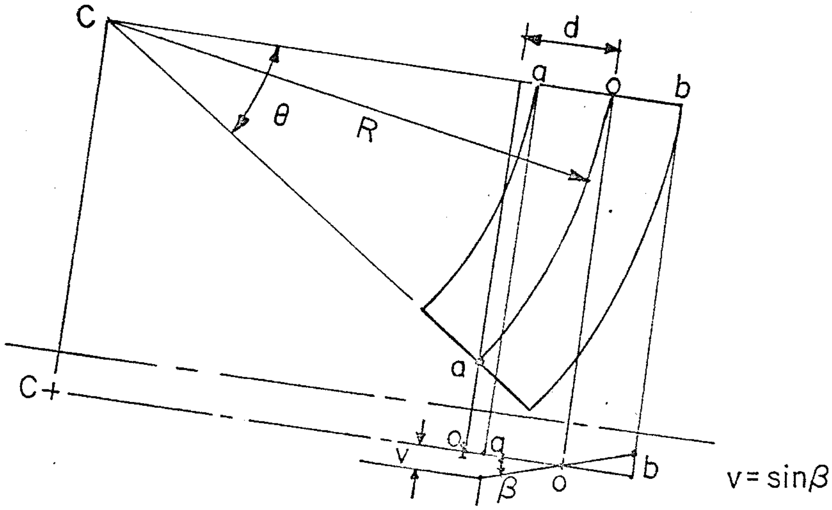

Figure 2.3. Plan View of Angular Displacement "β" Effect

By substituting equations (2.6) into equations (2.1), Saint-Venant's equations for a curved beam are derived, thus,

$$\left.\begin{aligned} M_x &= EI_{xx}\left(\frac{\beta}{R} - \frac{d^2v}{ds^2}\right) \\ M_z &= K\left(\frac{d\beta}{ds} + \frac{1}{R}\;\frac{dv}{ds}\right) \end{aligned}\right\} \qquad (2.7)$$

Figure 2.4 depicts an element of a curved beam ds in length with the stress resultants acting on the cut faces and the distributed loads applied along the elastic line. The positive signs are defined by the directions of all forces shown. The summation of force in the y-direction, give,

$$\frac{dN_y}{Rd\theta} = q_y \qquad (2.8)$$

The summation of moments about x and z directions respectively, is

$$N_y = \frac{1}{R}[M_x' + M_z] - m_x \qquad (2.9)$$

$$\frac{M_z'}{R} - \frac{M_x}{R} = - m_z \qquad (2.10)$$

where prime denotes differentiation with respect to θ.
By differentiating equation (2.9) with respect to θ and substitute into equations (2.8), give,

$$M_x'' + M_z' = Rm_x' + R^2q_y \qquad (2.11)$$

Thus, the resulting set of equilibrium equations is

$$\left.\begin{aligned} M_z' + M_x'' &= Rm_x' + R^2 q_y \\ M_z' - M_x &= -Rm_z \\ N_y &= \frac{1}{R}[M_x' + M_z] - m_x \end{aligned}\right\} \qquad (2.12)$$

Equations (2.7) and (2.12) are inapplicable for open cross-section curved beams where generally shear centers do not coincide with centroids. Complete derivation of such a theory for thin-walled, open section curved bars has been given by J. A. Cheney[22]. However, according to V. Z. Vlasov[23] equations (2.7) and (2.12) are still valid provided that beams have small initial curvature with the ratio of the largest sectional dimension to the radius of curvature of the order of 1/10 or less. The cross-sections must also be symmetrical in order to eliminate I_{xy}, the product of inertia.

In Vlasov's theory, the quantity of $\frac{a_x}{R}$ is neglected as compared to unity, where a_x is the coordinate of the shear center, and R is the radius of curvature of the centroidal axis. The stress resultant M_x is referred to the centroid, while the torsional moment M_z and shear N_y are referred to the shear center. All internal deflections and external applied loads are referred to the shear center. In deriving equations (2.12), all forces are referred to the centroidal axis, thus introducing some approximate characters.

In this thesis, Vlasov's equations are employed with the above-mentioned modifications.

2.3 Bending Of A Curved Beam Out Of It's Initial Plane

Equations (2.7) and (2.12) are ordinary linear differential equations. Exact solutions will depend upon the variations of the applied loads q_y, m_x and m_z. Furthermore, the following notations are adopted for the purpose of simplifying equations (2.7)

$$Y = \frac{v}{R} \qquad a = \frac{EI_{xx}}{R} \qquad \mu = \frac{K}{EI_{xx}} \tag{2.13}$$

Equations (2.7) then become

$$M_x = a\left(\beta - \frac{d^2y}{d\theta^2}\right) \qquad M_z = \mu a\left(\frac{d\beta}{d\theta} + \frac{dY}{d\theta}\right) \tag{2.14}$$

where the angle θ is measured from the bisector of the angle 2γ between the two points of support (Figure 2.5). The boundary conditions regardless of loading variations are assumed to be

$$\beta(\gamma) = \beta(-\gamma) = 0 \qquad Y(\gamma) = Y(-\gamma) = 0 \qquad \frac{dY(\gamma)}{d\theta} = \frac{dY(-\gamma)}{d\theta} = 0 \tag{2.15}$$

for clamped edges. Then, from equations (2.12), (2.14) and (2.15), solutions can be readily developed under a variety of loading variations.

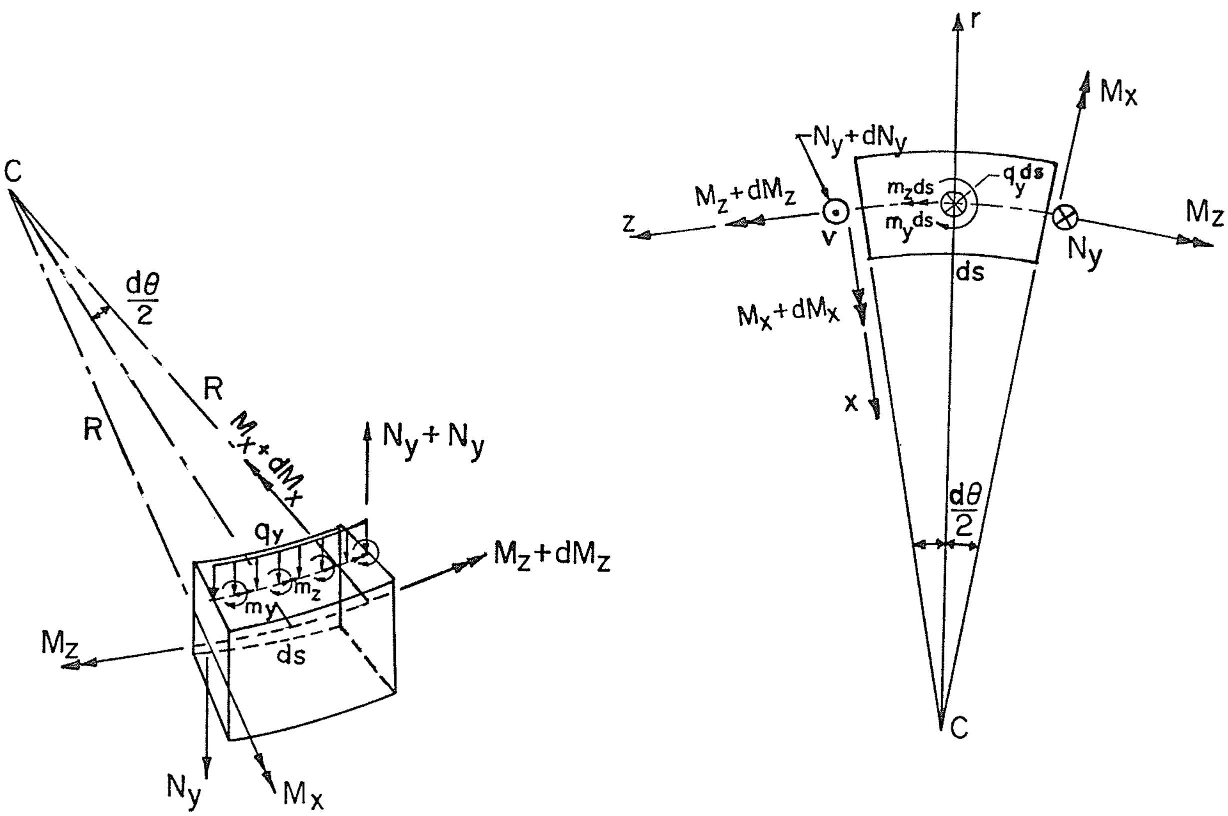

Figure 2.4. Forces and Moments on a curved Beam Element

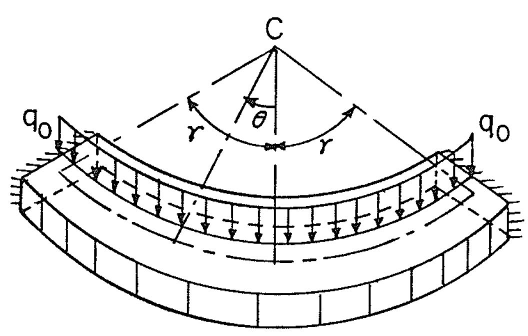

Figure 2.5 Built-in Curved Beam with u.d.l. shown

2.3.1 Beam Subjected to Loadings Having Cosine Variation ($n \neq 1$)

In this section, solutions of equations (2.12) are based on the assumption that beams are subjected to loadings having $\cos n\theta$ variation only. That is,

$$\left.\begin{aligned} q_y &= \Sigma H_n \cos n\theta \\ m_x &= \Sigma X_n \sin n\theta \\ m_x' &= \Sigma n X_n \cos n\theta \\ m_z &= \Sigma Z_n \cos n\theta \end{aligned}\right\} \quad \begin{array}{l}\text{where } H_n,\ X_n \text{ and } Z_n \text{ are the} \\ \text{magnitudes of each n value,} \\ \text{and } \Sigma = \sum\limits_{n=0,2,3,.....}\end{array} \tag{2.16}$$

Solutions are valid for each term of a complete harmonic series except for $n = 1$. A cosine variation is assumed for the loadings because it is a symmetrical function and thus satisfies the general assumptions in Chapter 1. Furthermore, by using the following notation,

$$\begin{aligned} A_n \cos n\theta &= R^2 H_n \cos n\theta \\ &\text{or} \\ A_n \cos n\theta &= nRX_n \cos n\theta \\ &\text{and} \\ B_n \cos n\theta &= -RZ_n \cos n\theta \end{aligned} \tag{2.17}$$

and q_y, m_x and m_z are in the positive direction, equations (2.12) become

$$\begin{aligned} M_z' + M_x'' &= A_n \cos n\theta \\ M_z' - M_x &= B_n \cos n\theta \\ N_y &= \frac{1}{R}(M_x' + M_z) - X_n \sin n\theta \end{aligned} \tag{2.18}$$

The complete solution of equations (2.14) and (2.18) using boundary condition equation (2.15) can be written as

$$M_x = C_1 \cos\theta + \frac{(A_n - B_n)}{1 - n^2} \cos n\theta \tag{2.19a}$$

$$M_z = C_1 \sin\theta + \frac{A_n - n^2 B_n}{1 - n^2} \frac{\sin n\theta}{n} \tag{2.19b}$$

$$N_y = \frac{A_n}{R} \frac{\sin n\theta}{n} - X_n \sin n\theta \tag{2.19c}$$

$$Y = C_2 + C_3 \cos\theta - \frac{C_1(1+\mu)}{2a\mu} \theta\sin\theta + \frac{B_n n^2(1+\mu) - A_n(1+n^2\mu)}{a\mu\,(n^2-1)^2} \cdot \left[\frac{\cos n\theta}{n^2} - \frac{1}{n^2}\right] \tag{2.19d}$$

$$\beta = -\left(\frac{C_1}{a\mu} + C_3\right)\cos\theta + \frac{C_1(1+\mu)}{2a\mu} \theta\sin\theta + \frac{A_n(1+\mu) - B_n(n^2+\mu)}{a\mu(n^2-1)^2} \cos n\theta \tag{2.19e}$$

where

$$C_1 = 2\left\{\frac{B_n n^2 - \frac{A_n(1+n^2\mu)}{1+\mu}}{(n^2-1)^2} \left(\sin\gamma\cos n\gamma - \cos\gamma\frac{\sin n\gamma}{n}\right) + \frac{(A_n - B_n)\mu}{(n^2-1)(1+\mu)} \sin\gamma\cos n\gamma\right\} \Big/ \left\{\frac{\mu-1}{1+\mu}\cos\gamma\sin\gamma + \gamma\right\} \tag{2.20a}$$

$$C_2 = \frac{1+\mu}{2a\mu}\left\{(\cos\gamma + \gamma\sin\gamma + \gamma\cos\gamma\cot\gamma)C_1 + 2\,\frac{B_n n^2 - \frac{A_n(1+n^2\mu)}{1+\mu}}{(n^2-1)^2} \cdot \left(\cot\gamma\,\frac{\sin n\gamma}{n} + \frac{1}{n^2} - \frac{\cos n\gamma}{n^2}\right)\right\} \tag{2.20b}$$

$$C_3 = -\frac{1+\mu}{2a\mu}\left\{(1+\gamma\cot\gamma)C_1 + 2\,\frac{B_n n^2 - \dfrac{A_n(1+n^2\mu)}{1+\mu}}{\sin\gamma(n^2-1)^2}\,\frac{\sin n\gamma}{n}\right\} \tag{2.20c}$$

For $n = 0$

$$\frac{\sin n\gamma}{n} = \gamma, \qquad \frac{\sin n\theta}{n} = \theta$$

$$\frac{1}{n^2} - \frac{\cos n\gamma}{n^2} = \frac{\gamma^2}{2}, \qquad \frac{\cos n\theta}{n^2} - \frac{1}{n^2} = -\frac{\theta^2}{2}$$

2.3.2 Beam Subjected To Loadings Having Cosine Variation (n = 1)

Equations (2.19's) in Section 2.3.1 do not hold for the case of $n = 1$. Solutions for such a case are presented in this section. In equations (2.12), the loading terms will be

$$\left.\begin{aligned} q_y &= H_1\cos\theta \\ m_x &= X_1\sin\theta \\ \therefore\ m_x' &= X_1\cos\theta \\ m_z &= Z_1\cos\theta \end{aligned}\right\} \tag{2.21}$$

where H_1, X_1 and Z_1 are the magnitudes for $n = 1$. Similar to Section 2.3.1, by using the notation

$$\begin{aligned} A_1\cos\theta &= R^2 H_1\cos\theta \\ &\text{or} \\ A_1\cos\theta &= R X_1\cos\theta \\ &\text{or} \\ B_1\cos\theta &= -R Z_1\cos\theta \end{aligned} \tag{2.22}$$

and q_y, m_x and m_z are in the positive direction, equations (2.12) become

$$\begin{aligned} M'_z + M''_x &= A_1 \cos\theta \\ M'_z - M_x &= B_1 \cos\theta \\ N_y &= \frac{1}{R}(M'_x + M_z) - X_1 \sin\theta \end{aligned} \tag{2.23}$$

Solutions of equations (2.23) are obtained by considering the effects of q_y, m_x and m_z separately. These effects can be combined using the superposition technique. The solution of equations (2.14), (2.15) and (2.23) with only A_1 considered, can be written as

$$M_x = (C_4 - \frac{A_1}{2})\cos\theta + \frac{A_1}{2}\,\theta\sin\theta \tag{2.24a}$$

$$M_z = C_4 \sin\theta - \frac{A_1}{2}\,\theta\cos\theta \tag{2.24b}$$

$$\begin{aligned} Y = C_6 + C_5 \cos\theta + \frac{1+\mu}{2a\mu}\left(\frac{A_1\mu}{1+\mu} - \frac{3A_1}{4} - C_4\right)\theta\sin\theta \\ + \frac{A_1(1+\mu)}{8a\mu}\,\theta^2\cos\theta \end{aligned} \tag{2.24c}$$

$$\begin{aligned} \beta = -\left(C_5 + \frac{C_4}{a\mu} + \frac{A_1}{2a\mu}\right)\cos\theta + \frac{1+\mu}{2a\mu}\left(C_4 - \frac{A_1}{4}\right)\theta\sin\theta \\ - \frac{A_1(1+\mu)}{8a\mu}\,\theta^2\cos\theta \end{aligned} \tag{2.24d}$$

where

$$C_4 = \left\{\frac{\sin\gamma(\cos\gamma + \gamma\sin\gamma) + \left(\frac{4\mu}{1+\mu} - 1\right)\gamma\cos^2\gamma}{\gamma + \cos\gamma\sin\gamma\,\left(1 - \frac{2}{1+\mu}\right)}\right\}\frac{A_1}{4} \tag{2.25a}$$

$$C_5 = \frac{1+\mu}{2a\mu}\{(\frac{A_1\mu}{1+\mu} - C_4)(1 + \gamma\cot\gamma) - \frac{A_1}{4}(3 + \gamma^2 + \gamma\cot\gamma)\} \tag{2.25b}$$

$$C_6 = \frac{1+\mu}{2a\mu}\{(C_4 - \frac{A_1\mu}{1+\mu})(\cos\gamma + \frac{\gamma}{\sin\gamma}) + \frac{A_1}{4}(3\cos\gamma + 3\gamma\sin\gamma + \gamma\cos\gamma\cot\gamma)\} \tag{2.25c}$$

The solution of equations (2.14), (2.15) and (2.23) with only B_1 considered, gives

$$M_x = C_7\cos\theta - \frac{B_1}{2}\theta\sin\theta \tag{2.26a}$$

$$M_z = (C_7 + \frac{B_1}{2})\sin\theta + \frac{B_1}{2}\theta\cos\theta \tag{2.26b}$$

$$Y = C_9 + C_8\cos\theta - \frac{1+\mu}{2a\mu}(C_7 - \frac{B_1}{4})\theta\sin\theta - \frac{B_1(1+\mu)}{8a\mu}\theta^2\cos\theta \tag{2.26c}$$

$$\beta = -(C_8 + \frac{C_7}{a\mu})\cos\theta + \frac{1+\mu}{2a\mu}(C_7 - \frac{B_1(\mu-3)}{4(1+\mu)})\theta\sin\theta + \frac{B_1(1+\mu)}{8a\mu}\theta^2\cos\theta \tag{2.26d}$$

where

$$C_7 = -\frac{B_1}{4}\{\frac{\cos\gamma(\gamma\cos\gamma-\sin\gamma) - \frac{\mu-3}{1+\mu}\gamma\sin^2\gamma}{\gamma + \frac{\mu-1}{1+\mu}\cos\gamma\sin\gamma}\} \tag{2.27a}$$

$$C_8 = -\frac{1+\mu}{2a\mu}\{C_7 - (1+\gamma^2)\frac{B_1}{4} + (C_7 + \frac{B_1}{4})\gamma\cot\gamma\} \tag{2.27b}$$

$$C_9 = \frac{1+\mu}{2a\mu}\{(\cos\gamma + \gamma\sin\gamma + \gamma\cos\gamma\cot\gamma)C_7 - (\cos\gamma + \gamma\sin\gamma - \gamma\cos\gamma\cot\gamma)\frac{B_1}{4}\} \tag{2.27c}$$

CHAPTER III

CIRCULAR ARCH THEORY

3.1 Introduction

The arch is a well-known fundamental structural unit. It can resist external loads more effectively than a straight beam because its resistance capacity is from internal axial compression as well as shear and moment. Two different theories have been developed to describe the structural behaviour of an arch. The General Arch Theory is subjected to approximations valid for the majority of structural arches. Most of the analysis techniques, namely, the unit load method, the elastic center method and the column analogy method, are governed by the above theory. The more exact theory which includes the effects of axial deformations is called a Deflection Theory[24]. Such theory is usually found to be nonlinear, and an exact solution is not yet available.

In this chapter, only the symmetrical circular arch is examined. The governing linear differential equations are obtained by considering the equilibrium conditions of a differential element. Forces and displacements relationships are derived from the stress-strain considerations. The exact solution of these equations is presented under certain boundary and loading conditions.

3.2 Governing Equations

It is assumed that the plane of curvature of the arch is also a plane of symmetry of the cross-section. External loads applied to the arch act only in this plane. Deformation, under such conditions, will also take place in this plane. Thus, the problem becomes a two-dimensional plane-strain problem. Furthermore, the principle of superposition and Navier's hypothesis is applicable. That is, the structure obeys the Hooke's Law, and a section that is plane before bending is plane afterwards. Finally, the small deformations are assumed.

The displacement functions are derived from the Euler-Bernoulli Beam Theory. Strain-strain relationships are established under the plane-strain condition. The moment and force equations are obtained by integrating over the entire cross-section.

In Figure 3.1, a differential element of a straight beam before and after deformation is shown. The deformed element has a radius of curvature ρ. The slope angle θ is considered to be small. The relation between θ and the displacement u is thus

$$\theta \simeq \tan\theta = \frac{\partial u}{\partial z} \tag{3.1}$$

The displacement functions for point c within the element given by Euler-Bernoulli, are

$$\begin{aligned} u(z,x) &= u(z) \\ w(z,x) &= w_0(z) + x\tan\theta = w_0(z) + xw_1(z) \end{aligned} \tag{3.2}$$

where

$$w_1 = \tan\theta = \frac{\partial u}{\partial z} \tag{3.3}$$

The same expression of equations (3.2) is extended to the elastic arch, where a small element is shown in Figure 3.2. The displacement functions thus become

$$\begin{aligned} u &= u(\theta) \\ w &= w_o(\theta) + xw_1 \\ v &= 0 \end{aligned} \tag{3.4}$$

The strain-displacement relationships expressed in polar coordinate are

$$\begin{aligned} \varepsilon_r &= \frac{\partial u}{\partial r} \qquad \varepsilon_\theta = \frac{1}{r}\frac{\partial w}{\partial \theta} + \frac{u}{r} \\ \gamma_{r\theta} &= \frac{\partial w}{\partial r} + \frac{1}{r}\frac{\partial u}{\partial \theta} - \frac{w}{r} \end{aligned} \tag{3.5}$$

Differentiating equations (3.4) with respect to r and θ, and substituting into equations (3.5), yields

$$\begin{aligned} \varepsilon_r &= \varepsilon_\xi = \gamma_{\theta\xi} = \gamma_{\xi r} = 0 \\ \varepsilon_\theta &= \frac{1}{r}\frac{dw_o}{d\theta} + \frac{x}{r}\frac{dw_1}{d\theta} + \frac{u}{r} \\ \gamma_{r\theta} &= \frac{1}{r}\frac{du}{d\theta} - \frac{w_o}{r} + \frac{R}{r}w_1 \end{aligned} \tag{3.6}$$

If shear strain is ignored, i.e. $\gamma_{r\theta} = 0$, Equations (3.6) give

$$w_1 = \frac{1}{R}\left(w_o - \frac{du}{d\theta}\right) \tag{3.7}$$

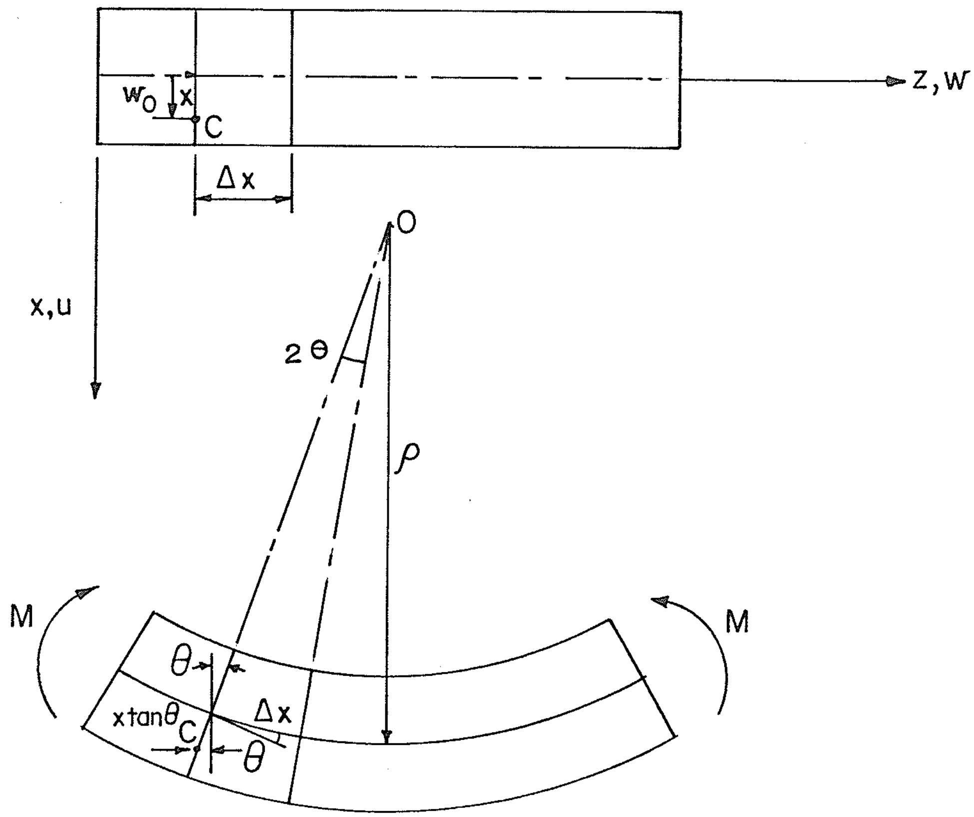

Figure 3.1 Euler - Bernouille Beam Element

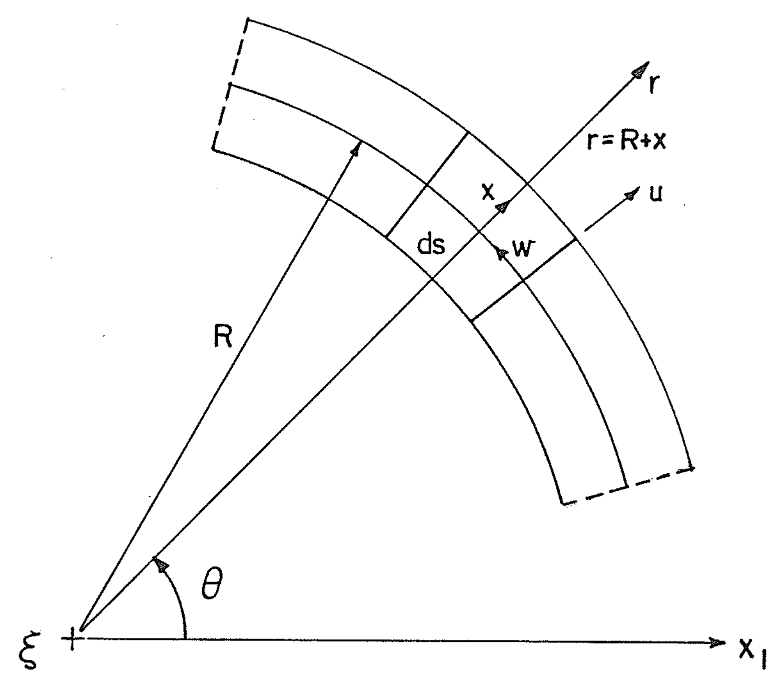

Figure 3.2 Circular Arch Element

Differentiating equation (3.7) with respect to θ and substituting into equations (3.6) yields

$$\frac{dw_1}{d\theta} = \frac{1}{R}\left(\frac{dw_o}{d\theta} - \frac{d^2u}{d\theta^2}\right) \tag{3.8}$$

$$\varepsilon_\theta = \frac{1}{R}\left[\left(u + \frac{dw_o}{d\theta}\right) + \frac{x}{R}\left(\frac{dw_o}{d\theta} - \frac{d^2u}{d\theta^2}\right)\right] \tag{3.9}$$

The theory of elasticity gives the following stress-strain relation as $\varepsilon_r = \varepsilon_\xi = 0$,

$$\sigma_\theta = E\varepsilon_\theta = \frac{E}{R}\left[\left(u + \frac{dw}{d\theta}\right) + \frac{x}{R}\left(\frac{dw}{d\theta} - \frac{d^2u}{d\theta^2}\right)\right] \tag{3.10}$$

The stress resultant N_θ and stress couple M_θ, defined as the normal force and bending moment acting on the cross-section, are the integrals of stress over the arch thickness.

$$\begin{aligned} N_z &= N_\theta = \int_A \sigma_\theta dA \\ M_y &= M_\theta = \int_A x\sigma_\theta dA \end{aligned} \tag{3.11}$$

The force-displacement relations are obtained by substituting equations (3.10) into (3.11),

$$N_z = \int_A \frac{E}{R}\left(u + \frac{dw}{d\theta}\right)dA + \int_A \frac{Ex}{R^2}\left(\frac{dw}{d\theta} - \frac{d^2u}{d\theta^2}\right)dA$$

$$= \frac{EA}{R}\left(u + \frac{dw}{d\theta}\right) \tag{3.12a}$$

$$M_y = \int_A \frac{xE}{R} (u + \frac{dw}{d\theta})dA + \int_A \frac{Ex^2}{R^2} (\frac{dw}{d\theta} - \frac{d^2u}{d\theta^2})dA$$

$$= \frac{EI_{yy}}{R^2} (\frac{dw}{d\theta} - \frac{d^2u}{d\theta^2}) \tag{3.12b}$$

where

$$\int_A xdA = 0$$

$$\int_A dA = A \text{ and } \int_A x^2 dA = I_{yy}$$

The governing differential equations are derived by considering the equilibrium conditions in a differential arch element as shown in Figure 3.3. The positive directions of all forces are defined as indicated. The summation of forces in the x and z directions give

$$\begin{aligned} \frac{1}{R} (N_z + N_x') &= q_x \\ N_x - N_z' &= Rq_z \end{aligned} \tag{3.13}$$

The summation of moment about y-direction yields

$$N_x = - \frac{M_y'}{R} + m_y \tag{3.14}$$

Differentiating equation (3.14) with respect to θ and substituting into equations (3.13), the equilibrium equation set can be written as

$$\begin{aligned} N_z - \frac{M_y''}{R} &= -m_y' + Rq_x \\ N_z' + \frac{M_y'}{R} &= -Rq_z + m_y \\ N_x &= - \frac{M_y'}{R} + m_y \end{aligned} \tag{3.15}$$

Again, equations (3.12) and (3.15) are not valid for open cross-section elastic arches. The more exact derivations will be those given by J. A. Cheney[22]. The approximate theory, proposed by V. Z. Vlasov[23] will again be used. All the related assumptions and recommendations will be followed as before.

3.3 Bending Of A Circular Fixed-Ends Arch

Equations (3.12) and (3.15) are ordinary linear differential equations for which exact solution can be found if the loading and boundary conditions are known. By using the following notation

$$k = \frac{EA}{R} \qquad \zeta = \frac{I_{yy}}{AR^2} \tag{3.16}$$

Equations (3.12) become

$$N_z = k\left(u + \frac{dw}{d\theta}\right) \qquad \frac{M_y}{R} = k\zeta\left(\frac{-d^2u}{d\theta^2} + \frac{dw}{d\theta}\right) \tag{3.17}$$

where the angle θ is measured from the bisector of the angle 2γ between the two supports (Figure 3.4). The built-in supports are described by the following boundary condition,

$$u(\gamma) = u(-\gamma) = 0 \qquad w(\gamma) = w(-\gamma) = 0 \qquad \frac{du}{d\theta}(\gamma) = \frac{du}{d\theta}(-\gamma) = 0 \tag{3.18}$$

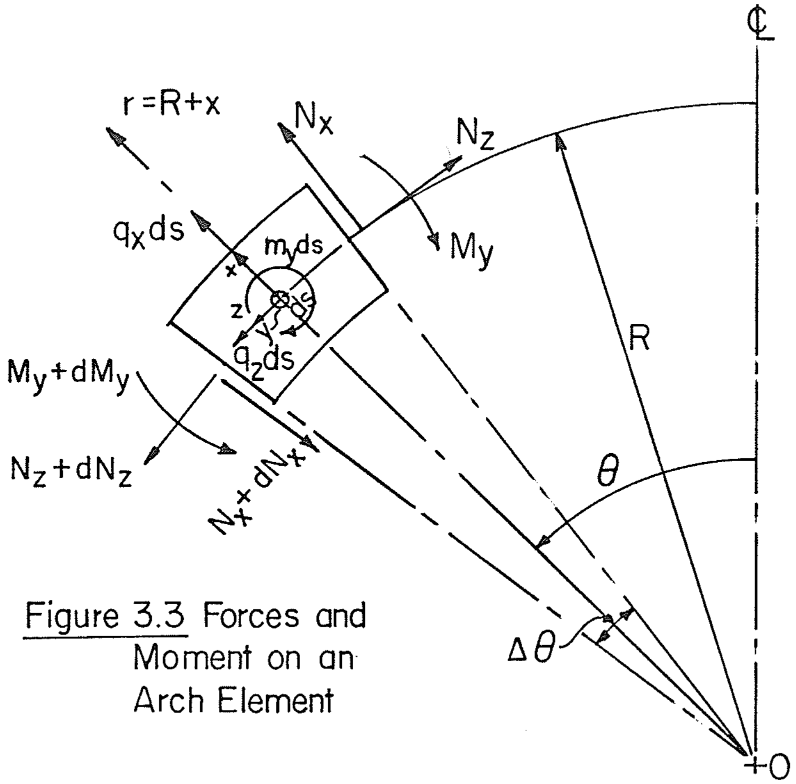

Figure 3.3 Forces and Moment on an Arch Element

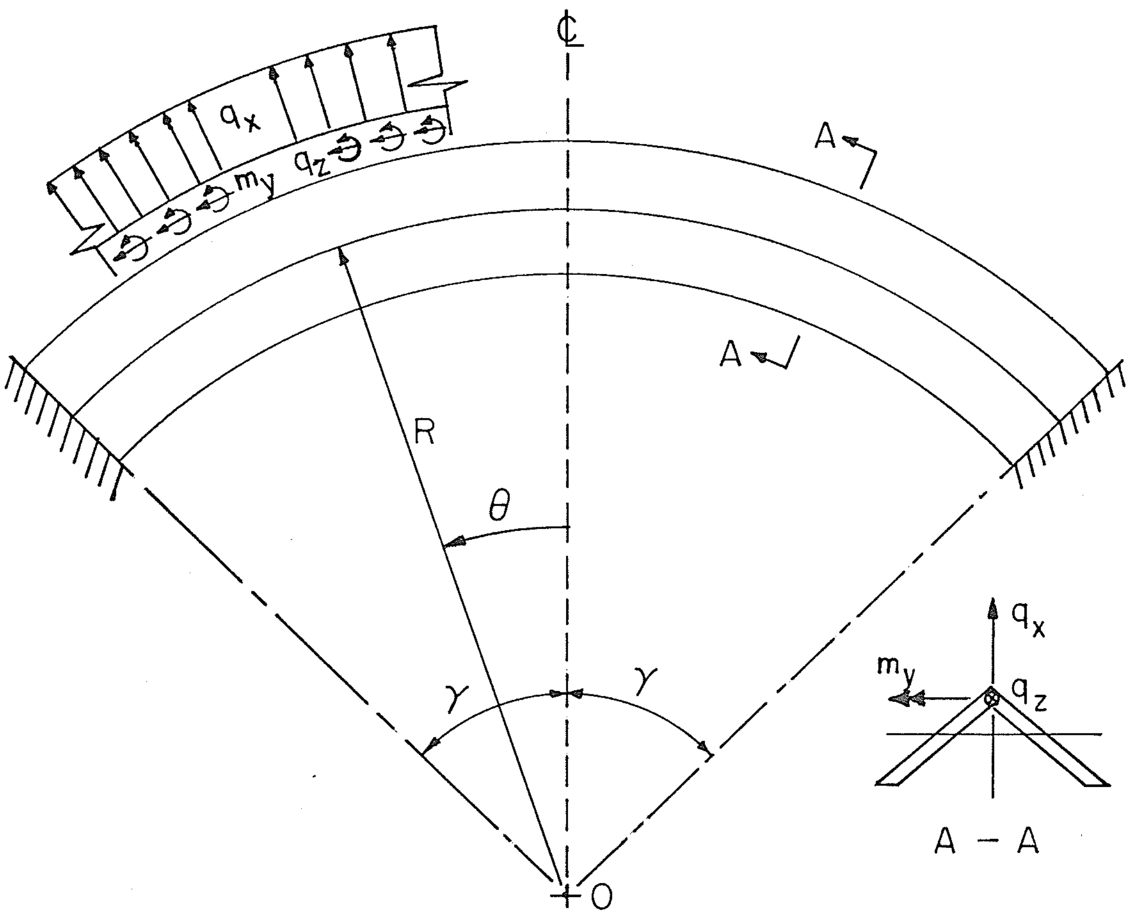

Figure 3.4 Fixed-End Circular Arch

3.3.1 Arch Subjected To Loading Having Sine and Cosine Variations ($n \neq 1$)

In this section, solutions of equations (3.15) are based on the assumption that the loading variations are cos$n\theta$ and sin$n\theta$. To be exact, the variation of q_x, q_z and m_y is

$$\left.\begin{aligned} q_x &= \Sigma V_n \cos n\theta \\ q_z &= \Sigma T_n \sin n\theta \\ m_y &= \Sigma U_n \sin n\theta \\ m_y' &= \Sigma n U_n \cos n\theta \end{aligned}\right\} \tag{3.19}$$

where V_n, T_n and U_n are the magnitudes for each n^{th} harmonic values. Solutions do not hold for the case of $n = 1$. Again, by using the notation

$$\begin{aligned} E_n \cos n\theta &= R V_n \cos n\theta \\ &\text{or} \\ E_n \cos n\theta &= -n U_n \cos n\theta \\ &\text{and} \\ F_n \sin n\theta &= (-R T_n + U_n) \sin n\theta \end{aligned} \tag{3.20}$$

where q_x, q_z and m_y are assumed in the positive direction, equations (3.15) become

$$\begin{aligned} N_z - \frac{M_y''}{R} &= E_n \cos n\theta \\ N_z' + \frac{M_y'}{R} &= F_n \sin n\theta \\ N_x &= -\frac{M_y'}{R} + U_n \sin n\theta \end{aligned} \tag{3.21}$$

The effects of any combinations of q_x, q_z and m_y can be found by superposition.

The complete solution of equations (3.17) and (3.21), using boundary conditions equations (3.18) can be written as

$$N_z = D_1 \cos\theta + \frac{(nF_n + E_n)}{1 - n^2} \cos n\theta \tag{3.22a}$$

$$\frac{M_y}{R} = D_3 - D_1 \cos\theta - \left(\frac{F_n}{n} + \frac{nF_n + E_n}{1 - n^2}\right)\cos n\theta \tag{3.22b}$$

$$N_x = U_n \sin n\theta - D_1 \sin\theta - \frac{n(nF_n + E_n)}{1 - n^2} \sin n\theta - F_n \sin n\theta \tag{3.22c}$$

$$u = -\frac{D_3}{k\zeta} + D_2 \cos\theta + \frac{D_1(1+\zeta)}{2k\zeta}\theta\sin\theta + \frac{1+\zeta}{k\zeta}\left(\frac{E_n}{(1-n^2)^2} + \frac{F_n(1+n^2\zeta)}{n(1+\zeta)(1-n^2)^2}\right)\cos n\theta \tag{3.22d}$$

$$w = \frac{D_3}{k\zeta}\theta + \left[\frac{D_1(\zeta-1)}{2k\zeta} - D_2\right]\sin\theta + \frac{D_1(1+\zeta)}{2k\zeta}\theta\cos\theta + \frac{1+\zeta}{k\zeta}\left[\frac{(nF_n+E_n)\zeta}{(1+\zeta)(1-n^2)} - \frac{E_n}{(1-n^2)^2} - \frac{F_n(1+n^2\zeta)}{n(1+\zeta)(1-n^2)^2}\right]\frac{\sin n\theta}{n} \tag{3.22e}$$

where

$$D_1 = 2\left\{\frac{\left[\frac{E_n}{(1-n^2)^2} + \frac{F_n(1+n^2\zeta)}{n(1+\zeta)(1-n^2)^2}\right]\left[\frac{\sin n\gamma}{n} - n\sin n\gamma - \gamma\cos n\gamma + n\gamma\cot\gamma\sin n\gamma\right]}{\gamma\cos\gamma + \gamma^2\sin\gamma + \gamma^2\cos\gamma\cot\gamma - \frac{2\sin\gamma}{1+\zeta}} - \frac{\frac{(nF_n+E_n)}{(1+\zeta)(1-n^2)}\;\frac{\sin n\gamma}{n}}{\gamma\cos\gamma + \gamma^2\sin\gamma + \gamma^2\cos\gamma\cot\gamma - \frac{2\sin\gamma}{1+\zeta}}\right\} \tag{3.23a}$$

$$D_2 = \frac{1+\zeta}{2k\zeta}\{[1+\cot\gamma]\, D_1 - 2\,\frac{nE_n + \frac{F_n(1+n^2\zeta)}{1+\zeta}}{(1-n^2)^2}\,\frac{\sin n\gamma}{\sin\gamma}\} \qquad (3.23b)$$

$$D_3 = \frac{1+\zeta}{2}\{[\cos\gamma + \gamma\sin\gamma + \gamma\cos\gamma\cot\gamma]\, D_1 + 2[\frac{E_n}{(1-n^2)^2} +$$

$$\frac{F_n(1+n^2\zeta)}{n(1+\zeta)(1-n^2)^2}]\cos n\gamma - 2\,\frac{nE_n + F_n\frac{1+n^2\zeta}{1+\zeta}}{(1-n^2)^2}\cot\gamma\sin n\gamma\} \qquad (3.23c)$$

For n = 0,

$$F_n = 0, \quad \frac{F_n}{n} = 0$$

$$\frac{\sin n\gamma}{n} = \gamma$$

$$\frac{\sin n\theta}{n} = \theta$$

3.3.2 Arch Subjected To Loadings Having Sine and Cosine Variations (n = 1)

In this section, solution of equations (3.15) for the case of n = 1 is presented. The variation assumed for q_x, q_z and m_y is

$$\left.\begin{aligned} q_x &= V_1\cos\theta \\ q_z &= T_1\sin\theta \\ m_y &= U_1\sin\theta \\ m_y' &= U_1\cos\theta \end{aligned}\right\} \qquad (3.24)$$

where V_1, T_1 and U_1 are magnitudes for n = 1. By using the notation

$$E_1\cos\theta = RV_1\cos\theta$$
or
$$E_1\cos\theta = -U_1\cos\theta \qquad (3.25)$$
and
$$F_1\sin\theta = (-RT_1 + U_1)\sin\theta$$

where q_x, q_z and m_y are assumed in the positive direction, equations (3.15) become

$$N_z - \frac{M''_y}{R} = E_1\cos\theta$$
$$N_z + \frac{M'_y}{R} = F_1\sin\theta \qquad (3.26)$$
$$N_x = -\frac{M'_y}{R} + U_1\sin\theta$$

The effects of any combination of q_x, q_z and m_y can be found by superimposing the individual effects.

The complete solution of equations (3.26) and (3.17), using boundary conditions equations (3.18), can be written as

$$N_z = D_{10}\cos\theta - D_{11}\theta\sin\theta \qquad (3.27a)$$

$$M_y = D_{14} + D_{15}\cos\theta + D_{16}\theta\sin\theta \qquad (3.27b)$$

$$N_x = -D_{12}\sin\theta - D_{13}\theta\cos\theta + U_1\sin\theta \qquad (3.27c)$$

$$u = D_7 + D_8\cos\theta + D_9\theta\sin\theta + \frac{K_2}{8}\theta^2\cos\theta \qquad (3.27d)$$

$$w = D_6\theta + D_5\sin\theta + D_4\theta\cos\theta + \frac{K_1}{8}\theta^2\sin\theta \qquad (3.27e)$$

where

$$L_1 = -\frac{E_1}{R}, \qquad L_2 = -\frac{F_1}{R} \qquad (3.28a)$$

$$L_3 = -E(AL_1 + AL_2 + \frac{I_{yy}L_1}{R^2} + \frac{I_{yy}L_2}{R^2}),\quad L_4 = -L_3 \tag{3.28b}$$

$$K_1 = \frac{L_3R^4}{E^2AI_{yy}}, \qquad K_2 = \frac{L_4R^4}{E^2AI_{yy}} \tag{3.28c}$$

$$B_1 = \frac{I_{yy}}{R^2} - A, \qquad B_2 = \frac{I_{yy}}{R^2} + A \tag{3.28d}$$

and

$$D_4 = \frac{1}{[(\frac{B_1}{B_2} -1) + \gamma^2 + (1+\gamma\cot\gamma)\gamma\cot\gamma]}\{\frac{L_1R^2}{EB_2} + K_2[(\frac{B_1}{B_2^2} - \frac{3}{4B_2})\frac{I_{yy}}{R^2} + (\gamma^2\cot^2\gamma + \gamma^2 - 1)\frac{B_1}{4B_2} + (1-\gamma\cot\gamma)\frac{\gamma\cot\gamma}{4}\} \tag{3.29a}$$

$$D_5 = (\frac{B_1}{B_2} -1-\gamma\cot\gamma)\ D_4 - \frac{L_1R^2}{EB_2} + K_2[(\frac{3}{4B_2} - \frac{B_1}{B_2^2})\frac{I_{yy}}{R^2} + \frac{B_1}{4B_2} - \frac{\gamma\cot\gamma}{4} + \frac{\gamma^2}{8} + \frac{B_1}{4B_2}\ \gamma\cot\gamma] \tag{3.29b}$$

$$D_6 = (\cos\gamma+\gamma\sin\gamma+\gamma\cos\gamma\cot\gamma)(D_4 - \frac{B_1K_2}{4B_2}) + \frac{\gamma\cos\gamma\cot\gamma}{4}K_2 \tag{3.29c}$$

$$D_7 = -D_6 \tag{3.29d}$$

$$D_8 = (1+\gamma\cot\gamma)\ D_4 + [(\cot\gamma - \frac{\gamma}{2})\frac{\gamma}{4} - (1+\gamma\cot\gamma)\frac{B_1}{4B_2}]K_2 \tag{3.29e}$$

$$D_9 = D_4 - \frac{B_1}{4B_2}\ K_2 \tag{3.29f}$$

$$D_{10} = \frac{EA}{R}\left[\left(1+\frac{B_1}{B_2}\right) D_4 - \frac{L_1R^2}{EB_2} + \left(\frac{3}{4B_2} - \frac{B_1}{B_2^2}\right)\frac{I_{yy}K_2}{R^2}\right] \tag{3.29g}$$

$$D_{11} = \frac{EAK_2}{4R}\left(1 + \frac{B_1}{B_2}\right) \tag{3.29h}$$

$$D_{12} = \frac{EI_{yy}}{R^3}\left[\left(1-\frac{B_1}{B_2}\right) D_4 + \frac{L_1R^2}{EB_2} + \left(\frac{1}{2} - \frac{3B_1}{4B_2} - \frac{3I_{yy}}{4B_2R^2} + \frac{B_1I_{yy}}{B_2^2R^2}\right) K_2\right] \tag{3.29i}$$

$$D_{13} = \frac{EI_{yy}K_2}{4R^3}\left(1-\frac{B_1}{B_2}\right) \tag{3.29j}$$

$$D_{14} = \frac{EI_{yy}}{R^2} D_6 \tag{3.29k}$$

$$D_{15} = \frac{EI_{yy}}{R^2}\left[\left(\frac{B_1}{B_2} - 1\right) D_4 - \frac{L_1R^2}{EB_2} + \left(\frac{3I_{yy}}{4B_2R^2} - \frac{B_1I_{yy}}{B_2^2R^2} + \frac{B_1}{2B_2} - \frac{1}{4}\right) K_2\right] \tag{3.29l}$$

$$D_{16} = \frac{EI_{yy}K_2}{4R^2}\left(1 - \frac{B_1}{B_2}\right) \tag{3.29m}$$

CHAPTER IV

METHOD OF ANALYSIS

4.1 Introduction

This chapter deals with the analysis of arched folded plates of revolution on simple spans. Such structures are composed of folds in the transverse direction, where each fold is symmetric and arches along the longitudinal direction. All folds are connected monolithically to each other along the common edges in order to develop the spatial rigidity of the components parts. The structure thus can be considered as:

(a) a continuous one-way slab spanning transversely between joints, and

(b) a series of open-section curved beams spanning longitudinally between end supports.

The analytical procedure presented in this chapter actually consists of three separate analyses:

(1) Elementary transverse slab analysis, in which all surface loads are assumed to be carried transversely to the joints by one-way slab bending only.

(2) Arch and curved-beam analyses for joint loads, in which the joint reactions from (1) are applied as

loads to the combined arch-curved beam system.

(3) Correction analysis, in which correction forces are determined and compatibility between two folds is ensured.

4.2 Elementary Transverse Slab Analysis

The objective of this analysis is to transform surface loads into the forms of joint loads and joint moments.

Roof structure is usually subjected to uniformly distributed surface loadings. At any unit transverse cross-sections, the system can be considered as a continuous one-way slab (Figure 4.1a) Since the structure is prismatic, such cross-section will be the same everywhere. Fictitious supports are placed at every joint along the entire span length in order to develop joint reactions (Figure 4.2b). Elementary transverse slab analysis is performed by analyzing the continuous one-way slab for the transverse distributed loads. The moment distribution technique may be used to compute the transverse moments $\overline{M}_j$ and the reactions $\overline{R}_j$ at each joint. Typical results of the transverse slab analysis is shown in Figure 4.1c.

The transverse reinforcement patterns will be designed according to the magnitude of the final transverse slab bending moments. The joint reactions will be applied as joint loads. There are no longitudinal stresses developed from this analysis.

Figure 4.1

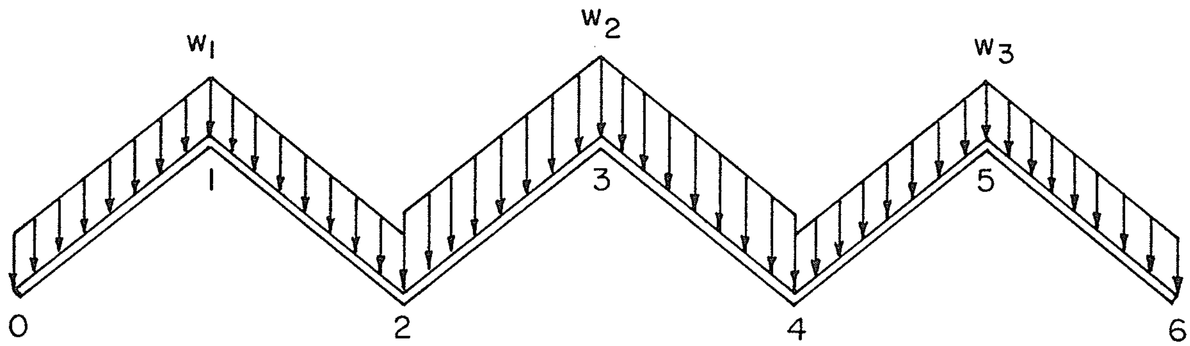

(a) Typical Transverse Cross-Section with u.d.L.

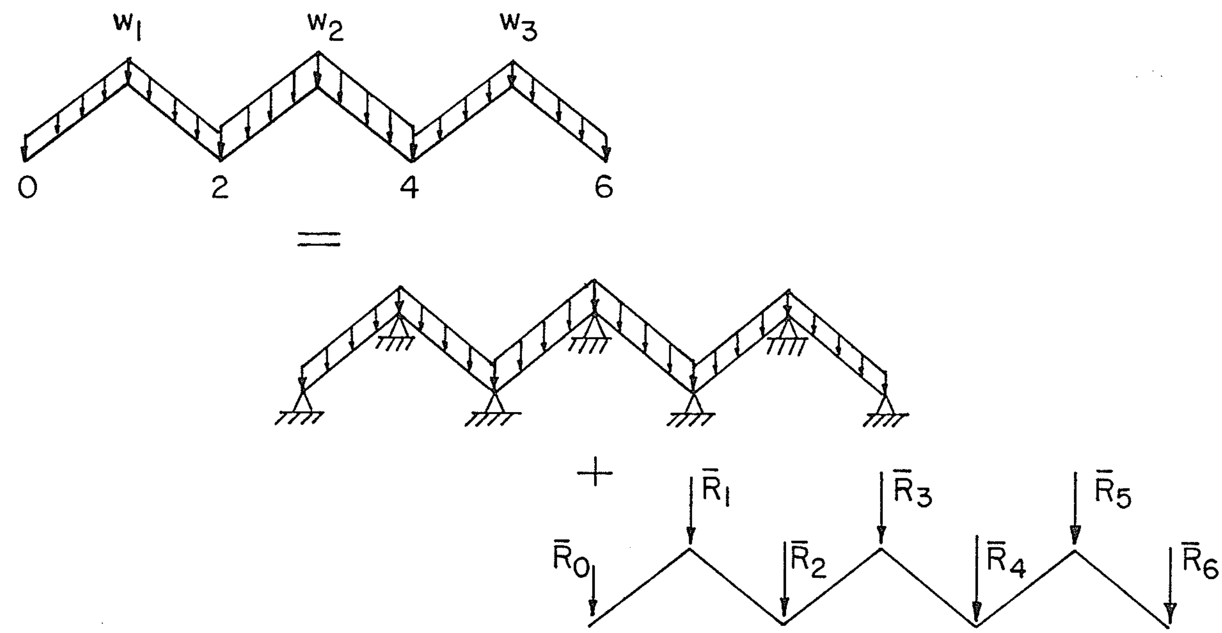

(b) The Principle of Fictitous Supports

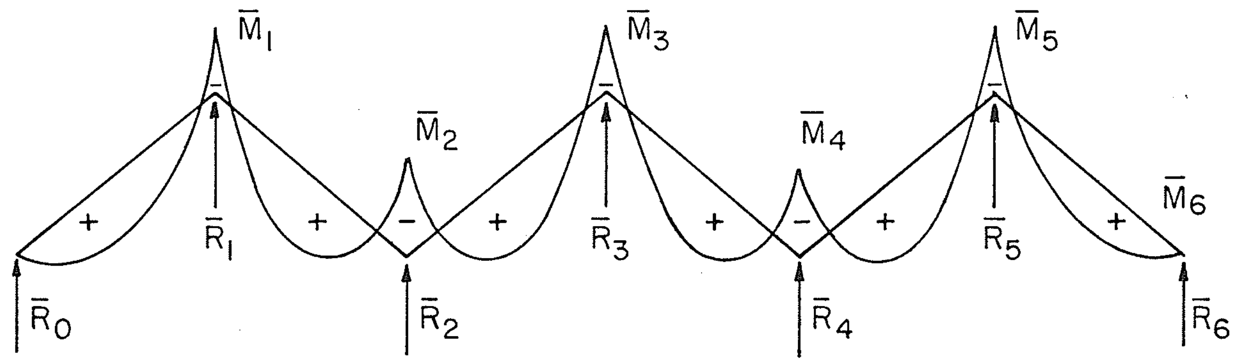

(c) Typical Transverse Slab Analysis Results

4.3 Longitudinal Arch and Curved-Beam Analysis

The joint reactions developed in section 4.2 are transmitted to the end supports by the combined arch and curved-beam system. The analysis is carried out by considering first, the Primary System, where longitudinal hinges are introduced along all interior joints to eliminate transverse joint moments and allow each folded unit to rotate freely. This primary system, however, is not statically determinate, and is not yet ready to be analyzed, therefore, the following steps are necessary.

(a) The joint loads $\overline{R}_j$ are resolved into inplane forces F_j only at the common interior joints between two folds where the joint j occurs between plates j and j+1 (Figure 4.2a). F_j can be obtained by the geometric relationships:

$$F_j^{\ell} = \overline{R}_j \frac{\cos\psi_{j+1}}{\sin\alpha_j} \quad \text{or} \tag{4.1a}$$

$$F_j^{r} = -\overline{R}_j \frac{\cos\psi_j}{\sin\alpha_j} \tag{4.1b}$$

where equation (4.1a) is applied to the plate to the left of joint j and equation (4.1b) to the right of joint j. The joint loads are positive downward, plate forces are positive from right to left. The angle ψ_j, representing the slope of plate j with the horizontal, is measured counterclockwise from the horizontal at the left joint. The angle α_j is measured clockwise from the continuation of plate j and j+1 (Figure 4.2b).

After joint loads are resolved into inplane forces at all the common joints, the primary system can be divided into a series of subsystems. Each primary subsystem consists of individual folded unit and is allowed to behave separately as an arch and curved beam. To make these subsystems applicable to the solutions derived in Chapters 2 and 3, inplane forces in each unit must be transferred to the shear centers. In Figure 4.2c, Q_j and P_j are the sum of forces in the vertical and horizontal directions, and Z_j is the moments sum at the shear center of unit j. From here on, only the interior common joints between folds are numbered, where the joint j now occurs between folds j-1 and j.

(b) Each primary subsystem subjected to loading Q_j is considered as an arch, and while subjected to P_j snd Z_j is considered as a curved beam. Loadings Q_j, P_j and Z_j have the same longitudinal variation as the joint loads $\overline{R}_j$ and hence the same as the external surface loads, i.e.,

$$(\overline{R}_j)_\theta \sim (Q_j)_\theta, (P_j)_\theta, (Z_j)_\theta = W(\theta)$$

which in the case of uniform loading is a constant.

The resulting internal forces and displacements for each subsystem can be obtained from the solutions in Section 2.3.1 and 3.3.1 for the case n=0 (Figure 4.3a). The longitudinal edge stresses are obtained from the internal forces at a cross-section by the simple flexural theory where tensile stress is taken as positive.

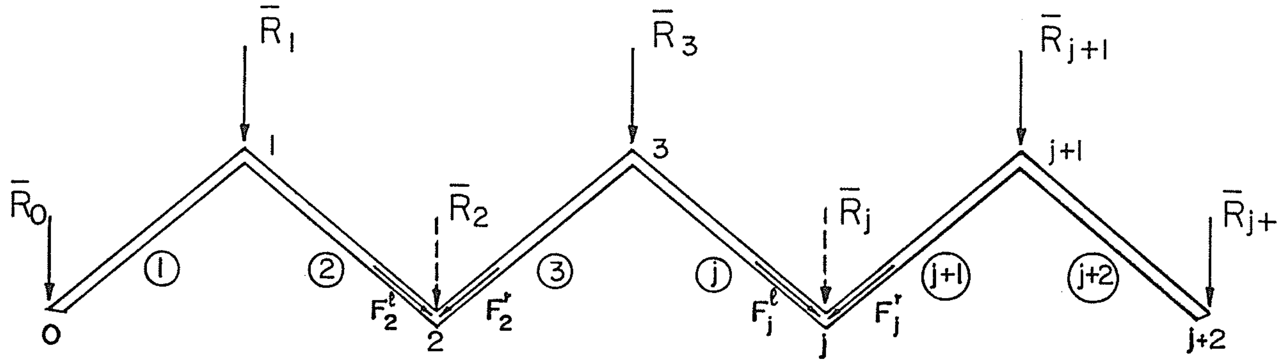

Figure 4.2 (a) Joint Loads Resolved into Inplane Forces

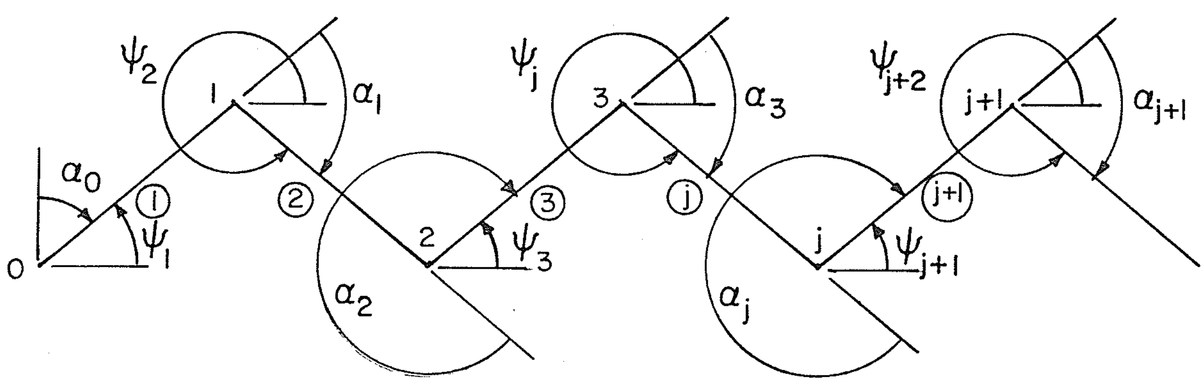

Figure 4.2 (b) Symbols and Orientations of a Transverse Cross-Section

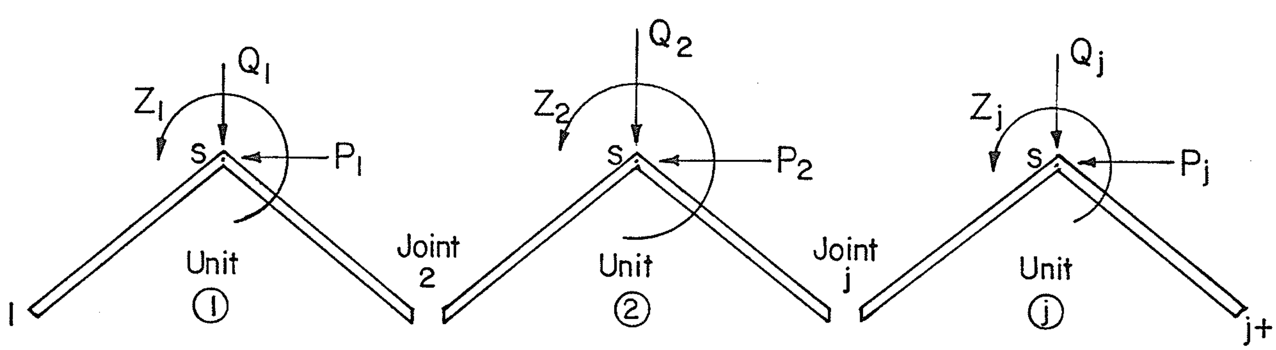

Figure 4.2 (c) Forces Referred to Shear Centers of each Unit

$$\sigma_j^r(\theta) = [\frac{N_z}{A} + \frac{M_x}{I_{xx}} b_j - \frac{M_y}{2I_{yy}} h_j]_{j,\theta} \text{ or} \tag{4.2a}$$

$$\sigma_j^\ell(\theta) = [\frac{N_z}{A} - \frac{M_x}{I_{xx}} b_j - \frac{M_y}{2I_{yy}} h_j]_{j,\theta} \tag{4.2b}$$

where A, I_{xx}, I_{yy}, b_j and h_j are cross-sectional properties (Figure 4.3b) of unit j, and N_z, M_x and M_y are internal force components which is function of θ. The right edge stress of unit j is given by equation (4.2a), while the left edge stress is given by equation (4.2b).

The edge displacements of unit j are different from those at the shear center. Due to effects of the internal rotation, the edge deflections are given by

$$u_j^r(\theta) = u_j(\theta) + \beta_j(\theta) \times b_j \tag{4.3a}$$

$$u_j^\ell(\theta) = u_j(\theta) - \beta_j(\theta) \times b_j \tag{4.3b}$$

$$v_j(\theta) = v_j(\theta) + \beta_j(\theta) \times h_j \tag{4.3c}$$

where u_j, v_j and β_j are the vertical, horizontal and rotational displacements at the shear center of unit j. Equation (4.3a) is valid for the right edge while equation (4.3b) is good for the left edge (Figure 4.3c). Equation (4.3c) is valid for both edges.

(c) The differences between the edge stresses and the edge deflections in each unit at every common joint are the errors:

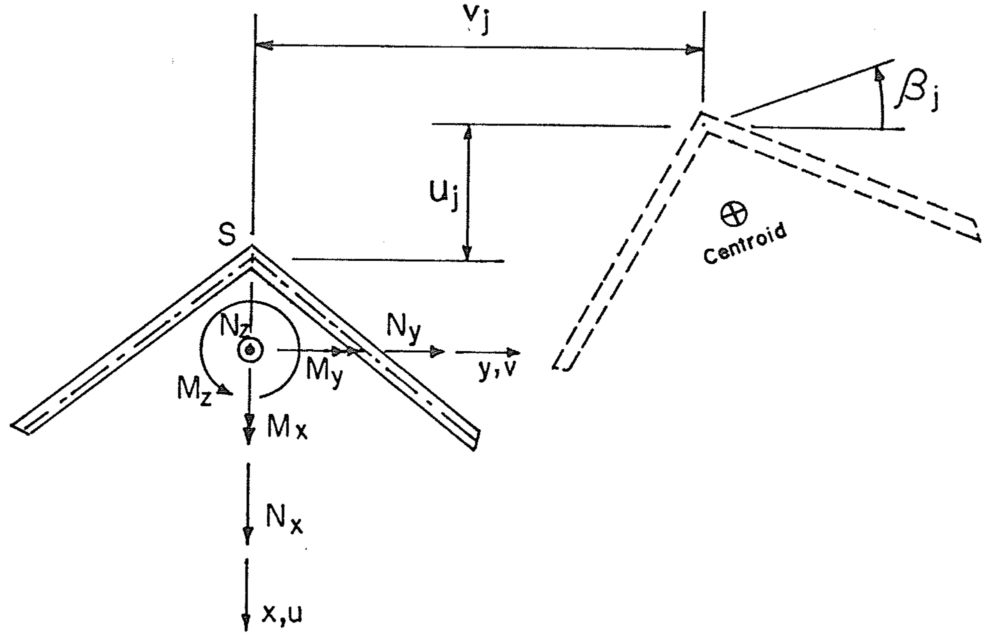

(a) Internal Forces and Displacements of Unit j

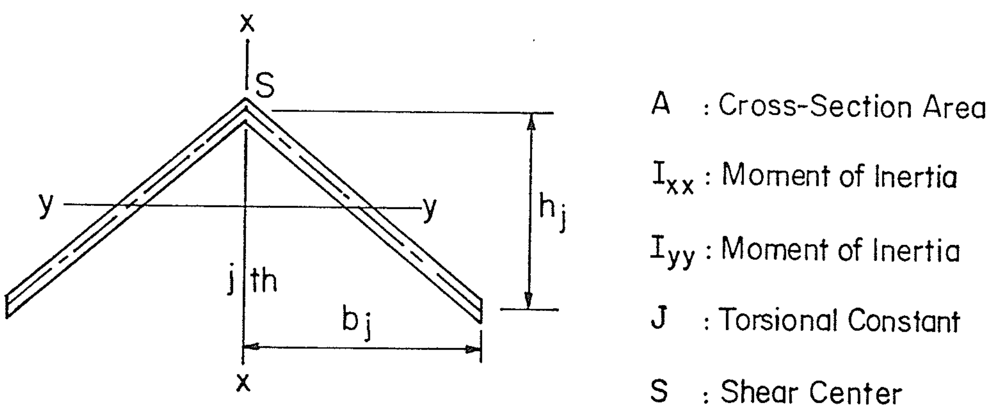

(b) Cross Sectional Properties of Unit j

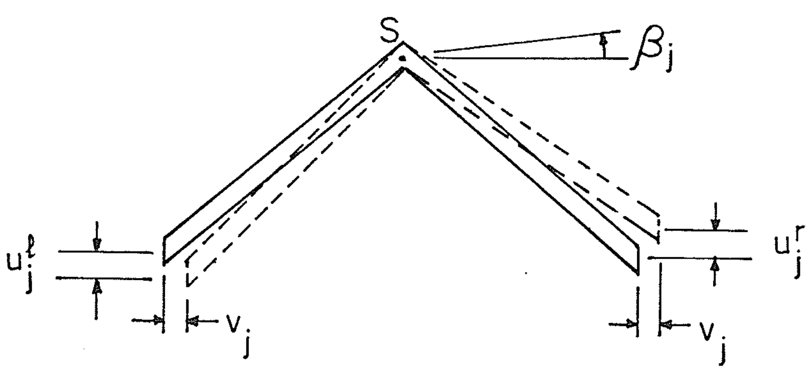

(c) Rotational Effects on Edge Deflection u, v

Figure 4.3

$$\Delta\sigma_j^L(\theta) = \sigma_{j-1,j}^r(\theta) - \sigma_{j,j}^\ell(\theta) \tag{4.5}$$

$$\Delta u_j^L(\theta) = u_{j-1,j}^r(\theta) - u_{j,j}^\ell(\theta) \tag{4.6}$$

$$\Delta v_j^L(\theta) = v_{j-1,j}(\theta) - v_{j,j}(\theta) \tag{4.7}$$

where the single subscript refers to a common joint value and the double subscript m,j to a value of unit m (where m = j-1 or j) at joint j. Figure 4.4a illustrates stress incompatibility at common joints while incompatibility of displacements is shown in Figure 4.4b.

4.4 Correction Analysis

The longitudinal edge stresses and edge deflections computed in Section 4.3 are initially determined on the assumption that each unit carries its loads independently of the others. Free edge stresses and displacements result which are not usually the same on the two sides of a common joint of two adjacent folds. That is, $\Delta\sigma_j^L$, Δu_j^L and Δv_j^L always exists for every joint j. These incompatibilities, however, are not allowed, and correction forces must be found to ensure compatibility between two folds.

To correct the differences in longitudinal stresses, longitudinal shears will develop at the joints to equalize the edge stresses (Figure 4.5). These shearing stresses are produced by the application of self-equilibrating longitudinal shear correction forces T_j at the joint j, which may be thought of as concentrated eccentric tensions or compressions. The longitudinal variation of these forces must be

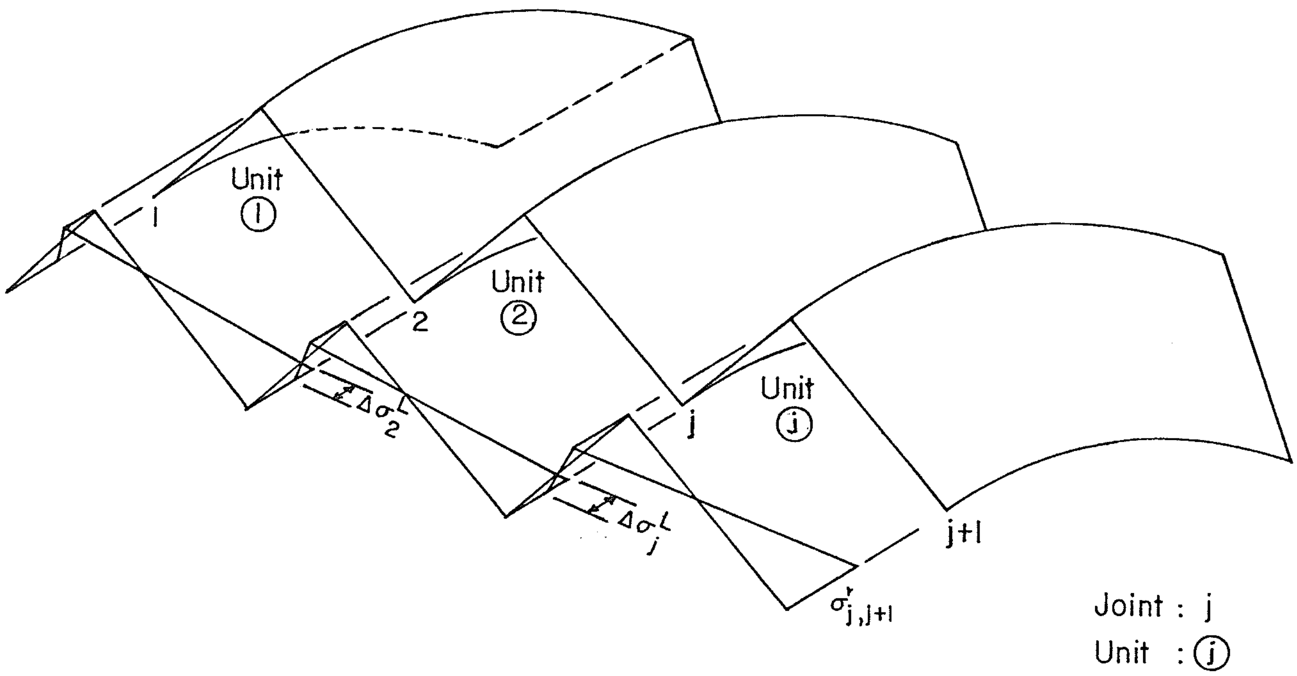

(a) Incompatible Longitudinal Edge Stresses due to Loadings

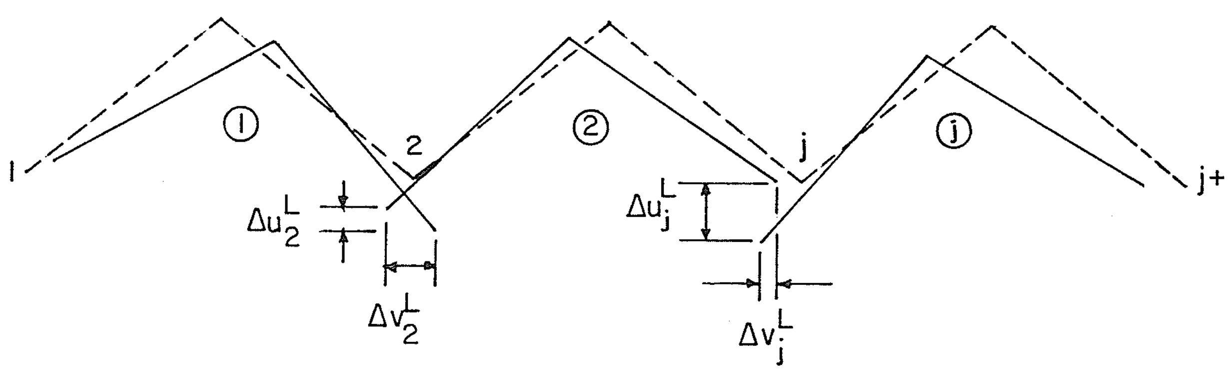

(b) Incompatible Edge Displacements

Figure 4.4 Edge Stress and Displacement Discrepancies at Common Joints

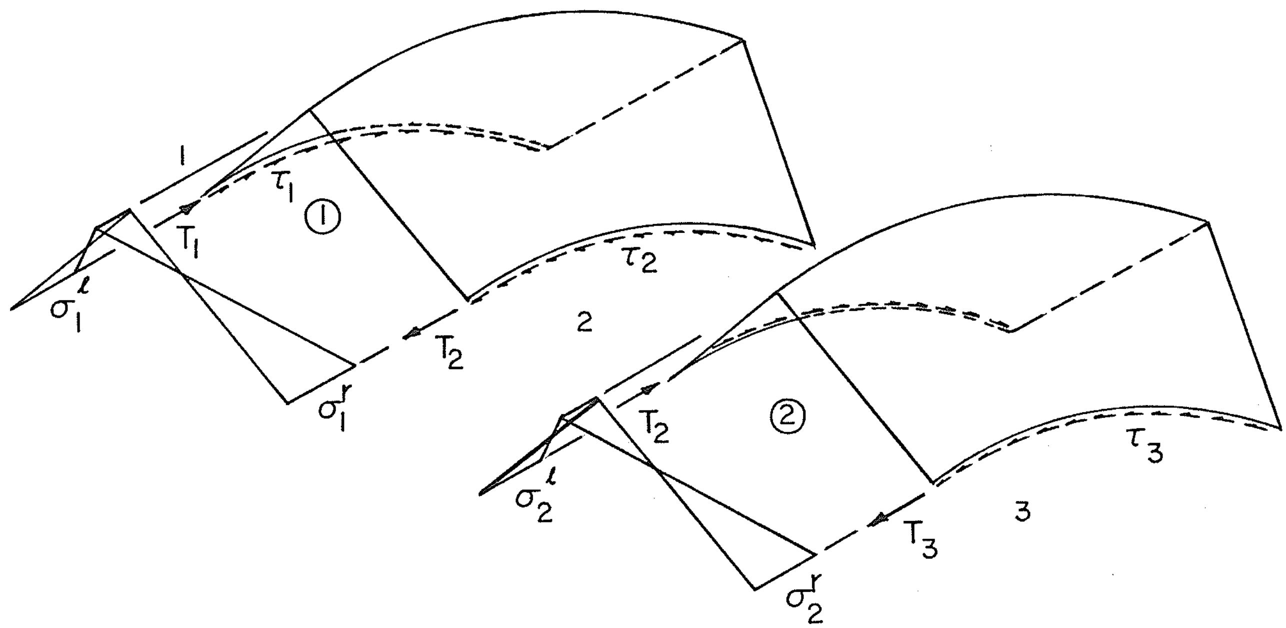

Figure 4.5 The Development of Longitudinal Shear Stress τ

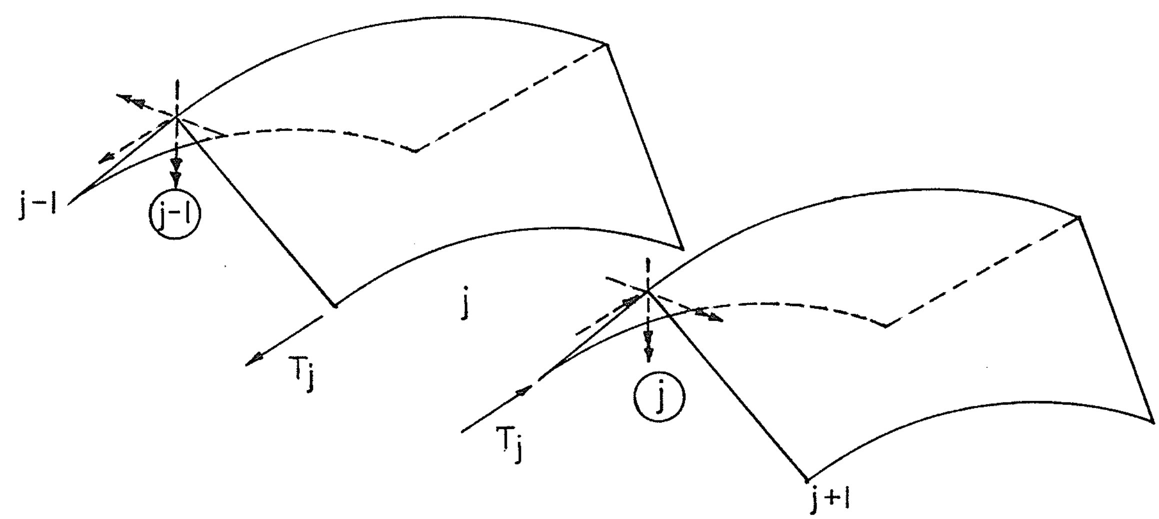

Figure 4.6 The Application of Stress Correction Force T_j

the same as that for the shearing stresses τ_j due to the way T_j is taken as

$$T_j = \tau_j t dz \tag{4.8}$$

where t is the cross-section thickness, and dz equals unity. The longitudinal normal stresses have the variation of $\cos\theta$, which is the same as the internal forces. To be consistent with those elasticity equations, the shear stresses τ must have a sine variation, which is anti-symmetric as compared to σ. Furthermore, each shear correction force T_j consists of a complete harmonic series of sine variation.

$$T_j = \sum_n T_{n,j} \sin n\theta \tag{4.9}$$

where n = 1, 2, 3, . . ., and $T_{n,j}$ is the unknown magnitude of the correction force for each n at joint j. Then, the shear correction force T_j is applied to the undeformed configuration of the structure at every common joint as shown in Figure 4.6. The longitudinal edge stresses and displacements in each unit due to unit shear correction force can be obtained from the solutions in Chapter 2 and 3. By the usual force transformation to the shear center, for example, the effects of unit j subjected to shear correction forces T_j and T_{j+1} are the sum of the individual (Figure 4.7). Therefore,

$$\sigma_j^r(\theta) = \bar{\sigma}_{j,j}^r(\theta) T_j + \bar{\sigma}_{j,j+1}^r(\theta) T_{j+1} \tag{4.10}$$

where $\bar{\sigma}_{j,j}^r$ is the right edge stresses of unit j due to T_j, and $\bar{\sigma}_{j,j+1}^r$ is the resulting right edge stresses of unit j due to T_{j+1}.

$$\sigma_j^\ell(\theta) = \bar{\sigma}_{j,j}^\ell(\theta)T_j + \bar{\sigma}_{j,j+1}^\ell(\theta)T_{j+1} \tag{4.11}$$

$$u_j^r(\theta) = \bar{u}_{j,j}^r(\theta)T_j + \bar{u}_{j,j+1}^r(\theta)T_{j+1} \tag{4.12}$$

$$u_j^\ell(\theta) = \bar{u}_{j,j}^\ell(\theta)T_j + \bar{u}_{j,j+1}^\ell(\theta)T_{j+1} \tag{4.13}$$

$$v_j(\theta) = \bar{v}_{j,j}(\theta)T_j + \bar{v}_{j,j+1}(\theta)T_{j+1} \tag{4.14}$$

where $\bar{u}_j^r$, $\bar{u}_j^\ell$, $\bar{v}_j$, $\bar{\sigma}_j^r$, and $\bar{\sigma}_j^\ell$ are obtained in the same way as in equations (4.3) and (4.2). The difference between the longitudinal edge stresses and the edge deflections in each unit at a common joint j are given by

$$\delta\sigma_j^T(\theta) = \sigma_{j-1}^r(\theta) - \sigma_j^\ell(\theta) \tag{4.15}$$

$$\delta u_j^T(\theta) = u_{j-1}^r(\theta) - u_j^\ell(\theta) \tag{4.16}$$

$$\delta v_j^T(\theta) = v_{j-1}(\theta) - v_j(\theta) \tag{4.17}$$

where the single subscript at the left side refers to a value at joint j, while the right side subscript refers to the value of unit j.

The vertical and horizontal edge displacement errors are to be corrected by applying a set of self-equilibrating vertical and horizontal correction forces at the joints. The correction forces are necessary only where relative joint displacements occur, thus their longitudinal variation must be the same as that for the displacements. The edge displacement variation is found to be symmetrical and therefore can be represented by a cosine function. The correction forces not only have cosine variation, but also consist of a complete harmonic series.

$$V_j = \sum_n V_{n,j} \cos n\theta \tag{4.18}$$

$$H_j = \sum_n H_{n,j} \cos n\theta \tag{4.19}$$

where n = 0, 1, 2, 3 . . . etc., $V_{n,j}$ and $H_{n,j}$ are the unknown magnitude of the correction forces for each n at joint j. Again, the displacement correction forces are applied to the undeformed shape of the structure at each common joint as shown in Figure 4.8. Using the solutions given in Chapters 2 and 3, the longitudinal edge stresses and displacements in each unit due to either V_j or H_j can be evaluated. For example, the results of unit j subjected to vertical displacement correction forces V_j and V_{j+1} (Figure 4.9) are

$$\sigma_j^r(\theta) = \bar{\sigma}_{j,j}^r(\theta)V_j + \bar{\sigma}_{j,j+1}^r(\theta)V_{j+1} \tag{4.20}$$

$$\sigma_j^\ell(\theta) = \bar{\sigma}_{j,j}^\ell(\theta)V_j + \bar{\sigma}_{j,j+1}^\ell(\theta)V_{j+1} \tag{4.21}$$

$$u_j^r(\theta) = \bar{u}_{j,j}^r(\theta)V_j + \bar{u}_{j,j+1}^r(\theta)V_{j+1} \tag{4.22}$$

$$u_j^\ell(\theta) = \bar{u}_{j,j}^\ell(\theta)V_j + \bar{u}_{j,j+1}^\ell(\theta)V_{j+1} \tag{4.23}$$

$$v_j(\theta) = \bar{v}_{j,j}(\theta)V_j + \bar{v}_{j,j+1}(\theta)V_{j+1} \tag{4.24}$$

The difference between the longitudinal edge stresses and displacements in each unit at a common joint j are given by

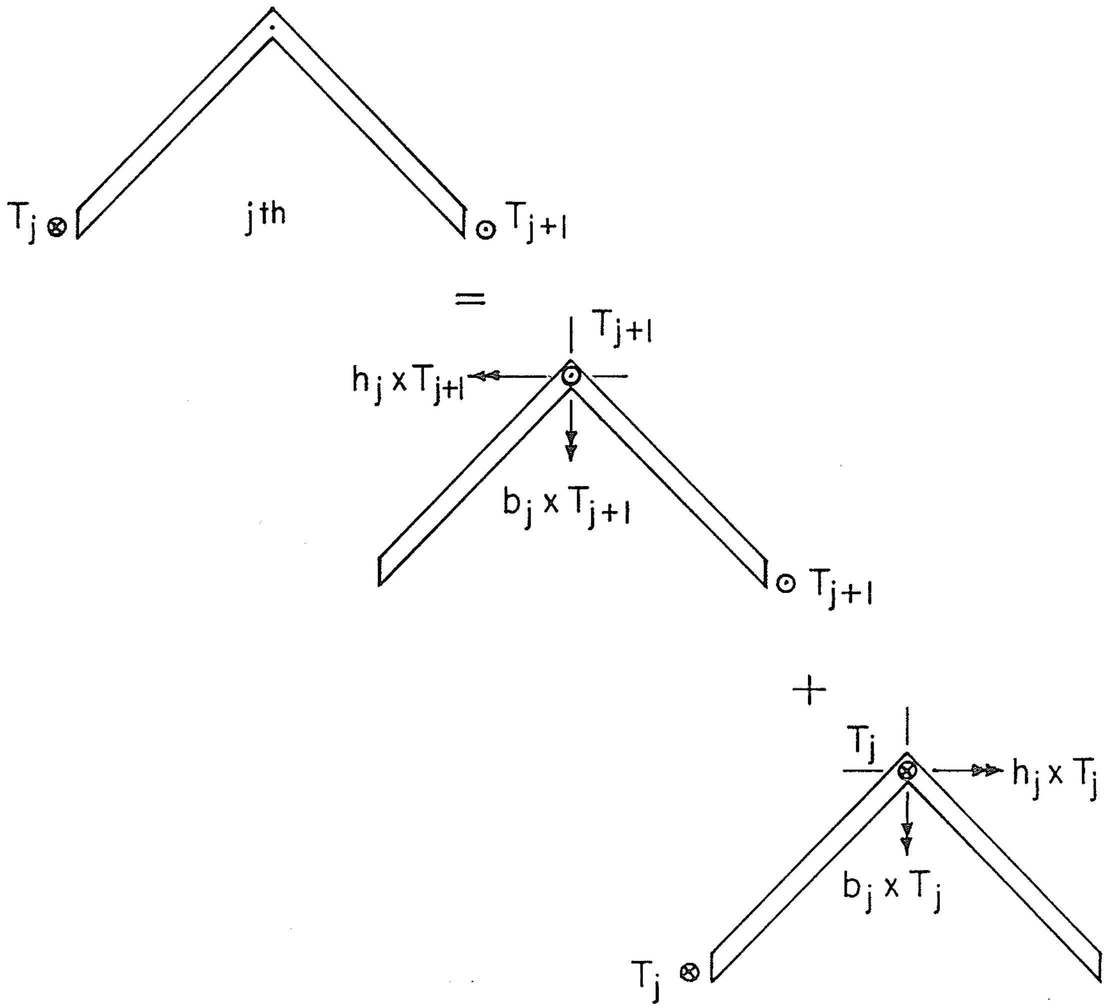

Figure 4.7 Unit j subjected to Stress Correction Force T_j and T_{j+1}

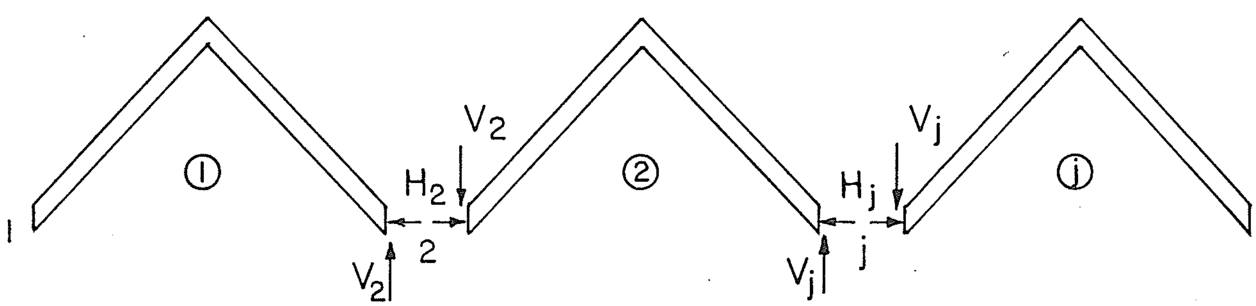

Figure 4.8 The Application of Displacement Correction Forces

$$\delta\sigma_j^V(\theta) = \sigma_{j-1}^r(\theta) - \sigma_j^\ell(\theta) \tag{4.25}$$

$$\delta u_j^V(\theta) = u_{j-1}^r(\theta) - u_j^\ell(\theta) \tag{4.26}$$

$$\delta v_j^V(\theta) = v_{j-1}(\theta) - v_j(\theta) \tag{4.27}$$

Similarly, the results of unit j subjected to horizontal displacement correction forces H_j and H_{j+1} (Figure 4.10) are

$$\sigma_j^r(\theta) = \bar{\sigma}_{j,j}^r(\theta)H_j + \bar{\sigma}_{j,j+1}^r(\theta)H_{j+1} \tag{4.28}$$

$$\sigma_j^\ell(\theta) = \bar{\sigma}_{j,j}^\ell(\theta)H_j + \bar{\sigma}_{j,j+1}^\ell(\theta)H_{j+1} \tag{4.29}$$

$$u_j^r(\theta) = \bar{u}_{j,j}^r(\theta)H_j + \bar{u}_{j,j+1}^r(\theta)H_{j+1} \tag{4.30}$$

$$u_j^\ell(\theta) = \bar{u}_{j,j}^\ell(\theta)H_j + \bar{u}_{j,j+1}^\ell(\theta)H_{j+1} \tag{4.31}$$

$$v_j(\theta) = \bar{v}_{j,j}(\theta)H_j + \bar{v}_{j,j+1}(\theta)H_{j+1} \tag{4.32}$$

and the difference between the longitudinal edge stresses and displacements in each unit at a common joint j are given by

$$\delta\sigma_j^H(\theta) = \sigma_{j-1}^r(\theta) - \sigma_j^\ell(\theta) \tag{4.33}$$

$$\delta u_j^H(\theta) = u_{j-1}^r(\theta) - u_j^\ell(\theta) \tag{4.34}$$

$$\delta v_j^H(\theta) = v_{j-1}(\theta) - v_j(\theta) \tag{4.35}$$

Actually, the correction forces V, H and T are applied to each common joint simultaneously. The difference in longitudinal edge stresses and displacements are obtained separately for each joint. Before simultaneous equations can be set up, the value of

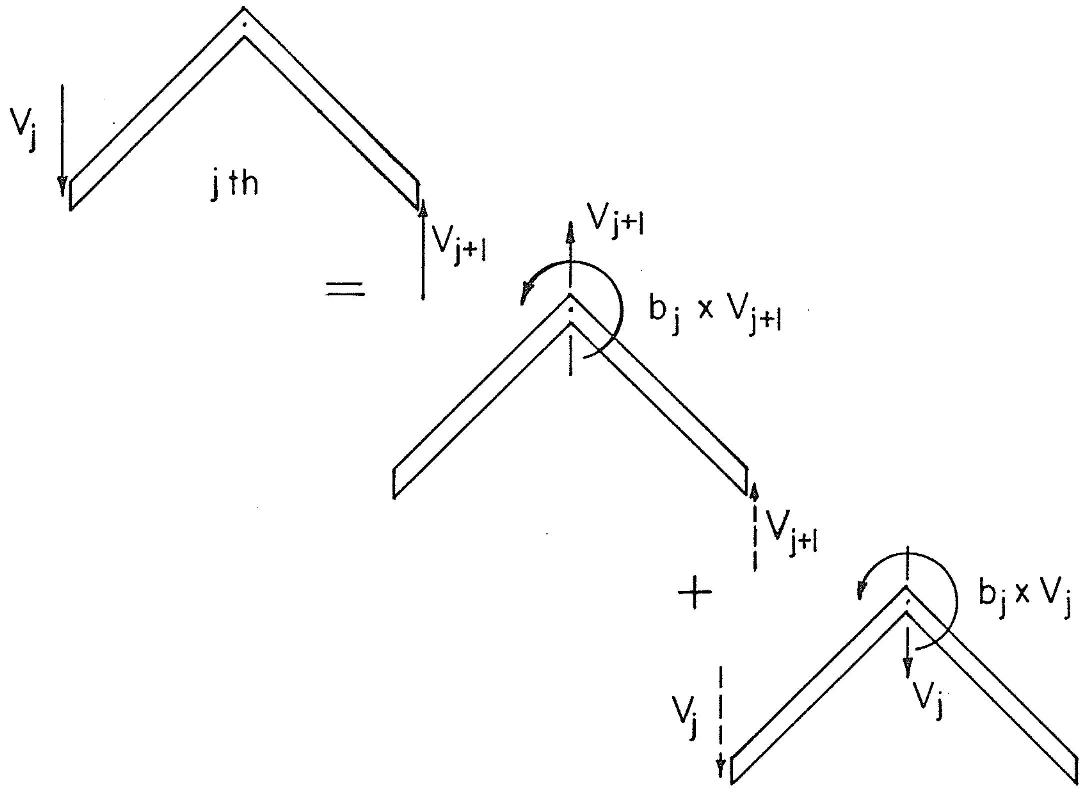

Figure 4.9 Unit j subjected to Vertical Correction Forces V_j and V_{j+1}

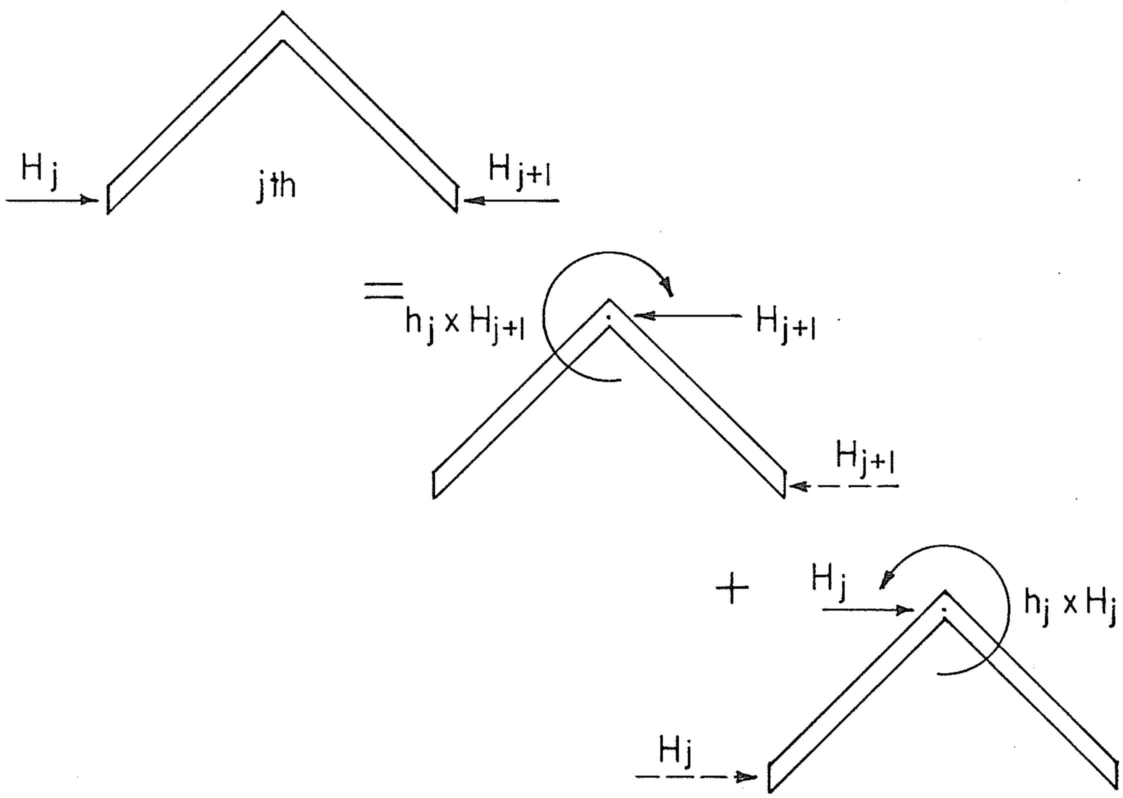

Figure 4.10 Unit j subjected to Horizontal Correction Forces H_j and H_{j+1}

n must be determined. The n value indicates the number of terms in a harmonic series and represents the number of locations along the common joints where compatibilities are to be imposed. For example, if n = 3, then at $\theta = \theta_1$, θ_2 and θ_3, the condition of compatibility in longitudinal stresses and displacements are ensured. The correction forces will take on terms like

$$V = V_0 + V_1 \cos\theta + V_2 \cos 2\theta$$

$$H = H_0 + H_1 \cos\theta + H_2 \cos 2\theta$$

$$T = T_1 \sin\theta + T_2 \sin 2\theta + T_3 \sin 3\theta + T_4 \sin 4\theta$$

It can be seen that T has one more term than V and H, because due to the natural restraints at the end supports only longitudinal stresses need to be corrected at boundaries.

Simultaneous equations are set up based on the compatibility relation.

$$\delta_j\text{'s} + \Delta_j^L\text{'s} = 0 \qquad (4.36)$$

For example, at joint j, the simultaneous equations using matrix notation are as outlined on the following page. Equation (4.37) is continued for every joint. Total number of unknowns is equal to

No. of interior common joints x (3n + 1) .

The techniques of solving simultaneous equations are many. The most popular one is the Gauss-Elimination Method. However, when the number of unknowns becomes bigger, even with the aid of the electronic digital computer, the above technique proved to be ineffective. In such cases Gauss-Seidel iteration may be used.

$$
\underbrace{\begin{bmatrix}
\delta u_j^V(\theta_1)+\delta u_j^H(\theta_1)+\delta u_j^T(\theta_1) \\
\delta u_j^V(\theta_2)+\delta u_j^H(\theta_2)+\delta u_j^T(\theta_2) \\
\vdots \\
\delta u_j^V(\theta_n)+\delta u_j^H(\theta_n)+\delta u_j^T(\theta_n) \\
\delta v_j^V(\theta_1)+\delta v_j^H(\theta_1)+\delta v_j^T(\theta_1) \\
\vdots \\
\vdots \\
\delta v_j^V(\theta_n)+\delta v_j^H(\theta_n)+\delta v_j^T(\theta_n) \\
\delta \sigma_j^V(\theta_1)+\delta \sigma_j^H(\theta_1)+\delta \sigma_j^T(\theta_1) \\
\vdots \\
\vdots \\
\delta \sigma_j^V(\theta_n)+\delta \sigma_j^H(\theta_n)+\delta \sigma_j^T(\theta_n) \\
\delta \sigma_j^V(\gamma)+\delta \sigma_j^H(\gamma)+\delta \sigma_j^T(\gamma)
\end{bmatrix}}_{(3n+1)\times(3n+1)}
\underbrace{\begin{bmatrix}
V_{0,j} \\ V_{1,j} \\ \vdots \\ V_{n,j} \\ H_{0,j} \\ H_{1,j} \\ \vdots \\ H_{n,j} \\ T_{1,j} \\ T_{2,j} \\ \vdots \\ T_{n,j} \\ T_{n+1,j}
\end{bmatrix}}_{(3n+1)\times 1}
=
\underbrace{\begin{bmatrix}
-\Delta u_j^L(\theta_1) \\
-\Delta u_j^L(\theta_2) \\
\vdots \\
-\Delta u_j^L(\theta_n) \\
-\Delta v_j^L(\theta_1) \\
-\Delta v_j^L(\theta_2) \\
\vdots \\
-\Delta v_j^L(\theta_n) \\
-\Delta \sigma_j^L(\theta_1) \\
-\Delta \sigma_j^L(\theta_2) \\
\vdots \\
-\Delta \sigma_j^L(\theta_n) \\
-\Delta \sigma_j^L(\gamma)
\end{bmatrix}}_{(3n+1)\times 1}
\qquad (4.37)
$$

4.5 Superposition

The final displaced configurations of the structure are obtained by superimposing the effects due to the joint loads and the correction forces. The longitudinal normal edge stresses and displacements of each unit subjected to joint loads are previously stored. The magnitudes of the correction forces are obtained by solving equation (4.37), then applying the results to each unit. The results of each unit due to each component of these correction forces are combined and added to those previously stored values to give the final answer.

Stress and displacements compatibilities are expected especially at the specified locations of each joint. If the number of locations selected are appropriate, the results in-between are found to be satisfactory. More precise results will be obtained with larger values of n.

CHAPTER V

APPLICATION OF THE ANALYSIS METHOD

5.1 Introduction

The objective of this chapter is to illustrate the analysis of arched folded plates based on the method presented in the preceding chapter.

A two-folds roof structure is selected for this purpose. Results will be compared with those given by the Finite Element Method.

5.2 Example - Layout

The dimensioning of the structure is usually governed by the following variables such as span length, plate thickness, plate depth and slope, and finally radius of rotation. The effects of these variables are briefly discussed.

(1) Ratio of span length to the total width of the cross-section, L/B:-Deflections will be smaller as L/B decreases. As L/B increases and > 5, the longitudinal stresses tend to approach those values which would be obtained from an arch analysis of the entire cross-section. The transverse moments will also rapidly increase with L/B.

(2) Ratio of overall depth of the cross-section to the radius of curvature, h/R:-This ratio should be in the order of 1/10 or less.

The smaller the ratio, the more accurate analysis will be.

(3) The plate slopes should not be too flat or too deep. The steeper slopes are always difficult to cast. A slope between 30° to 45° would be ideal.

(4) The plate thickness:-A thin slab is difficult and costly to cast. Thickness of 3 to 4 inches should provide sufficient moment capacity.

The choice of the type of cross-section is restricted to symmetrical cross-sections only. Although other type of symmetric cross-sections are possible, however, the simple V-shape is considered to be basic here.

The single span two-folds arched folded-plate roof shown in Figure 5.1 has been analyzed for a uniformly distributed loads over the inclined surface of the roof.

The loading was as follows:

	Unit 1	Unit 2
Concrete Dead Load (150 pcf)	37.5 psf	50 psf
Other Dead Load	37.5 psf	150 psf
Live Load	35.0 psf	50 psf
TOTAL ROOF LOAD W	100.0 psf	250 psf

The properties of the system are tabulated in Table 1.

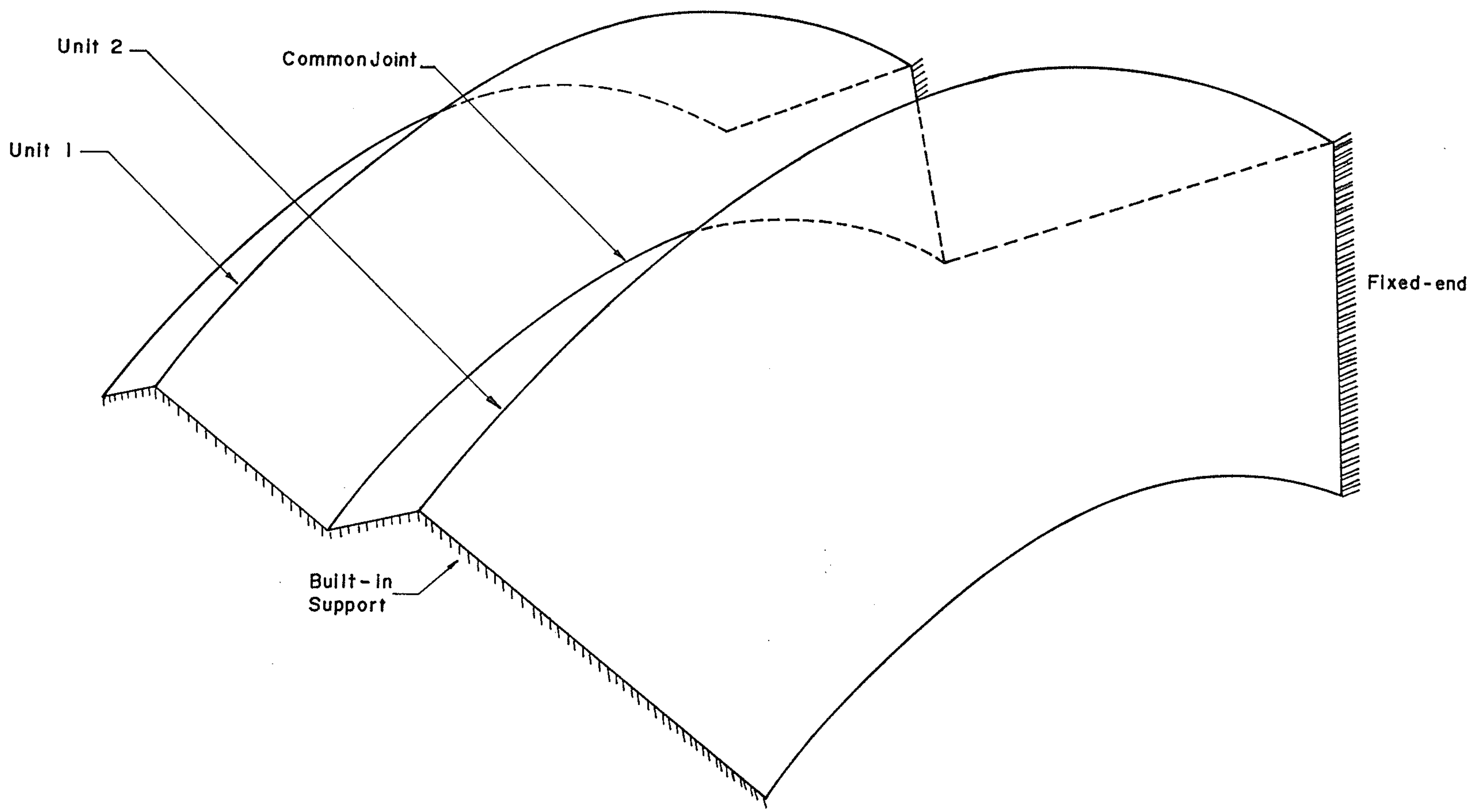

Figure 5.1 Two-Folds Arched-Folded-Plate Roof

TABLE 1 - Properties of the System

(a) Plates

Unit	Plate No.	Length, d (ft)	Thickness (in)	$\psi°$	I_{xx} (ft^4)	I_{yy} (ft^4)	J (ft^4)	A (ft^2)	R (ft)	$\gamma°$
1	1	4	3	30	8.00	0.6667	0.04167	2.00	50	45
	2	4	3	-30						
2	3	8	4	30	85.35	7.11	0.1975	5.334	51	45
	4	8	4	-30						

(b) Joints

Joint No.	Common Joint	$\alpha°$	sin α
0	No	60	0.8660
1	No	60	0.8660
2	Yes	330	0.5000
3	No	60	0.8660
4	No	60	0.8660

TABLE 1 continued

(c) Moment Distribution Constants

Joint	Plate	Relative Stiffness K_r	Distribution Factor
0		0	0
	1		
		3	3/7
1			
		4	4/7
	2		
		4	4/8.74
2			
		4.74	4.74/8.74
	3		
		4	4/7
3			
		3	3/7
	4		
4		0	0

5.3 Example - Analysis

A. Elementary Transverse Slab Analysis

A typical one foot strip of slab continuous over the supports is analyzed by moment distribution (Figure 5.2a). The fixed end moments are distributed and the resulting reactions and transverse moments at the supports are computed in Table 2 and shown in Figure 5.2b.

TABLE 2 - Transverse Moments and Joint Reactions For A Typical Cross-Section

0	1		2		3		4	Joint
1		2		3		4		Plate
01	10	12	21	23	32	34	43	Member
0	3	4	4	4.74	4	3	0	Relative Stiffness K_r
0	.428	.572	.457	.543	.572	.428	0	Distribution Factor DF
0	-173	116	-116	1155	-1155	1730	0	Fixed End Moments ft-lb/ft
0	-47	47	-506	506	-1603	1603	0	Final Moments M ft-lb/ft
-13	13	-132	132	-159	159	233	-233	M/d cosψ lb/ft
200	200	200	200	1000	1000	1000	1000	Wd/2 lb/ft
187	213	68	332	841	1159	1233	767	Total Vertical Shear lb/ft
187	281		1173		2392		767	Joint Reactions $\bar{R}_j$ lb/ft

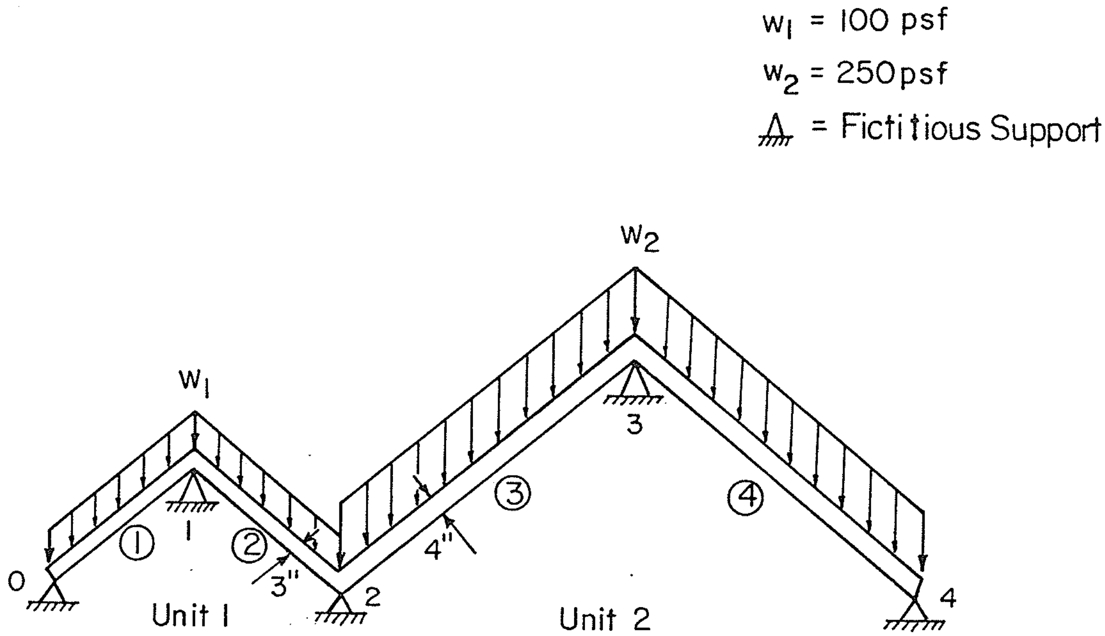

(a) One Way Slab bending

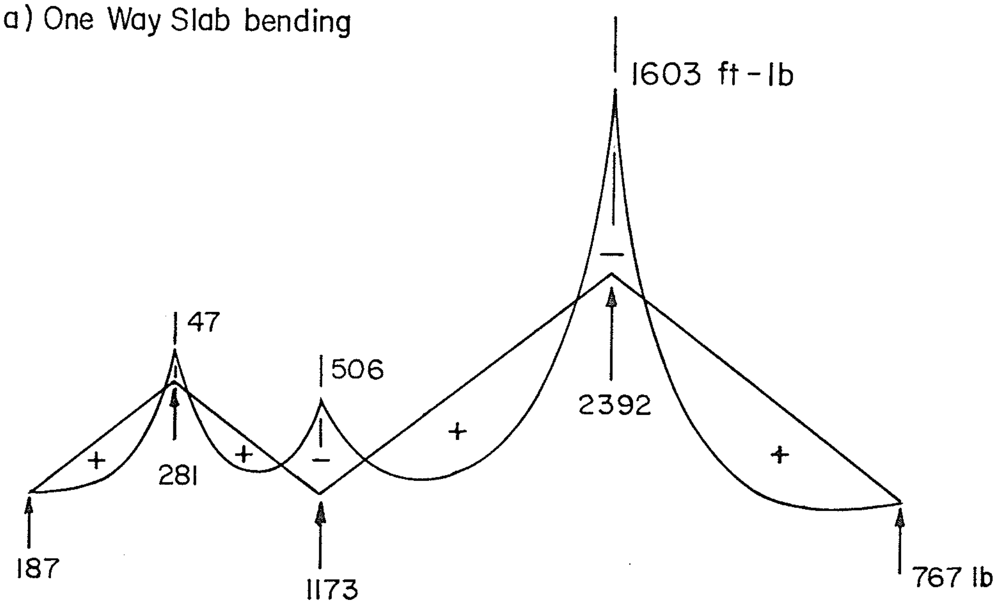

(b) Transverse Moments and Joint Reactions Results

Figure 5.2 Transverse Slab Analysis

B. Longitudinal Arch and Curved-Beam Analysis

(a) Inplane Forces - The joint reactions are resolved into inplane forces according to equation (4.1) only at the common joint 2.

$$F_2^{\ell} = -1173 \text{ lb.} \qquad F_2^{r} = 1173 \text{ lb.}$$

The shear center of unit 1 and 2 are at joint 1 and 3 respectively. The joint reactions $\bar{R}_0$, $\bar{R}_4$ and the vertical components of the inplane forces are transferred to the respective shear center, such that

$$Q_1 = 187 + 281 + 1173 \sin 30° = 1054.5 \text{ lb.}\downarrow$$

$$P_1 = 0$$

$$Z_1 = 3.464\ (187 - 1173 \sin 30°) = -1383.87 \text{ ft-lb.}$$

$$Q_2 = 767 + 2392 + 1173 \sin 30° = 3745.5 \text{ lb.}\downarrow$$

$$P_2 = 0$$

$$Z_2 = 6.928\ (1173 \sin 30° - 767) = -1250.51 \text{ ft-lb.}$$

(b) The primary subsystem subjected to loads Q_j is analyzed as an arch; and when subjected to loads P_j and Z_j is considered as a curved beam. Using the solutions presented in Section 2.3.1 and 3.3.1 for the case n = 0, the internal forces and displacements for each subsystem can be obtained. The edge stresses and edge deflections are evaluated according to equations (4.2) and (4.3). The results at θ equals to 0°, 15°, 30° and 45° for unit 1 and 2 are recorded in Table 3a.

TABLE 3a

Unit 1	θ°	σ_1^r (lb/ft²)	u_1^r (in)	v_1 (in)
a. Arch Case $E_n = 50x(-1054.5)$ $F_n^n = 0$	0 15 30 45	-19931.07272 -22005.40983 -28087.05852 -37761.56448	-0.06923 -0.05445 -0.02098 0.00	--- --- --- ---
b. Curved Beam Case $A_n = 0$ $B_n^n = -50x(-1383.87)$	0 15 30 45	-29627.94168 -29639.28157 -29672.52847 -29725.41666	-0.06414 -0.05635 -0.03399 0.00	0.01164 0.00574 -0.00488 0.00
Summation of a and b	0 15 30 45	-49559.01440 -51644.69140 -57759.58699 -67486.98114	-0.13337 -0.11080 -0.05497 0.00	0.01164 0.00574 -0.00488 0.00

Unit 2	θ°	σ_2^ℓ (lb/ft²)	u_2^ℓ (in)	v_2 (in)
a. Arch Case $E = 51x(-3745.5)$ $F_n^n = 0$	0 15 30 45	-18316.35752 -23658.44007 -39320.63364 -64235.58561	-0.09219 -0.07251 -0.02794 0.0	--- --- --- ---
b. Curved Beam Case $A_n = 0$ $B_n^n = -51x(-1250.51)$	0 15 30 45	5154.09139 5154.96785 5157.53748 5161.62517	0.01137 0.00999 0.00603 0.00	-0.00217 -0.00232 -0.00215 0.00
Summation of a and b	0 15 30 45	-13162.25613 -18503.47222 -34163.09616 -59073.96044	-0.08082 -0.06252 -0.02191 0.00	-0.00217 -0.00232 -0.00215 0.00

(c) The errors in longitudinal edge stresses and edge deflection at joint 2 are computed from equations (4.5) and (4.7) and recorded in Table 3b.

TABLE 3b

$\theta°$	$\Delta\sigma^L_2$ (psf)	Δu^L_2 (in)	Δv^L_2 (in)
0	-36396.74828	-0.05255	0.01381
15	-33141.21918	-0.04828	0.00806
30	-23596.49083	-0.03306	-0.00273
45	- 8413.0207	---	---

C. Correction Analysis

The value of n is chosen to be 3. That is, the correction forces applied at joint 2 have the following form, and the compatibility conditions at θ chosen at 0°, 15° and 30° are imposed.

$$V_2 = V_{0,2} + V_{1,2} \cos\theta + V_{2,2} \cos 2\theta$$

$$H_2 = H_{0,2} + H_{1,2} \cos\theta + H_{2,2} \cos 2\theta \qquad (5.1)$$

$$T_2 = T_{1,2} \sin\theta + T_{2,2} \sin 2\theta + T_{3,2} \sin 3\theta + T_{4,2} \sin 4\theta$$

Each term of the harmonic series are applied to the undeformed configuration of the structure shown in Figure 5.3. The solutions are obtained according to Table 4.

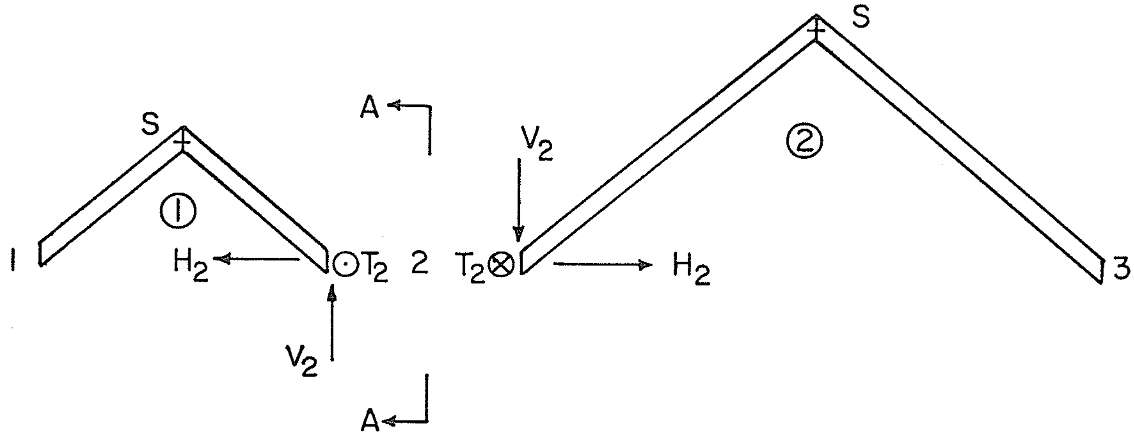

$$V_2 = V_{0,2} + V_{1,2}\cos\theta + V_{2,2}\cos 2\theta$$

$$H_2 = H_{0,2} + H_{1,2}\cos\theta + H_{2,2}\cos 2\theta$$

$$T_2 = T_{1,2}\sin\theta + T_{2,2}\sin 2\theta + T_{3,2}\sin 3\theta + T_{4,2}\sin 4\theta$$

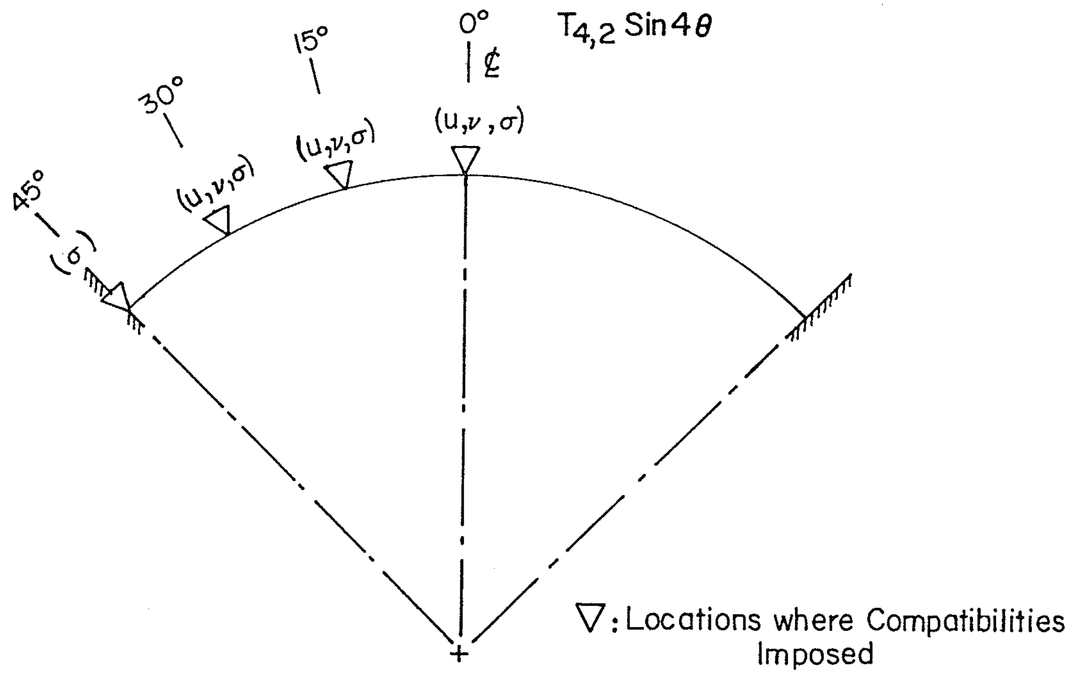

Section A–A

Figure 5.3 The Application of Correction Forces T, V & H

TABLE 4

Correction Force	Terms	n	A_n Unit 1	A_n Unit 2	B_n Unit 1	B_n Unit 2	E_n Unit 1	E_n Unit 2	F_n Unit 1	F_n Unit 2
V_2	$V_{0,2}$	0	0	0	-50x(3.464)	-51x(6.928)	50x(1)	51x(-1)	0	0
	$V_{1,2}\cos\theta$	1	0	0	-50x(3.464)	-51x(6.928)	50x(1)	51x(-1)	0	0
	$V_{2,2}\cos 2\theta$	2	0	0	-50x(3.464)	-51x(6.928)	50x(1)	51x(-1)	0	0
H_2	$H_{0,2}$	0	50^2x(1)	51^2x(-1)	-50x(-2.00)	-51x(4.00)	0	0	0	0
	$H_{1,2}\cos\theta$	1	50^2x(1)	51^2x(-1)	-50x(-2.00)	-51x(4.00)	0	0	0	0
	$H_{2,2}\cos 2\theta$	2	50^2x(1)	51^2x(-1)	-50x(-2.00)	-51x(4.00)	0	0	0	0
T_2	$T_{1,2}\sin\theta$	1	1x50x(-3.464)	1x51x(-6.928)	0	0	-1x(2.00)	-1x(-4.00)	-50x(1)+(2.00)	-51x(-1)+(-4.0)
	$T_{2,2}\sin 2\theta$	2	2x50x(-3.464)	2x51x(-6.928)	0	0	-2x(2.00)	-2x(-4.00)	-50x(1)+(2.00)	-51x(-1)+(-4.0)
	$T_{3,2}\sin 3\theta$	3	3x50x(-3.464)	3x51x(-6.928)	0	0	-3x(2.00)	-3x(-4.00)	-50x(1)+(2.00)	-51x(-1)+(-4.0)
	$T_{4,2}\sin 4\theta$	4	4x50x(-3.464)	4x51x(-6.928)	0	0	-4x(2.00)	-4x(-4.00)	-50x(1)+(2.00)	-51x(-1)+(-4.0)

The longitudinal normal edge stresses and displacement due to correction forces V_2, H_2 and T_2 are calculated from equations (4.20)-(4.24), equations (4.28)-(4.32) and equations (4.10)-(4.14) respectively. The differences in longitudinal edge stresses and deflections at joint 2 due to each of the correction forces are obtained from equations (4.25)-(4.27), equations (4.33)-(4.35) and equations (4.15)-(4.17) accordingly. The results are recorded in Table 5.

The simultaneous equations set up on the basis of equation (4.26) and presented according to equation (4.27) are as shown following Table 5.

TABLE 5

(a)	Term	$\theta°$	δu_2^V	δv_2^V	$\delta\sigma_2^V$
V_2	$V_{0,2}$	0	0.00032	-0.00004	126.51481
		15	0.00027	-0.00003	129.94336
		30	0.00015	0.0000003	139.99534
		45	0.0	0.0	155.98574
	$V_{1,2}$	0	0.00060	-0.00015	113.07389
		15	0.00037	-0.00011	122.49207
		30	-0.00007	-0.000028	139.44067
		45	0.0	0.0	131.49910
	$V_{2,2}$	0	0.00136	-0.00044	76.19363
		15	0.00062	-0.00032	102.21034
		30	-0.00063	-0.00010	137.27466
		45	0.0	0.0	66.40147

(b)	Term	$\theta°$	δu_2^H	δv_2^H	$\delta\sigma_2^H$
H_2	$H_{0,2}$	0	0.00129	-0.00262	- 81.93825
		15	0.00051	-0.00247	- 50.37005
		30	-0.00085	-0.00212	42.18324
		45	0.0	0.0	189.41426
	$H_{1,2}$	0	0.00124	-0.00244	- 79.08068
		15	0.00050	-0.00229	- 47.77438
		30	-0.00081	-0.00195	42.06121
		45	0.0	0.0	178.58729
	$H_{2,2}$	0	0.00111	-0.00193	- 71.09152
		15	0.00043	-0.00181	- 40.54660
		30	-0.00072	-0.00150	41.47119
		45	0.0	0.0	148.78533

Table 5 continued

(c)	Term	θ°	δu_2^T	δv_2^T	$\delta \sigma_2^T$
T_2	$T_{1,2}$	0 15 30 45	-0.00032 -0.00013 +0.00020 0.0	0.00013 0.000099 0.000034 0.0	13.31576 2.18806 - 19.77059 - 19.79238
	$T_{2,2}$	0 15 30 45	-0.00059 -0.00023 +0.00036 0.0	0.00024 0.00018 0.000061 0.0	26.58266 3.71378 - 38.10300 - 27.08445
	$T_{3,2}$	0 15 30 45	-0.00076 -0.00028 +0.00047 0.0	0.00030 0.00022 0.000075 0.0	39.39091 3.96205 - 53.26825 - 15.79659
	$T_{4,2}$	0 15 30 45	-0.00083 -0.00028 +0.00051 0.0	0.00031 0.00023 0.000074 0.0	50.80227 2.44401 - 63.21682 10.53125

$$
\begin{bmatrix}
\delta u_2^{V_0,2}(0^\circ) & \delta u_2^{H_0,2}(0^\circ) & \delta u_2^{T_1,2}(0^\circ) & \delta u_2^{V_1,2}(0^\circ) & \delta u_2^{H_1,2}(0^\circ) & \delta u_2^{T_2,2}(0^\circ) & \delta u_2^{V_2,2}(0^\circ) & \delta u_2^{H_2,2}(0^\circ) & \delta u_2^{T_3,2}(0^\circ) & \delta u_2^{T_4,2}(0^\circ) \\
\delta v_2^{V_0,2}(0^\circ) & & & & & & & & & \\
\delta \sigma_2^{V_0,2} & \delta \sigma_2^{H_0,\bar{2}} & \delta \sigma_2^{T_1,\bar{2}} & \delta \sigma_2^{V_1,\bar{2}} & \delta \sigma_2^{H_1,\bar{2}} & \delta \sigma_2^{T_2,\tilde{2}} & \delta \sigma_2^{V_2,\bar{2}} & \delta \sigma_2^{H_2,\bar{2}} & \delta \sigma_2^{T_3,\bar{2}} & \delta \sigma_2^{T_4,\bar{2}} \\
\cdot & & & & & & & & & \\
\cdot & & & & & & & & & \\
\delta u_2^{V_0,2}(30^\circ) & & & & & & & & & \\
\delta v_2^{V_0,2}(30^\circ) & \delta v_2^{H_0,\bar{2}}(30^\circ) & \delta v_2^{T_1,\bar{2}}(30^\circ) & \delta v_2^{V_1,\bar{2}}(30^\circ) & \delta v_2^{H_1,\bar{2}}(30^\circ) & \delta v_2^{T_2,\bar{2}}(30^\circ) & \delta v_2^{V_2,\bar{2}}(30^\circ) & \delta v_2^{H_2,\bar{2}}(30^\circ) & \delta v_2^{T_3,\bar{2}}(30^\circ) & \delta v_2^{T_4,\bar{2}}(30^\circ) \\
\delta \sigma_2^{V_0,2}(45^\circ) & \delta \sigma_2^{H_0,2}(45^\circ) & \delta \sigma_2^{T_1,2}(45^\circ) & \delta \sigma_2^{V_1,2}(45^\circ) & \delta \sigma_2^{H_1,2}(45^\circ) & \delta \sigma_2^{T_2,2}(45^\circ) & \delta \sigma_2^{V_2,2}(45^\circ) & \delta \sigma_2^{H_2,2}(45^\circ) & \delta \sigma_2^{T_3,2}(45^\circ) & \delta \sigma_2^{T_4,2}(45^\circ)
\end{bmatrix}
\times
\begin{bmatrix}
V_{0,2} \\ H_{0,2} \\ T_{1,2} \\ V_{1,2} \\ H_{1,2} \\ T_{2,2} \\ V_{2,2} \\ H_{2,2} \\ T_{3,2} \\ T_{4,2}
\end{bmatrix}
=
\begin{bmatrix}
-\Delta u_2^L(0^\circ) \\ -\Delta v_2^L(0^\circ) \\ -\Delta \sigma_2^L(0^\circ) \\ -\Delta u_2^L(15^\circ) \\ -\Delta v_2^L(15^\circ) \\ -\Delta \sigma_2^L(15^\circ) \\ -\Delta u_2^L(30^\circ) \\ -\Delta v_2^L(30^\circ) \\ -\Delta \sigma_2^L(30^\circ) \\ -\Delta \sigma_2^L(45^\circ)
\end{bmatrix}
$$

Equation (5.2)

The solutions of equation (5.1) are found as follows:

$$\begin{aligned}
V_{0,2} &= -\ 2944.86106 && \text{lb/ft} \\
H_{0,2} &= 9501.40318 && \text{lb/ft} \\
T_{1,2} &= -248953.67749 && \text{ft-lb/ft} \\
V_{1,2} &= 4109.03864 && \text{lb/ft} \\
H_{1,2} &= -\ 13648.94789 && \text{lb/ft} \\
T_{2,2} &= 264018.11955 && \text{ft-lb/ft} \\
V_{2,2} &= -\ 856.34874 && \text{lb/ft} \\
H_{2,2} &= 4352.32604 && \text{lb/ft} \\
T_{3,2} &= -123606.19378 && \text{ft-lb/ft} \\
T_{4,2} &= 23302.62672 && \text{ft-lb/ft}
\end{aligned} \tag{5.3}$$

D. Superposition

To obtain the final longitudinal edge stresses and displacements, the magnitude of the correction forces in equation (5.3) are applied back to the structure at the common joints according to their corrected directions. Subsequently, the correction forces are transferred to the shear centers of their respective units. The results are again obtained from the solutions presented in Chapters 2 and 3 for various loading cases. Then, using the principle of superposition, the effects from the correction forces are combined with those due to joint loads calculated previously to give the final results as shown in Table 6.

The final value of the longitudinal edge stresses and deflections of unit 1 and 2 at joint 2 are plotted against θ in Figure 5.4.

TABLE 6

Unit 1

$\theta°$	σ_1^r (psf)	u_1^r (in)	v_1^r (in)
0*	-27064.76436	-0.09606	0.01035
10	-28133.74616	-0.08636	0.00924
15*	-29298.74526	-0.07512	0.00791
20	-30933.24935	-0.06077	0.00624
30*	-37832.89467	-0.02820	0.00263
35	-44318.57361	-0.01456	0.00070
45*	-55266.29357	0.0	0.0

Unit 2

$\theta°$	σ_2^ℓ (psf)	u_2^ℓ (in)	v_2^ℓ (in)
0*	-27065.37198	-0.09606	0.01036
10	-27967.39349	-0.08658	0.00930
15*	-29297.92963	-0.07512	0.00791
20	-31397.19269	-0.06035	0.00603
30*	-37833.69426	-0.02821	0.00264
35	-42004.96116	-0.01530	0.00195
45*	-55265.10136	0.0	0.0

* Locations where compatibility conditions are imposed

Fig. 5.4 (a) Plot of σ_f vs. θ

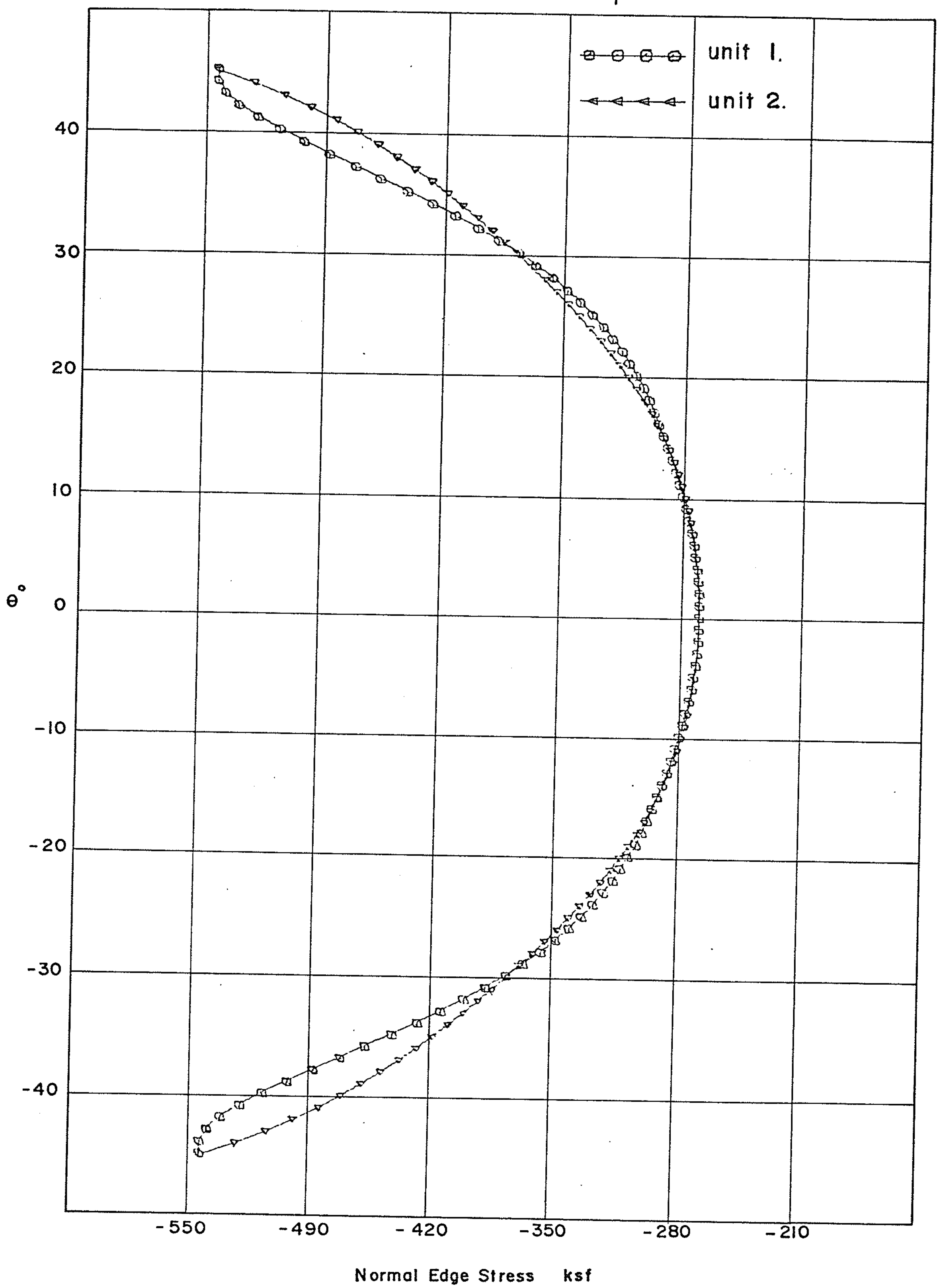

Fig. 5.4(b) Plot of u_f vs θ

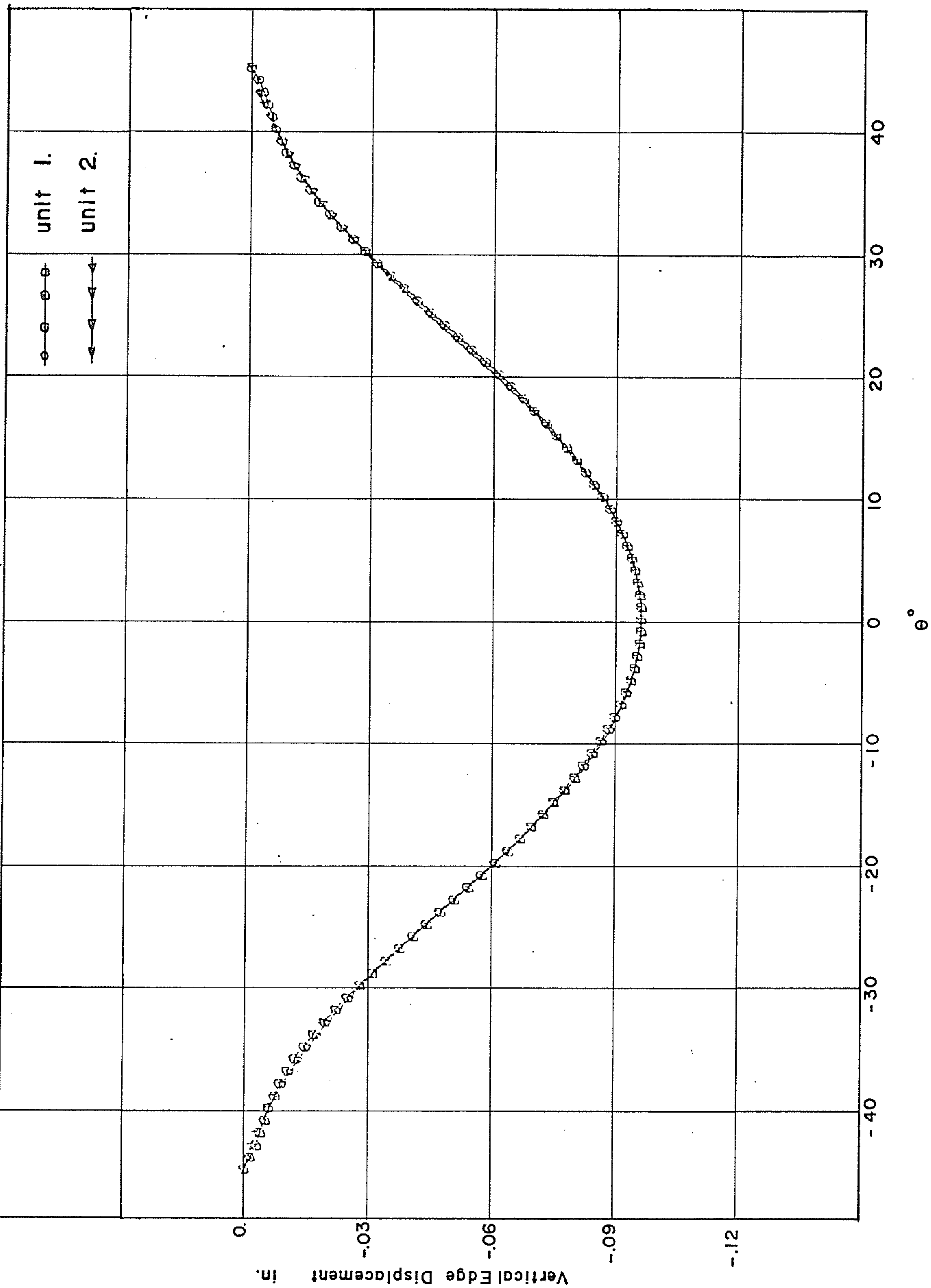

Fig. 5.4 (c) Plot of v_f vs θ

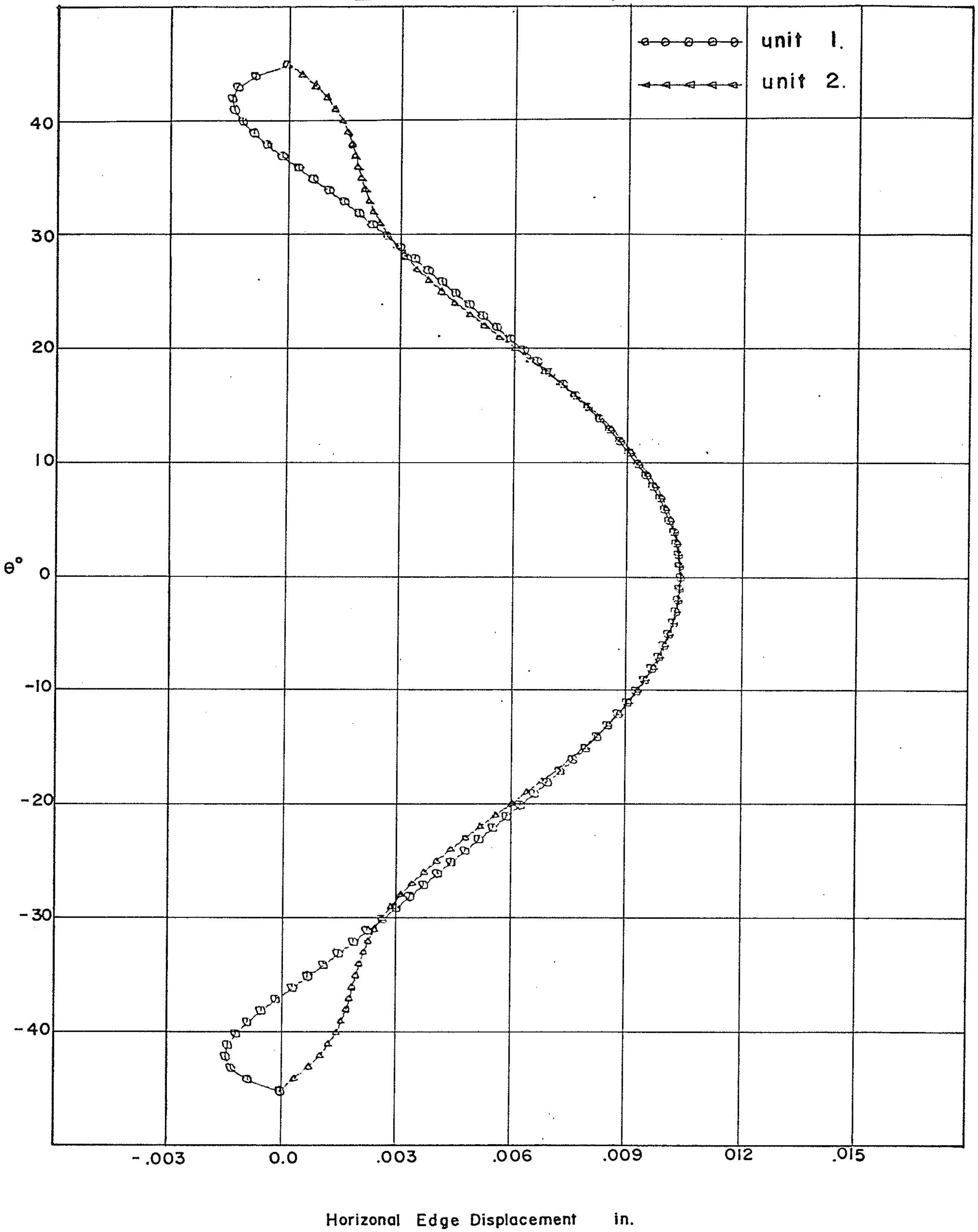

5.4 Analysis By The Finite Element Method

From the classical thin-shell theory, it is possible to generate differential equations of equilibrium or continuity, which have been solved for only special geometric forms and certain specific boundary conditions. It is evidenced that the theory cannot adequately deal with shell structures having arbitrary geometric shapes and boundary conditions, such as the arched folded plates of revolution. However, a completely new approach for the solution of problems in continuum mechanics, using matrix alegbra and the digital computer, was introduced in the 50's and later became known as the finite element method. This method was first applied to the plane stress problems and was subsequently extended to the plates and shells analysis with satisfactory results. The major advantages of the finite element method are the ability to accommodate arbitrary geometry and boundary conditions together with variable thickness, variable material properties, discontinuities in the shell surface, and general loading conditions.

The two-fold arched folded plate roof which is the subject of the present study is analyzed by the finite element method using a computer program developed by Johnson and Smith[26]. The roof surface is idealized by an assemblage of flat quadrilateral elements as shown in Figure 5.5. The material properties of each element are assumed to be homogeneous, isotropic and linearly elastic. The global and surface coordinates for each node, the boundary conditions and the nodal loads are among the input data to the program which are shown in Appendix I.

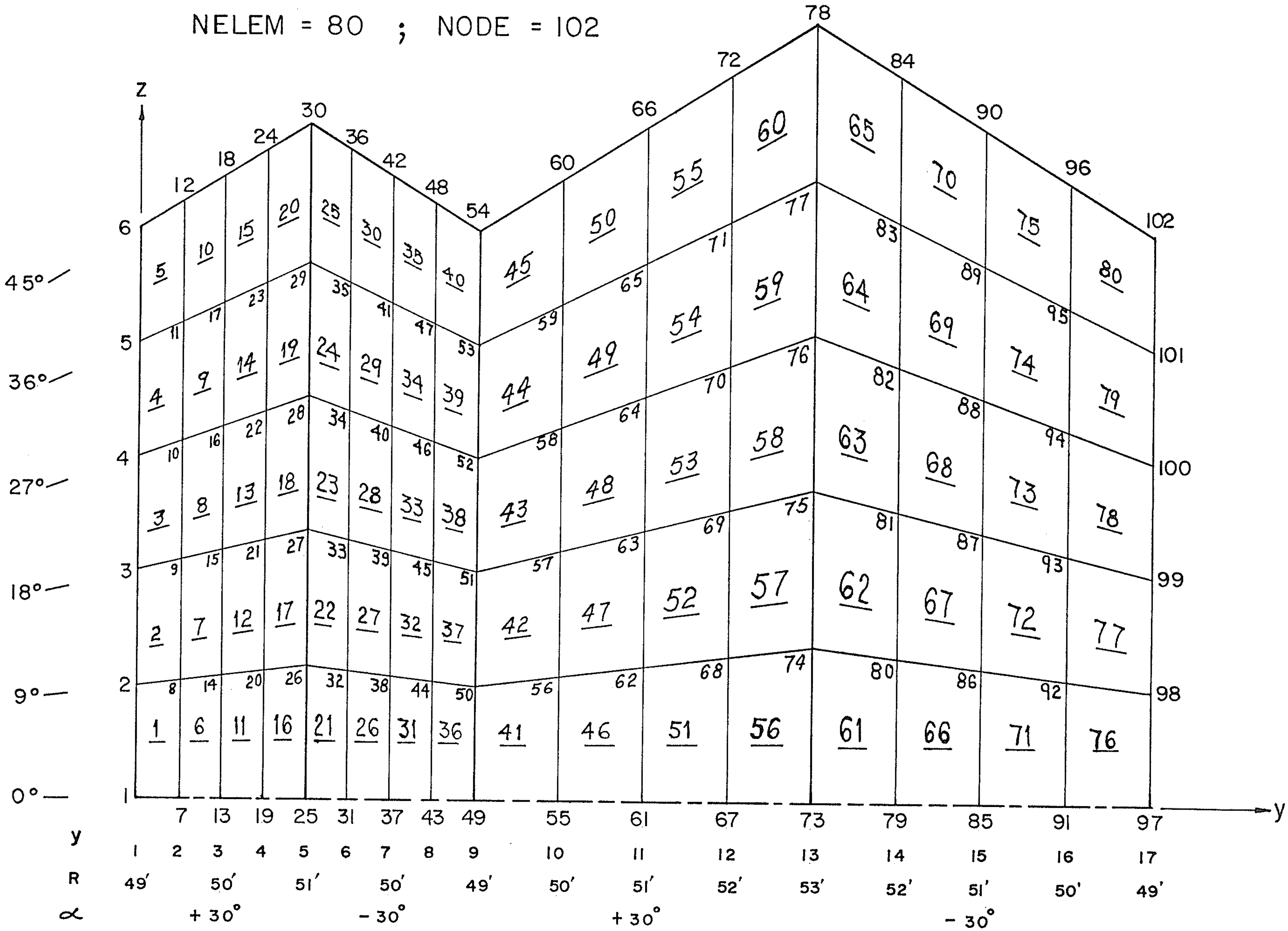

Figure 5.5 Quadrilateral Element Mesh with Nodal and Element Numbering

The global coordinate system x, y, z, as indicated in Figure 5.5, is chosen for the structure. Nodal coordinates are calculated by the following expressions:

$$
\begin{aligned}
x &= R\cos\theta \\
y &= s\cos\alpha \\
z &= R\sin\theta
\end{aligned}
\tag{5.4}
$$

where, R, s, α and θ are defined in Figure 5.6.

The surface coordinate system ξ_1, ξ_2, ξ_3 is characterized by the fact that ξ_3 is normal to the surface at each node, while ξ_1 and ξ_2 are tangent to the surface at each nodal point. Referring to Figure 5.6, the vector $\bar{r}$ from origin 0 to node I is defined as

$$\bar{r} = R\cos\theta\bar{i} + s\cos\alpha\bar{j} + R\sin\theta\bar{k} \tag{5.5}$$

The unit tangental vectors ξ_1 and ξ_2 are defined by

$$\xi_1 = \frac{1}{|\frac{\partial\bar{r}}{\partial s}|}\frac{\partial\bar{r}}{\partial s} \quad \text{and} \quad \xi_2 = \frac{1}{|\frac{\partial\bar{r}}{\partial\theta}|}\frac{\partial\bar{r}}{\partial\theta} \tag{5.6}$$

where $|\frac{\partial\bar{r}}{\partial s}|$ and $|\frac{\partial\bar{r}}{\partial\theta}|$ are the magnitudes, and have the values of

$$
\begin{aligned}
|\frac{\partial\bar{r}}{\partial s}| &= \sqrt{|\frac{\partial\bar{r}}{\partial s}|^2} = \sqrt{\sin^2\alpha\cos^2\theta+\cos^2\alpha+\sin^2\alpha\sin^2\theta} = 1 \\
|\frac{\partial\bar{r}}{\partial\theta}| &= \sqrt{|\frac{\partial\bar{r}}{\partial\theta}|^2} = \sqrt{s^2\sin^2\alpha\sin^2\theta+s^2\sin^2\alpha\cos^2\theta} = s\sin\alpha
\end{aligned}
\tag{5.7}
$$

Therefore,

$$
\begin{aligned}
\xi_1 &= \sin\alpha\cos\theta\bar{i}+\cos\alpha\bar{j}+\sin\alpha\sin\theta\bar{k} \\
\xi_2 &= -\sin\theta\bar{i}+\cos\theta\bar{k}
\end{aligned}
\tag{5.8}
$$

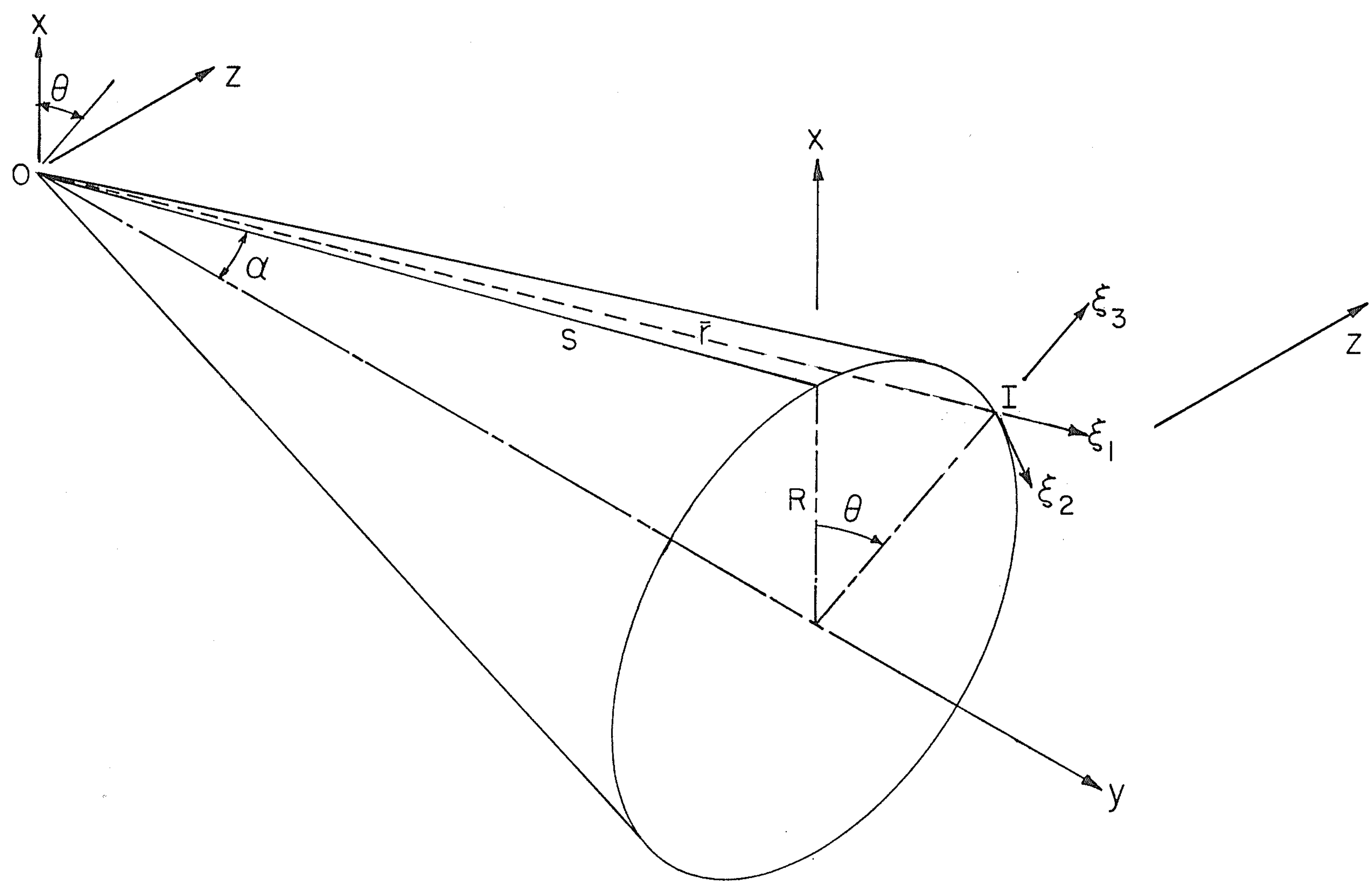

Figure 5.6. The Global and Surface Coördinate System

The normal, ξ_3, is generated by the cross-product of ξ_1 and ξ_2. The angles α and θ are defined in such way that the cross-product of ξ_1 and ξ_2 consistently have an outward normal ξ_3. Careful attention must be paid to nodal points having sudden change of slope where ξ_1 is approximated by

$$\xi_1 = \bar{J} \tag{5.9}$$

The boundary conditions allow specified displacements at any nodal point. A five degree-of-freedom nodal point displacement system for the assemblage is utilized. These five degrees of freedom consist of three linear translations and two rotations, and are defined as follows:

$D_1 \equiv$ Translation in surface ξ_1-direction.
$D_2 \equiv$ Translation in surface ξ_2-direction.
$D_3 \equiv$ Translation in surface ξ_3-direction.
$D_4 \equiv$ Rotation about ξ_1 coordinate.
$D_5 \equiv$ Rotation about ξ_2 coordinate.

The boundary conditions for this example are specified at two special locations. At the fix-end support, all nodal displacement components are equal to zero. At the axis of symmetry only D_2 and D_4 are zero. To be exact, rotation about the global y-coordinate at the symmetry axis are zero; however, this is not allowed in the programme due to local base coordinate system was chosen.

The original loading in the previous analysis is taken as uniformly radial distributed pressure over the inclined surface of the roof. The programme allows uniform pressure loads UPL which are normal to the surface of the element only; however, nodal loads are permitted with considerable flexibility. The five nodal load components P_1 to P_5 at each node correspond in an energy sense to the five nodal point displacement components D_1 to D_5. Due to the above programme restriction, the original UPL is converted into nodal point loads having components P_1 and P_3 only. Input nodal force values for each loaded nodes are listed in Appendix I.

The output of the computer programme contains the following information:

(1) Reprint all the input data.

(2) Nodal joint displacements D_1-D_5 are expressed in the base coordinate system which in this case is the surface coordinate system.

(3) The quantities of element stress resultants are printed with respect to the average plane coordinate system. The sign convention for these quantities are illustrated in Figure 5.7 for surface coordinates. These stress resultants can be assumed to be acting at the centroid of the quadrilateral element.

(4) Averaged nodal stress results are also among the output. These quantities are the averaged element stress resultants in all the elements surrounding a given node expressed with respect to the surface coordinate system.

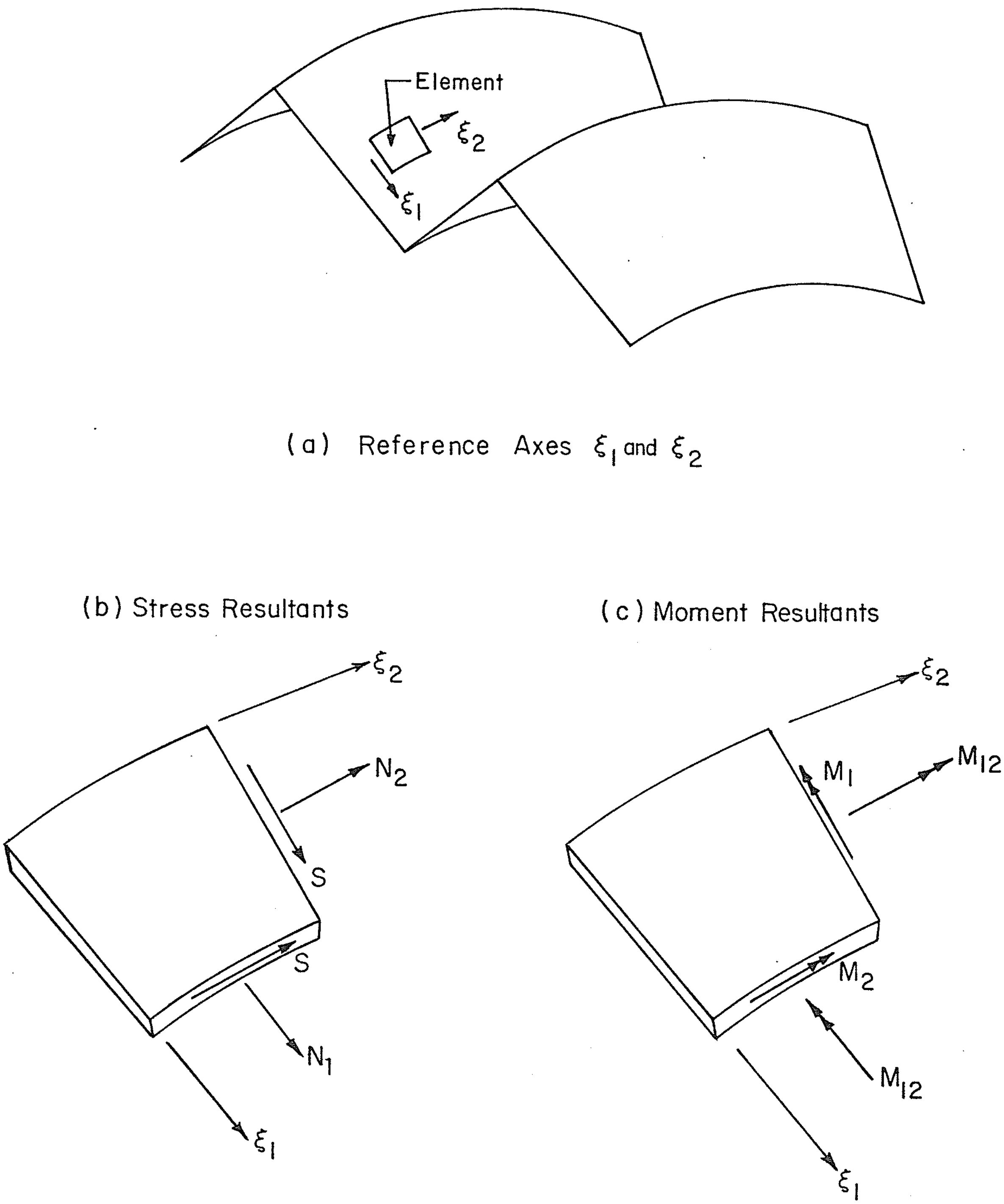

Figure 5.7 Shell Stresses and Moments

Previous structural analysis of the arched folded plate roof yields longitudinal direct stresses and displacements only at the common joint of the two units, which are comparable with stress resultant N_2, displacement components D_1 and D_3 of nodal points 49-54 from the shell analysis. Results of the element stress resultants for element 36-45 and nodal displacements for nodes 49-54, together with the distribution of transverse bending moments M_2 at mid-span are plotted in Figure 5.8.

Fig. 5.8 (a) Plot of F. E. M.'s Results

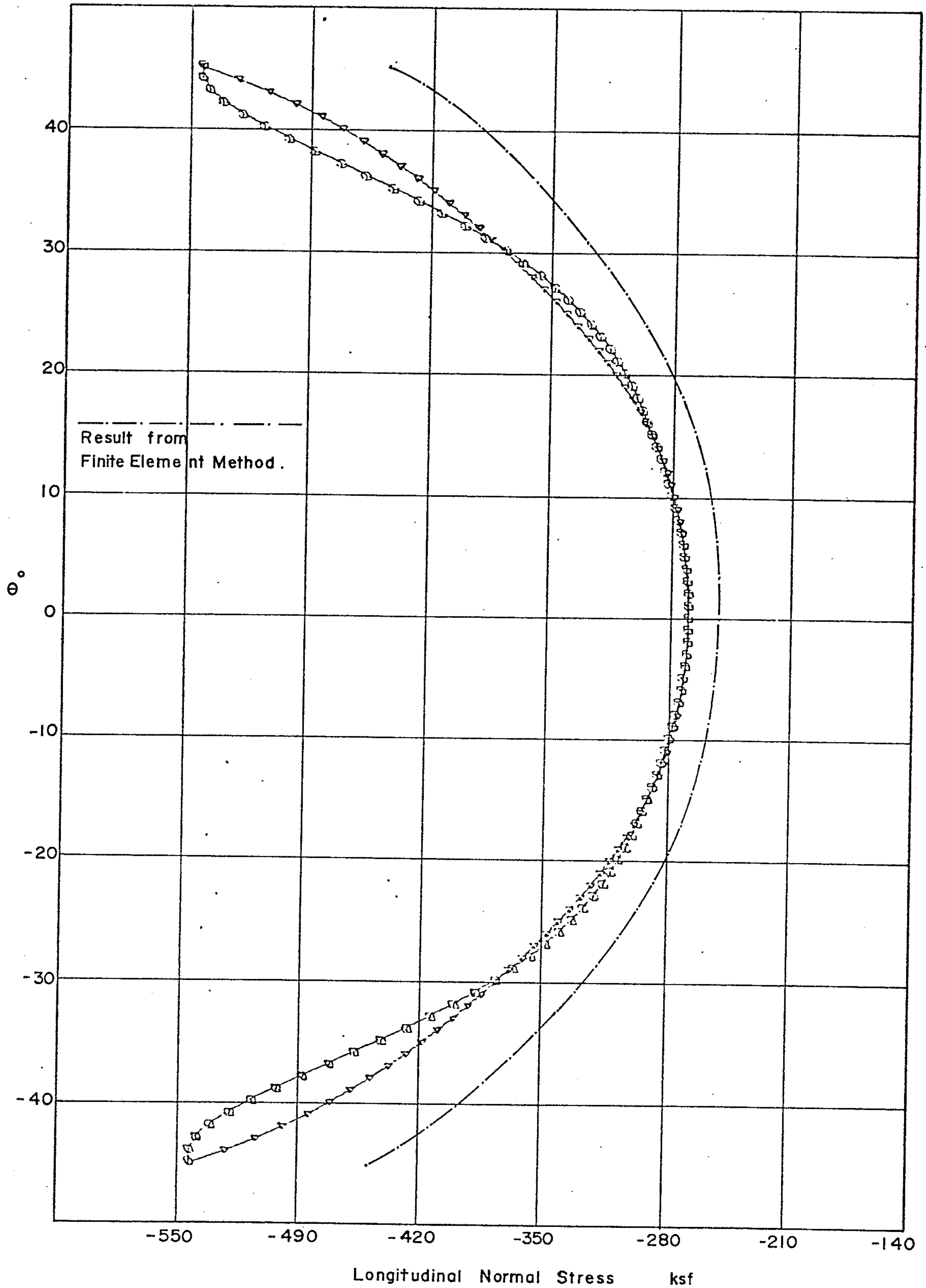

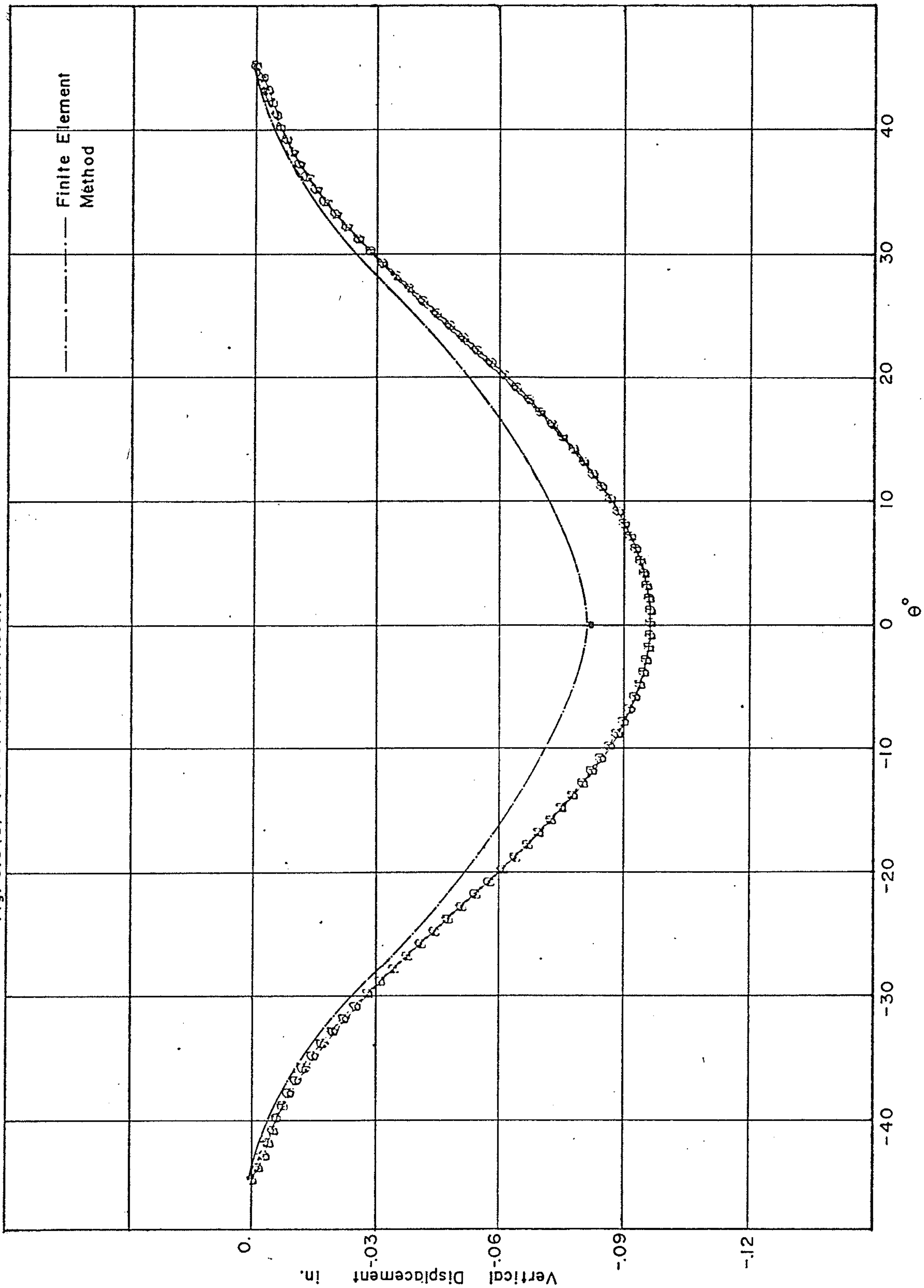

Fig. 5.8(b) Plot of F.E.M. Results

Fig. 5.8 (c) Plot of F.E.M. Results

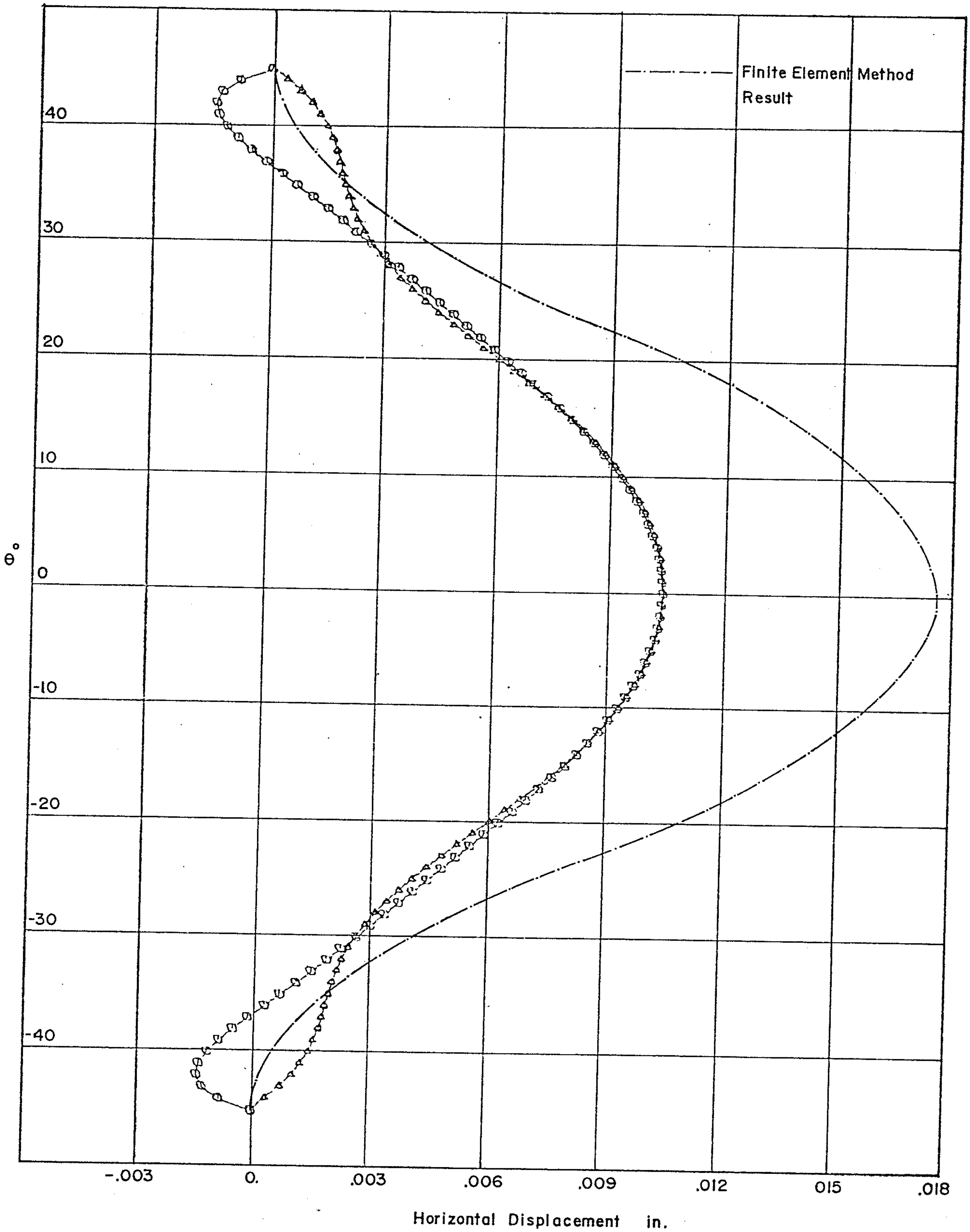

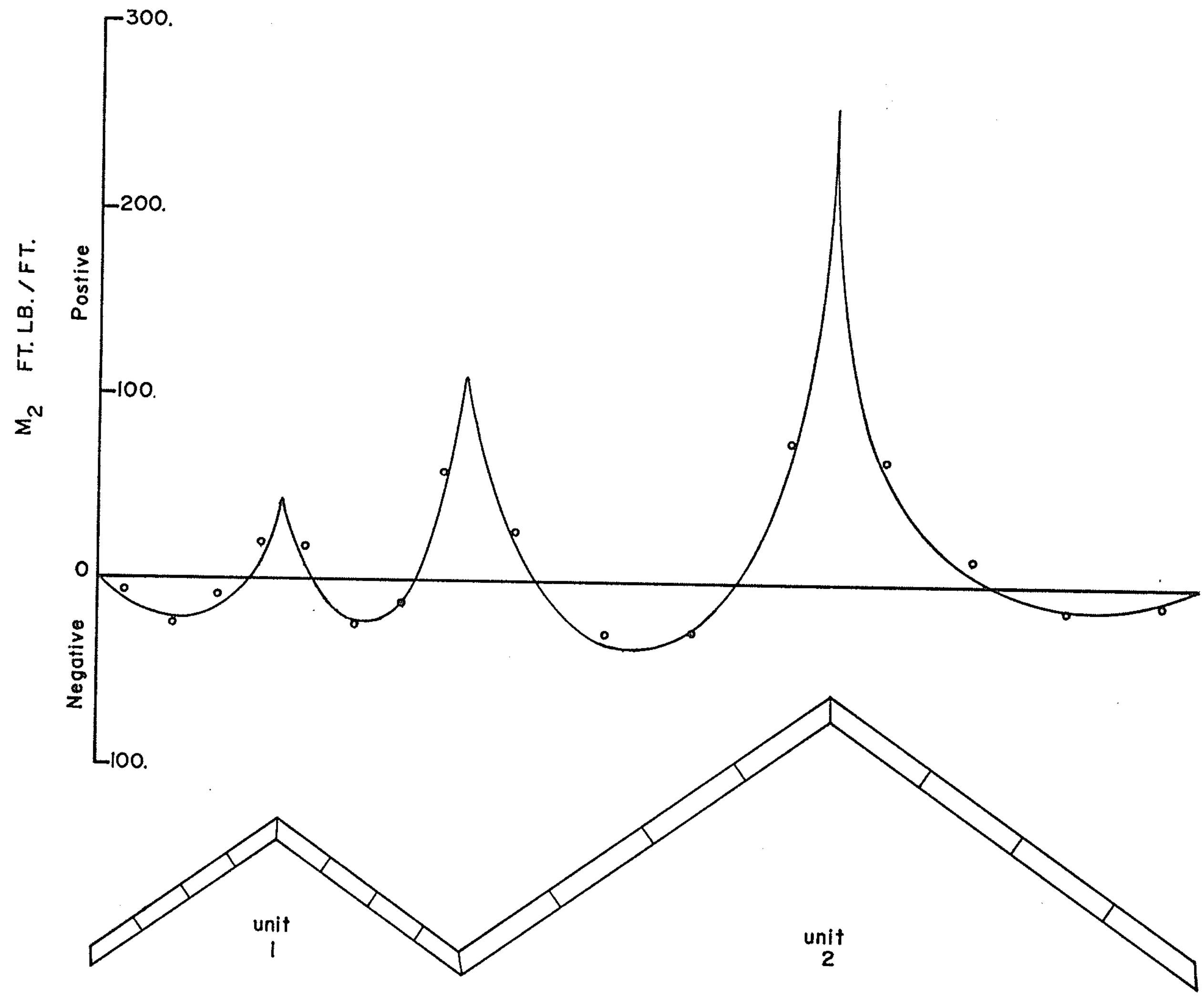

Figure 5.8 (d) Distribution of Transverse Bending Moments M_2 at Mid-Span.

CHAPTER VI

CONCLUSIONS

6.1 Conclusions

The stress resultants and displacements along the common joint of the arched folded plate roof, obtained by the structural analysis are compared with the results of a finite element analysis using shell theory. The comparisons are summarized in Figure 5.8a, b, c and d.

Figure 5.8a shows reasonably good agreement in the vertical displacement component values between the two methods of analysis. These vertical displacement values are referred to edge displacements u in the structural analysis and nodal displacements D_3 expressed in the surface coordinate ξ_3 in the finite element analysis. For locations having sudden change of slope, the outward normal ξ_3 is referred to the same direction as to the edge displacement u.

Nodal displacement components D_1 in the finite element analysis are expressed in the surface coordinate ξ_1-direction, which is parallel to the global horizontal axis for locations having sudden change of slope. The edge displacements v in the structural analysis are referred to the same direction. Figure 5.8b shows no significant difference in the horizontal displacement values from the two analyses, although some discrepencies were observed.

The stress resultants in shell theory are actually force per unit length of surface. Values of the longitudinal direct stress N_2 in the finite element analysis should therefore be divided by the element thickness. Due to the fact that the structure did not have an overall uniform plate thickness, separate element thickness was used for elements at the trough. Stresses produced by plate bending moments M_1 are not included in the longitudinal membrane stresses because they contribute less than 5 per cent of the final stress values. The longitudinal direct stresses yielded by the two methods of analysis are both expressed with respect to the same direction such that they can be compared. Figure 5.8c shows some disagreement in the longitudinal direct stress values between the two methods of analysis. The simple structural analysis yields higher stress values, while discrepancies become larger towards the fixed-end support. The overall stress distribution pattern, however, are in a reasonable good agreement between the two.

Transverse bending is represented in the shell analysis by the moment M_2 shown in Figure 5.7. The maximum M_2 values would generally occur near the center of the long span; therefore, the distribution of transverse moments M_2 obtained from the finite element analysis at mid-span is shown in Figure 5.8d. Comparison between the two is relatively meaningless at this stage as a final rotation correction was not made at the common joint in the structural analysis.

Values of the transverse direct stress N_1, the inplane shear S, and of the plate torsional moments M_{12} were not examined in detail as they were found to be less significant from normal structural design consideration. Consequently, values of N_1, M_{12} and S are not compared.

Despite the fact that values of longitudinal direct stress obtained from both methods of analysis compared favourably only in some degree, and there is no comparison in transverse moment values; it may be concluded that the structural theory proposed in this thesis can predict satisfactorily the internal forces and the deflection behaviour of an arched folded plates structure under load at this early development stage. The theory, however, will be far from perfect without any further research.

6.2 Comments For Further Study

The proposed structural theory obviously does not comprise a completely satisfactory solution to the problem of arched folded plates of revolution. Thus, the techniques of the theory are open to improvement and refinement. However, there were two notable areas in which improvement to the techniques used could have resulted in major improvements in the qualitative results obtained.

1) Under the current theory, rotation was allowed at the common joints such that the original angle α_j in Figure 4.2b was not maintained as the structure displaced. This rotational error can be eliminated by the incorporation of rotation correction within the correction analysis, such that the conditions of displacement, stress and rotation compatibility at each common joint of the structure are ensured. Improvement in the correction analysis would not only

contribute greatly to the accuracy of the results, but also allow the more accurate determination of the final transverse moments.

2) The final longitudinal direct stresses and displacements of the structure at the common joints could be improved. This can be done by increasing the number of locations where compatibility conditions are to be imposed. Locations near the support are highly preferable. Consequently, those discrepancies between units observed in Figure 5.4 can be removed.

It was recognized that the range of applicability of the proposed structural theory was very limited. Quite often the theory was found restricted to many geometric limitations as indicated in the early chapters. It was apparent that another approach to the problem of the arched folded plates structure was desirable. The consideration of plate strips, rather than the whole unit itself, would be very beneficial.

REFERENCES

1. Ehlers, G., "Ein neues Konstruktionsprinzip", Bauingenieur, Vol. 9, 1930, Pg. 125.

2. Craemer, H., "Theorie der Faltwerke", Beton und Eisen, Vol. 29, 1930, P. 276.

3. Gruber, E., "Berechnung Prismatischer Scheibenwerke", Internatl. Assoc. of Bridge and Structural Engrg. Memoirs, Vol. 1, 1932, P. 225.

4. Winter, G. and Pei, M., "Hipped plate Construction", J. American Concrete Institute, Vol. 32, January, 1947.

5. Gruening, G., "Die Nebenspannungen in Prismatischen Faltwerken", Ingenieur-Archir., Vol. 3, No. 4, 1932.

6. Vlassow, W. Z., "Structural Mechanics of Shells", Moskwa, 1936.

7. Gaafar, I., "Hipped Plate Analysis Considering Joint Displacement", Transactions, ASCE, Vol. 119, 1954.

8. Yitzhaki, David, "Prismatic and Cylindrical Shell Roofs", Haifa Science Publishers, Haifa, Israel, 1958.

9. Goldberg, J. E. and Leve, H. L., "Theory of Prismatic Folded Plate Structures", International Assn. of Bridges and Structural Engrg., No. 17, Zurich.

10. Phase I Report of the Task Committee on Folded Plate Construction, J. Struct. Div. ASCE, Vol. 90, December, 1963.

11. Edwards, Harry H., "Facts on Precast-Prestressed Folded Plate Slabs", Modern Concrete, Vol. 24, No. 2, June, 1960.

12. Marguerre, K., "Zur Theories der gerkrummten Plate grosser Formanderung", Proc. 5th Internatl. Congress of Appl. Mech., 1938.

13. Apeland, K. and Popov, E. P.,"Analysis of Bending Stresses in Translational Shells", Proc. of the Colloquium on Simplified Calculation Methods, Brussels, 1961.

14. Shah, A. H., and Lansdown, A. M., "Dead and Wind Load Analysis of Arched Folded Plate", IASS, July, 1972.

15. Moorman, R. B., "Folded-Plate Analysis of Thin-Walled Beam", 1960, Symposium on the Mechanics of Plates and Shells, Poly. Inst. of Brooklyn, N. Y.

16. Yitzhaki, D. and Reiss, Max, "Analysis of Folded Plates", J. Struct. Div., ASCE, Vol. 88, Oct. 1962.

17. Billington, David P., "Thin Shell Concrete Structures", Chapter 8, McGraw Hill Book Company, 1965.

18. Simpson, H., "Design of Folded Plate Roofs", Proc. Paper 1508, ASCE, Vol. 84, January, 1958.

19. Saint-Venant, Barre de, "Memoire sur le calcul de la resistance et de la flexion des pieces solids a simple on a double courbure, en prenant simultanement en consideration les divers efforts auxquels elles peuvent etre soumises dans tous les sens", Compt. Rend. Vol. 17, 1873.

20. Marcus, H., "Abriss einer allgemeinen Theorie des eigenspannten Tragers mit vaumlich gefundener Mittelinie", Z. Bauwesen, 1914.

21. Pippard, A. J., "The Stress Analysis of Bow Girders", Building Research Tech. Paper No. 1, Dept. of Scientific and Industrial Research, His Majesty's Stationery Office, London, England, 1926.

22. Cheney, J. A., "Bending and Buckling of Thin-Walled Open-Section Rings", J. Eng. Mech. Div. ASCE, October, 1963.

23. Vlasov, V. Z., "Thin-Walled Elastic Beams", The Israel Program For Science Translations, Jerusalem, 1961.

24. Borg, S. F. and Gennaro, J. J., "Modern Structural Analysis", Chapter 7, Van Nostrand Reinhold Company, 1969.

25. Volterra, E., "Deflections of a Circular Beam Out of Its Initial Plane", Paper No. 2727, Trans. Am. Soc. Civil Engrs., Vol. 120, 1955.

26. Johnson, C. P. and Smith, P. G., "A Computer Programme For the Analysis of Thin Shells", Dept. of Civil Engrg., University of California, Berkeley, 1969.

APPENDIX I

NODAL COORDINATES AND DIRECTION COSINES FOR SURFACE COORDINATES E1 AND E2 BAR

NODE	X ft.	Y ft.	Z ft.	E1X	E1Y	E1Z	E2X	F2Y	E2Z
1	49.0000	0.0	0.0	0.500000	0.866000	0.0	0.0	0.0	1.000000
2	48.3967	0.0	7.66530	0.493800	0.866000	0.078200	-0.156400	0.0	0.987700
3	46.6018	0.0	15.1418	0.475500	0.866000	0.154500	-0.309000	0.0	0.951100
4	43.6593	0.0	22.2455	0.445500	0.866000	0.227000	-0.454000	0.0	0.891000
5	39.6418	0.0	28.8015	0.404500	0.866000	0.293900	-0.587800	0.0	0.809000
6	34.6482	0.0	34.6482	0.328000	0.866000	0.377400	-0.754700	0.0	0.656100
7	49.5000	0.866000	0.0	0.500000	0.866000	0.0	0.0	0.0	1.000000
8	48.8906	0.866000	7.74350	0.493800	0.866000	0.078200	-0.156400	0.0	0.987700
9	47.0773	0.866000	15.2963	0.475500	0.866000	0.154500	-0.309000	0.0	0.951100
10	44.1048	0.866000	22.4725	0.445500	0.866000	0.227000	-0.454000	0.0	0.891000
11	40.0463	0.866000	29.0954	0.404500	0.866000	0.293900	-0.587800	0.0	0.809000
12	35.0018	0.866000	35.0018	0.328000	0.866000	0.377400	-0.754700	0.0	0.656100
13	50.0000	1.73210	0.0	0.500000	0.866000	0.0	0.0	0.0	1.000000
14	49.3844	1.73210	7.82170	0.493800	0.866000	0.078200	-0.156400	0.0	0.987700
15	47.5528	1.73210	15.4508	0.475500	0.866000	0.154500	-0.309000	0.0	0.951100
16	44.5503	1.73210	22.6995	0.445500	0.866000	0.227000	-0.454000	0.0	0.891000
17	40.4509	1.73210	29.3893	0.404500	0.866000	0.293900	-0.587800	0.0	0.809000
18	35.3553	1.73210	35.3553	0.328000	0.866000	0.377400	-0.754700	0.0	0.656100
19	50.5000	2.59810	0.0	0.500000	0.866000	0.0	0.0	0.0	1.000000
20	49.8783	2.59810	7.89990	0.493800	0.866000	0.078200	-0.156400	0.0	0.987700
21	48.0284	2.59810	15.6053	0.475500	0.866000	0.154500	-0.309000	0.0	0.951100
22	44.9958	2.59810	22.9265	0.445500	0.866000	0.227000	-0.454000	0.0	0.891000
23	40.8554	2.59810	29.6831	0.404500	0.866000	0.293900	-0.587800	0.0	0.809000
24	35.7089	2.59810	35.7089	0.328000	0.866000	0.377400	-0.754700	0.0	0.656100
25	51.0000	3.46410	0.0	0.0	1.000000	0.0	0.0	0.0	1.000000
26	50.3721	3.46410	7.97820	0.0	1.000000	0.0	-0.156400	0.0	0.987700
27	48.5039	3.46410	15.7599	0.0	1.000000	0.0	-0.309000	0.0	0.951100
28	45.4413	3.46410	23.1535	0.0	1.000000	0.0	-0.454000	0.0	0.891000
29	41.2599	3.46410	29.9770	0.0	1.000000	0.0	-0.587800	0.0	0.809000
30	36.0624	3.46410	36.0624	0.0	1.000000	0.0	-0.707100	0.0	0.707100
31	50.5000	4.33010	0.0	-0.500000	0.866000	0.0	0.0	0.0	1.000000
32	49.8783	4.33010	7.89990	-0.493800	0.866000	-0.078200	-0.156400	0.0	0.987700
33	48.0284	4.33010	15.6053	-0.475500	0.866000	-0.154500	-0.309000	0.0	0.951100
34	44.9958	4.33010	22.9265	-0.445500	0.866000	-0.227000	-0.454000	0.0	0.891000
35	40.8554	4.33010	29.6831	-0.404500	0.866000	-0.293900	-0.587800	0.0	0.809000
36	35.7089	4.33010	35.7089	-0.328000	0.866000	-0.377400	-0.754700	0.0	0.656100
37	50.0000	5.19620	0.0	-0.500000	0.866000	0.0	0.0	0.0	1.000000
38	49.3844	5.19620	7.82170	-0.493800	0.866000	-0.078200	-0.156400	0.0	0.987700
39	47.5528	5.19620	15.4508	-0.475500	0.866000	-0.154500	-0.309000	0.0	0.951100
40	44.5503	5.19620	22.6995	-0.445500	0.866000	-0.227000	-0.454000	0.0	0.891000
41	40.4509	5.19620	29.3893	-0.404500	0.866000	-0.293900	-0.587800	0.0	0.809000
42	35.3553	5.19620	35.3553	-0.328000	0.866000	-0.377400	-0.754700	0.0	0.656100
43	49.5000	6.06220	0.0	-0.500000	0.866000	0.0	0.0	0.0	1.000000
44	48.8906	6.06220	7.74350	-0.493800	0.866000	-0.078200	-0.156400	0.0	0.987700
45	47.0773	6.06220	15.2963	-0.475500	0.866000	-0.154500	-0.309000	0.0	0.951100
46	44.1048	6.06220	22.4725	-0.445500	0.866000	-0.227000	-0.454000	0.0	0.891000
47	40.0463	6.06220	29.0954	-0.404500	0.866000	-0.293900	-0.587800	0.0	0.809000
48	35.0018	6.06220	35.0018	-0.328000	0.866000	-0.377400	-0.754700	0.0	0.656100
49	49.0000	6.92820	0.0	0.0	1.000000	0.0	0.0	0.0	1.000000
50	48.3967	6.92820	7.66530	0.0	1.000000	0.0	-0.156400	0.0	0.987700
51	46.6018	6.92820	15.1418	0.0	1.000000	0.0	-0.309000	0.0	0.951100
52	43.6593	6.92820	22.2455	0.0	1.000000	0.0	-0.454000	0.0	0.891000
53	39.6418	6.92820	28.8015	0.0	1.000000	0.0	-0.587800	0.0	0.809000
54	34.6482	6.92820	34.6482	0.0	1.000000	0.0	-0.707100	0.0	0.707100
55	50.0000	8.66030	0.0	0.500000	0.866000	0.0	0.0	0.0	1.000000
56	49.3844	8.66030	7.82170	0.493800	0.866000	0.078200	-0.156400	0.0	0.987700
57	47.5528	8.66030	15.4508	0.475500	0.866000	0.154500	-0.309000	0.0	0.951100
58	44.5503	8.66030	22.6995	0.445500	0.866000	0.227000	-0.454000	0.0	0.891000
59	40.4509	8.66030	29.3893	0.404500	0.866000	0.293900	-0.587800	0.0	0.809000
60	35.3553	8.66030	35.3553	0.328000	0.866000	0.377400	-0.754700	0.0	0.656100
61	51.0000	10.3923	0.0	0.500000	0.866000	0.0	0.0	0.0	1.000000
62	50.3721	10.3923	7.97820	0.493800	0.866000	0.078200	-0.156400	0.0	0.987700
63	48.5039	10.3923	15.7599	0.475500	0.866000	0.154500	-0.309000	0.0	0.951100

64	45.4413	10.3923	23.1535	0.445500	0.866000	0.227000	-0.454000	0.0	0.891000
65	41.2599	10.3923	29.9770	0.404500	0.866000	0.293900	-0.587800	0.0	0.809000
66	36.0624	10.3923	36.0624	0.328000	0.866000	0.377400	-0.754700	0.0	0.656100
67	52.0000	12.1244	0.0	0.500000	0.866000	0.0	0.0	0.0	1.000000
68	51.3598	12.1244	8.13460	0.493800	0.866000	0.078200	-0.156400	0.0	0.987700
69	49.4549	12.1244	16.0689	0.475500	0.866000	0.154500	-0.309000	0.0	0.951100
70	46.3323	12.1244	23.6075	0.445500	0.866000	0.227000	-0.454000	0.0	0.891000
71	42.0689	12.1244	30.5648	0.404500	0.866000	0.293900	-0.587800	0.0	0.809000
72	36.7695	12.1244	36.7695	0.328000	0.866000	0.377400	-0.754700	0.0	0.656100
73	53.0000	13.8564	0.0	0.0	1.000000	0.0	0.0	0.0	1.000000
74	52.3475	13.8564	8.29100	0.0	1.000000	0.0	-0.156400	0.0	0.987700
75	50.4060	13.8564	16.3779	0.0	1.000000	0.0	-0.309000	0.0	0.951100
76	47.2233	13.8564	24.0615	0.0	1.000000	0.0	-0.454000	0.0	0.891000
77	42.8779	13.8564	31.1526	0.0	1.000000	0.0	-0.587800	0.0	0.809000
78	37.4767	13.8564	37.4766	0.0	1.000000	0.0	-0.707100	0.0	0.707100
79	52.0000	15.5885	0.0	-0.500000	0.866000	0.0	0.0	0.0	1.000000
80	51.3598	15.5885	8.13460	-0.493800	0.866000	-0.078200	-0.156400	0.0	0.987700
81	49.4549	15.5885	16.0689	-0.475500	0.866000	-0.154500	-0.309000	0.0	0.951100
82	46.3323	15.5885	23.6075	-0.445500	0.866000	-0.227000	-0.454000	0.0	0.891000
83	42.0689	15.5885	30.5648	-0.404500	0.866000	-0.293900	-0.587800	0.0	0.809000
84	36.7695	15.5885	36.7695	-0.328000	0.866000	-0.377400	-0.754700	0.0	0.656100
85	51.0000	17.3205	0.0	-0.500000	0.866000	0.0	0.0	0.0	1.000000
86	50.3721	17.3205	7.97820	-0.493800	0.866000	-0.078200	-0.156400	0.0	0.987700
87	48.5039	17.3205	15.7599	-0.475500	0.866000	-0.154500	-0.309000	0.0	0.951100
88	45.4413	17.3205	23.1535	-0.445500	0.866000	-0.227000	-0.454000	0.0	0.891000
89	41.2599	17.3205	29.9770	-0.404500	0.866000	-0.293900	-0.587800	0.0	0.809000
90	36.0624	17.3205	36.0624	-0.328000	0.866000	-0.377400	-0.754700	0.0	0.656100
91	50.0000	19.0526	0.0	-0.500000	0.866000	0.0	0.0	0.0	1.000000
92	49.3844	19.0526	7.82170	-0.493800	0.866000	-0.078200	-0.156400	0.0	0.987700
93	47.5528	19.0526	15.4508	-0.475500	0.866000	-0.154500	-0.309000	0.0	0.951100
94	44.5503	19.0526	22.6995	-0.445500	0.866000	-0.227000	-0.454000	0.0	0.891000
95	40.4509	19.0526	29.3893	-0.404500	0.866000	-0.293900	-0.587800	0.0	0.809000
96	35.3553	19.0526	35.3553	-0.328000	0.866000	-0.377400	-0.754700	0.0	0.656100
97	49.0000	20.7846	0.0	-0.500000	0.866000	0.0	0.0	0.0	1.000000
98	48.3967	20.7846	7.66530	-0.493800	0.866000	-0.078200	-0.156400	0.0	0.987700
99	46.6018	20.7846	15.1418	-0.475500	0.866000	-0.154500	-0.309000	0.0	0.951100
100	43.6593	20.7846	22.2455	-0.445500	0.866000	-0.227000	-0.454000	0.0	0.891000
101	39.6418	20.7846	28.8015	-0.404500	0.866000	-0.293900	-0.587800	0.0	0.809000
102	34.6482	20.7846	34.6482	-0.328000	0.866000	-0.377400	-0.754700	0.0	0.656100

ELEMENT NODAL POINT NUMBERS AND MATERIAL PROPERTIES

ELEMENT	I	J	K	L	MODULUS psf.	THICKNESS ft.	POISSON'S R	NODE DIFFERENCE
1	1	7	8	2	0.43200000D 09	0.2500	0.1500	7
2	2	8	9	3	0.43200000D 09	0.2500	0.1500	7
3	3	9	10	4	0.43200000D 09	0.2500	0.1500	7
4	4	10	11	5	0.43200000D 09	0.2500	0.1500	7
5	5	11	12	6	0.43200000D 09	0.2500	0.1500	7
6	7	13	14	8	0.43200000D 09	0.2500	0.1500	7
7	8	14	15	9	0.43200000D 09	0.2500	0.1500	7
8	9	15	16	10	0.43200000D 09	0.2500	0.1500	7
9	10	16	17	11	0.43200000D 09	0.2500	0.1500	7
10	11	17	18	12	0.43200000D 09	0.2500	0.1500	7
11	13	19	20	14	0.43200000D 09	0.2500	0.1500	7
12	14	20	21	15	0.43200000D 09	0.2500	0.1500	7
13	15	21	22	16	0.43200000D 09	0.2500	0.1500	7
14	16	22	23	17	0.43200000D 09	0.2500	0.1500	7
15	17	23	24	18	0.43200000D 09	0.2500	0.1500	7
16	19	25	26	20	0.43200000D 09	0.2500	0.1500	7
17	20	26	27	21	0.43200000D 09	0.2500	0.1500	7
18	21	27	28	22	0.43200000D 09	0.2500	0.1500	7
19	22	28	29	23	0.43200000D 09	0.2500	0.1500	7
20	23	29	30	24	0.43200000D 09	0.2500	0.1500	7
21	25	31	32	26	0.43200000D 09	0.2500	0.1500	7
22	26	32	33	27	0.43200000D 09	0.2500	0.1500	7
23	27	33	34	28	0.43200000D 09	0.2500	0.1500	7
24	28	34	35	29	0.43200000D 09	0.2500	0.1500	7
25	29	35	36	30	0.43200000D 09	0.2500	0.1500	7
26	31	37	38	32	0.43200000D 09	0.2500	0.1500	7
27	32	38	39	33	0.43200000D 09	0.2500	0.1500	7
28	33	39	40	34	0.43200000D 09	0.2500	0.1500	7
29	34	40	41	35	0.43200000D 09	0.2500	0.1500	7
30	35	41	42	36	0.43200000D 09	0.2500	0.1500	7
31	37	43	44	38	0.43200000D 09	0.2500	0.1500	7
32	38	44	45	39	0.43200000D 09	0.2500	0.1500	7
33	39	45	46	40	0.43200000D 09	0.2500	0.1500	7
34	40	46	47	41	0.43200000D 09	0.2500	0.1500	7
35	41	47	48	42	0.43200000D 09	0.2500	0.1500	7
36	43	49	50	44	0.43200000D 09	0.2500	0.1500	7
37	44	50	51	45	0.43200000D 09	0.2500	0.1500	7
38	45	51	52	46	0.43200000D 09	0.2500	0.1500	7
39	46	52	53	47	0.43200000D 09	0.2500	0.1500	7
40	47	53	54	48	0.43200000D 09	0.2500	0.1500	7
41	49	55	56	50	0.43200000D 09	0.3333	0.1500	7
42	50	56	57	51	0.43200000D 09	0.3333	0.1500	7
43	51	57	58	52	0.43200000D 09	0.3333	0.1500	7
44	52	58	59	53	0.43200000D 09	0.3333	0.1500	7
45	53	59	60	54	0.43200000D 09	0.3333	0.1500	7
46	55	61	62	56	0.43200000D 09	0.3333	0.1500	7
47	56	62	63	57	0.43200000D 09	0.3333	0.1500	7
48	57	63	64	58	0.43200000D 09	0.3333	0.1500	7
49	58	64	65	59	0.43200000D 09	0.3333	0.1500	7
50	59	65	66	60	0.43200000D 09	0.3333	0.1500	7
51	61	67	68	62	0.43200000D 09	0.3333	0.1500	7
52	62	68	69	63	0.43200000D 09	0.3333	0.1500	7
53	63	69	70	64	0.43200000D 09	0.3333	0.1500	7
54	64	70	71	65	0.43200000D 09	0.3333	0.1500	7
55	65	71	72	66	0.43200000D 09	0.3333	0.1500	7
56	67	73	74	68	0.43200000D 09	0.3333	0.1500	7
57	68	74	75	69	0.43200000D 09	0.3333	0.1500	7
58	69	75	76	70	0.43200000D 09	0.3333	0.1500	7
59	70	76	77	71	0.43200000D 09	0.3333	0.1500	7
60	71	77	78	72	0.43200000D 09	0.3333	0.1500	7
61	73	79	80	74	0.43200000D 09	0.3333	0.1500	7
62	74	80	81	75	0.43200000D 09	0.3333	0.1500	7
63	75	81	82	76	0.43200000D 09	0.3333	0.1500	7

64	76	82	83	77	0.43200000D	09	0.3333	0.1500	7
65	77	83	84	78	0.43200000D	09	0.3333	0.1500	7
66	79	85	86	80	0.43200000D	09	0.3333	0.1500	7
67	80	86	87	81	0.43200000D	09	0.3333	0.1500	7
68	81	87	88	82	0.43200000D	09	0.3333	0.1500	7
69	82	88	89	83	0.43200000D	09	0.3333	0.1500	7
70	83	89	90	84	0.43200000D	09	0.3333	0.1500	7
71	85	91	92	86	0.43200000D	09	0.3333	0.1500	7
72	86	92	93	87	0.43200000D	09	0.3333	0.1500	7
73	87	93	94	88	0.43200000D	09	0.3333	0.1500	7
74	88	94	95	89	0.43200000D	09	0.3333	0.1500	7
75	89	95	96	90	0.43200000D	09	0.3333	0.1500	7
76	91	97	98	92	0.43200000D	09	0.3333	0.1500	7
77	92	98	99	93	0.43200000D	09	0.3333	0.1500	7
78	93	99	100	94	0.43200000D	09	0.3333	0.1500	7
79	94	100	101	95	0.43200000D	09	0.3333	0.1500	7
80	95	101	102	96	0.43200000D	09	0.3333	0.1500	7

BOUNDARY CONDITIONS OF POINTS HAVING SPECIFIED DISPLS.
D1,D2,D3, ARE TRANSLATIONS IN BASE COORDINATES. D4,D5 ARE ROTATIONS IN SURFACE COORDINATES.

NODE	D1	D2	D3	D4	D5	D1	D2	D3	D4	D5
6	1	1	1	1	1	0.0	0.0	0.0	0.0	0.0
12	1	1	1	1	1	0.0	0.0	0.0	0.0	0.0
18	1	1	1	1	1	0.0	0.0	0.0	0.0	0.0
24	1	1	1	1	1	0.0	0.0	0.0	0.0	0.0
30	1	1	1	1	1	0.0	0.0	0.0	0.0	0.0
36	1	1	1	1	1	0.0	0.0	0.0	0.0	0.0
42	1	1	1	1	1	0.0	0.0	0.0	0.0	0.0
48	1	1	1	1	1	0.0	0.0	0.0	0.0	0.0
54	1	1	1	1	1	0.0	0.0	0.0	0.0	0.0
60	1	1	1	1	1	0.0	0.0	0.0	0.0	0.0
66	1	1	1	1	1	0.0	0.0	0.0	0.0	0.0
72	1	1	1	1	1	0.0	0.0	0.0	0.0	0.0
78	1	1	1	1	1	0.0	0.0	0.0	0.0	0.0
84	1	1	1	1	1	0.0	0.0	0.0	0.0	0.0
90	1	1	1	1	1	0.0	0.0	0.0	0.0	0.0
96	1	1	1	1	1	0.0	0.0	0.0	0.0	0.0
102	1	1	1	1	1	0.0	0.0	0.0	0.0	0.0
1	0	1	0	1	0	0.0	0.0	0.0	0.0	0.0
7	0	1	0	1	0	0.0	0.0	0.0	0.0	0.0
13	0	1	0	1	0	0.0	0.0	0.0	0.0	0.0
19	0	1	0	1	0	0.0	0.0	0.0	0.0	0.0
25	0	1	0	1	0	0.0	0.0	0.0	0.0	0.0
31	0	1	0	1	0	0.0	0.0	0.0	0.0	0.0
37	0	1	0	1	0	0.0	0.0	0.0	0.0	0.0
43	0	1	0	1	0	0.0	0.0	0.0	0.0	0.0
49	0	1	0	1	0	0.0	0.0	0.0	0.0	0.0
55	0	1	0	1	0	0.0	0.0	0.0	0.0	0.0
61	0	1	0	1	0	0.0	0.0	0.0	0.0	0.0
67	0	1	0	1	0	0.0	0.0	0.0	0.0	0.0
73	0	1	0	1	0	0.0	0.0	0.0	0.0	0.0
79	0	1	0	1	0	0.0	0.0	0.0	0.0	0.0
85	0	1	0	1	0	0.0	0.0	0.0	0.0	0.0
91	0	1	0	1	0	0.0	0.0	0.0	0.0	0.0
97	0	1	0	1	0	0.0	0.0	0.0	0.0	0.0

TOTAL APPLIED NODAL POINT FORCES LOAD CASE 1 lbs.

NODE	P1	P2	P3	P4	P5
1	-97.0000	0.0	-168.000	0.0	0.0
2	-193.000	0.0	-335.000	0.0	0.0
3	-193.000	0.0	-335.000	0.0	0.0
4	-193.000	0.0	-335.000	0.0	0.0
5	-193.000	0.0	-335.000	0.0	0.0
6	0.0	0.0	0.0	0.0	0.0
7	-194.000	0.0	-336.500	0.0	0.0
8	-388.000	0.0	-673.000	0.0	0.0
9	-388.000	0.0	-673.000	0.0	0.0
10	-388.000	0.0	-673.000	0.0	0.0
11	-388.000	0.0	-673.000	0.0	0.0
12	0.0	0.0	0.0	0.0	0.0
13	-196.500	0.0	-340.000	0.0	0.0
14	-393.000	0.0	-680.000	0.0	0.0
15	-393.000	0.0	-680.000	0.0	0.0
16	-393.000	0.0	-680.000	0.0	0.0
17	-393.000	0.0	-680.000	0.0	0.0
18	0.0	0.0	0.0	0.0	0.0
19	-198.500	0.0	343.500	0.0	0.0
20	-397.000	0.0	-687.000	0.0	0.0
21	-397.000	0.0	-687.000	0.0	0.0
22	-397.000	0.0	-687.000	0.0	0.0
23	-397.000	0.0	-687.000	0.0	0.0
24	0.0	0.0	0.0	0.0	0.0
25	0.0	0.0	-398.000	0.0	0.0
26	0.0	0.0	-796.000	0.0	0.0
27	0.0	0.0	-796.000	0.0	0.0
28	0.0	0.0	-796.000	0.0	0.0
29	0.0	0.0	-796.000	0.0	0.0
30	0.0	0.0	0.0	0.0	0.0
31	198.500	0.0	343.500	0.0	0.0
32	397.000	0.0	-687.000	0.0	0.0
33	397.000	0.0	-687.000	0.0	0.0
34	397.000	0.0	-687.000	0.0	0.0
35	397.000	0.0	-687.000	0.0	0.0
36	0.0	0.0	0.0	0.0	0.0
37	196.500	0.0	-340.000	0.0	0.0
38	393.000	0.0	-680.000	0.0	0.0
39	393.000	0.0	-680.000	0.0	0.0
40	393.000	0.0	-680.000	0.0	0.0
41	393.000	0.0	-680.000	0.0	0.0
42	0.0	0.0	0.0	0.0	0.0
43	194.000	0.0	-336.500	0.0	0.0
44	388.000	0.0	-673.000	0.0	0.0
45	388.000	0.0	-673.000	0.0	0.0
46	388.000	0.0	-673.000	0.0	0.0
47	388.000	0.0	-673.000	0.0	0.0
48	0.0	0.0	0.0	0.0	0.0
49	0.0	0.0	-1165.00	0.0	0.0
50	0.0	0.0	-2330.00	0.0	0.0
51	0.0	0.0	-2330.00	0.0	0.0
52	0.0	0.0	-2330.00	0.0	0.0
53	0.0	0.0	-2330.00	0.0	0.0
54	0.0	0.0	0.0	0.0	0.0
55	-980.000	0.0	-1700.00	0.0	0.0
56	-1960.00	0.0	-3400.00	0.0	0.0
57	-1960.00	0.0	-3400.00	0.0	0.0
58	-1960.00	0.0	-3400.00	0.0	0.0
59	-1960.00	0.0	-3400.00	0.0	0.0
60	0.0	0.0	0.0	0.0	0.0
61	-1000.00	0.0	-1735.00	0.0	0.0
62	-2000.00	0.0	-3470.00	0.0	0.0
63	-2000.00	0.0	-3470.00	0.0	0.0

64	-2000.00	0.0	-3470.00	0.0	0.0
65	-2000.00	0.0	-3470.00	0.0	0.0
66	0.0	0.0	0.0	0.0	0.0
67	-1020.00	0.0	-1770.00	0.0	0.0
68	-2040.00	0.0	-3540.00	0.0	0.0
69	-2040.00	0.0	-3540.00	0.0	0.0
70	-2040.00	0.0	-3540.00	0.0	0.0
71	-2040.00	0.0	-3540.00	0.0	0.0
72	0.0	0.0	0.0	0.0	0.0
73	0.0	0.0	-2060.00	0.0	0.0
74	0.0	0.0	-4120.00	0.0	0.0
75	0.0	0.0	-4120.00	0.0	0.0
76	0.0	0.0	-4120.00	0.0	0.0
77	0.0	0.0	-4120.00	0.0	0.0
78	0.0	0.0	0.0	0.0	0.0
79	1020.00	0.0	-1770.00	0.0	0.0
80	2040.00	0.0	-3540.00	0.0	0.0
81	2040.00	0.0	-3540.00	0.0	0.0
82	2040.00	0.0	-3540.00	0.0	0.0
83	2040.00	0.0	-3540.00	0.0	0.0
84	0.0	0.0	0.0	0.0	0.0
85	1000.00	0.0	-1735.00	0.0	0.0
86	2000.00	0.0	-3470.00	0.0	0.0
87	2000.00	0.0	-3470.00	0.0	0.0
88	2000.00	0.0	-3470.00	0.0	0.0
89	2000.00	0.0	-3470.00	0.0	0.0
90	0.0	0.0	0.0	0.0	0.0
91	980.000	0.0	-1700.00	0.0	0.0
92	1960.00	0.0	-3400.00	0.0	0.0
93	1960.00	0.0	-3400.00	0.0	0.0
94	1960.00	0.0	-3400.00	0.0	0.0
95	1960.00	0.0	-3400.00	0.0	0.0
96	0.0	0.0	0.0	0.0	0.0
97	485.000	0.0	-840.000	0.0	0.0
98	970.000	0.0	-1680.00	0.0	0.0
99	970.000	0.0	-1680.00	0.0	0.0
100	970.000	0.0	-1680.00	0.0	0.0
101	970.000	0.0	-1680.00	0.0	0.0
102	0.0	0.0	0.0	0.0	0.0